UNIVERSITA' DEGLI STUDI DI PADOVA

Dipartimento di Scienze Chimiche
Corso di Laurea Magistrale in Chimica

TESI DI LAUREA MAGISTRALE

One step synthesis of foldamers with a Tridimensional Catalytic center for C-C bond formation

Relatore:
Prof. Alessandro Moretto

Controrelatore:
Prof.ssa Barbara Fresch

Laureanda**:**
Beatrice Marcon

Anno Accademico 2021-2022

INDEX

1. PURPOSE OF THIS WORK

Peptides have been extensively exploited as efficient catalysts in a variety of reactions. Their structures and functionalities can be varied by changing amino acid components and by rationally designing their secondary structures, such as α-helix, β-turn and β-sheet, in order to build suitable reaction environments around catalytic centers. Foldamers have emerged as synthetic, conformationally well-defined mimics of proteins and other biopolymers, in the way to allow chemists to expand the narrow range of structural components that build up natural proteins. Thus, foldamers have been designed to carry out protein-like functions of binding, catalysis and signal relay. Recently, Gellman and co-workers, exploiting a combination of α- and β-amino acids, developed a set of foldamers carrying on their surface one primary amine and one secondary amine functions at varying sequence positions. A foldamer featuring the two functionalities spaced by one helical turn proved to be a potent catalyst for macrocycle formation from linear dialdehyde precursors through carbon-carbon bond formation. The high efficiency of the system is related to the rigid foldamer conformation, which allows spatial control of the relative positioning of the catalytic diad. We speculated that if one of the functionalities of the catalytic diad can be placed directly into the backbone of a helical foldamer rather than at a side-chain position, then the versatility of the system could be expanded, possibly opening the way to catalytic triads.

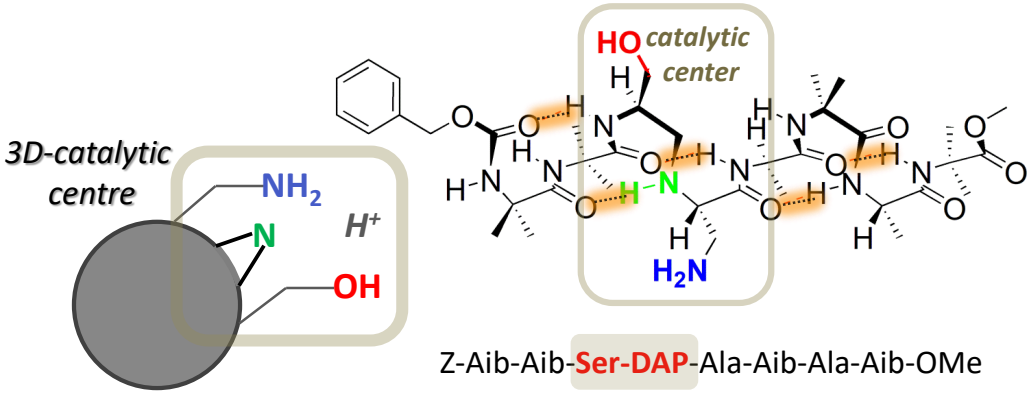

To this aim, peptide-based foldamers containing a -CH_2-NH- moiety as replacement of one peptide bond (Ψ[CH_2NH] in the notation for peptide bond surrogates) represent

suitable candidates. Concerning the helical foldameric scaffold, we relied on the well documented ability of α-aminoisobutyric acid (Aib), to promote stable and highly populated α-/3_{10}-helical conformations when combined with protein amino acids in α-peptides even of limited main-chain length. In this work, we report on the catalytic properties of foldamers designed on the basis of the considerations outlined above, which displayed high efficiency to template a C-C bond macrocyclization mediated by primary/secondary amine *via* imine-enamine chemistry, as well as examples of aldol condensation reactions.

2. INTRODUCTION

Enzymes are very interesting catalysts in the chemical field. They are proteins that selectively bind a substrate and lead to its chemical transformation by stabilizing the transition state. They are also non-toxic, environmentally friendly and capable to performing difficult chemical reactions with relative ease.[1] For these reasons they are of great interest for chemical industries, even if they show some disadvantages due to their vulnerability caused by high production costs, low thermal stability, low tolerance to solvent conditions and poor adaptability to abiotic chemical transformations. Furthermore, enzymatic catalysis depends on the positioning of functional groups within the active site, making their design difficult and synthetically elaborate. In this scenario there has been a growing demand for the development of catalysts that can mimic these natural models while overcoming their limitations. In recent decades, one solution has been the construction of catalytic sites within short peptide sequences.[2] In fact, peptides, as well as giving the possibility to create backbones with various reactive groups, allow to control the reactivity through the use of non-covalent interactions, such as hydrogen bonds, between catalyst and substrate. Many examples show that these oligomers are good catalysts for a variety of reactions such as S_N1 substitutions,[3] glycosylation[4] and for other enantioselective reactions.[5] To control the catalytic activity, it is not only necessary to have the right functional groups, but also particular substrate-catalyst interactions that allow the correct approach and orientation of the reactants, just like enzymes. To do this, a structural rigidity is required to bring the reaction sites into the correct distance and position. One solution for this need is foldamers.

2.1 Foldamers

The uniqueness of biopolymers, such as proteins or RNAs, is that they adopt specific and compact conformations, capable of performing catalysis or other molecular tasks. This has inspired and increased interest in synthetic foldamers. As proteins and RNAs have different structures, so by modifying and investigating possible backbone structures, different types of synthetic foldamers with different folding behaviors can

be obtained.[6] After these considerations, it is possible to define foldamers as oligomers or polymers that are strongly disposed to adopt specific conformations in solution.[7] It is clear at this point the potential behind the development of these molecules. Developing new molecules that adopt ordered solutions not only allows us to gain a deeper understanding of biological macromolecules, but also to find new polymers that can perform functions not yet seen in nature. A protein is a high molecular weight molecule, composed of a set of secondary structures. A single foldamer cannot be a good mimic of these biopolymers; conversely, a set of foldamers could be. Thus, while *foldamer* is defined to a secondary structure, in the same way a *tyligomer* is associated with a tertiary or quaternary conformation.[8] The chain conformation is defined by non-covalent interactions between non-adjacent monomer units, i.e., between atoms not of the same unit. This is a characteristic of secondary structures. Currently, most of the known foldamers have an alpha-helix structure, which requires particular types of hydrogen bonding to associate.[8] It is easier to find information on isolated helices than on isolated sheets, and this leads to greater access to knowledge to design systems that can fold into a helix conformation. Suitably engineered these helices could self-assemble to give tertiary or quaternary structures.[9] However, this field has not yet been much explored and current studies have focused on secondary structures, especially helices, of foldamers that can catalyze different types of reactions.

At this point is of particular interest for a chemist the design of the foldamer, in fact it is necessary to choose the right sequence of amino acids that allows then to bring the functional groups designated to catalysis in the right position of the helix, for example near the helical fold. As can be seen in one of the examples from the group of Gellman et al. for the aldol condensation reaction (*Figure 2.1)*[10]

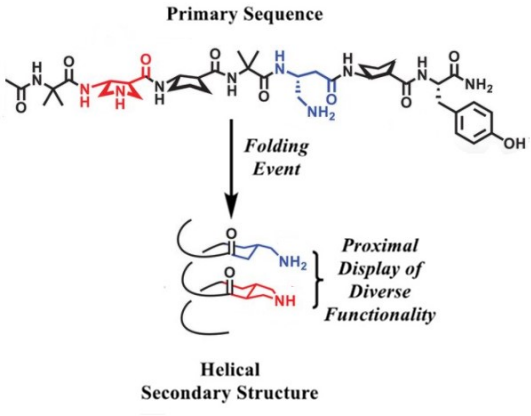

Figure 2.1 Primary sequence of generic foldamer and representation of the helical secondary structure that results in the alignment of functional groups from a common helical face.

While foldamers have the disadvantage compared to biomacromolecules of having side chains and substrates exposed to the solvent and limitations on the arrangement of side chains, they have a great advantage. These systems allow, in fact, to have predictable secondary structures that are very stable at short lengths. In this way it is possible to predetermine the spatial distance of the reactive groups by carefully selecting the design of the amino acid sequence.

2.2 α- and 3_{10} helices

As has been mentioned, most of the currently known foldamers have an alpha-helix structure, which is the most common secondary structure among peptides. The other main structure present among helical peptides is helix 3_{10}. These two types of helices differ primarily in their intramolecular C=O···H-N hydrogen bonding pattern, which is type $i \rightarrow i + 3$ in the 3_{10} helix and type $i \rightarrow i + 4$ in the alpha-helix. *(Figure2.2)*

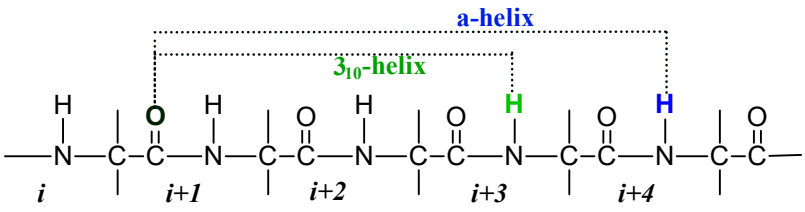

Figure 2.2 C=O···H–N H-bonds: i ← i+3 for the 310- helix and i ← i+4 for the α-helix

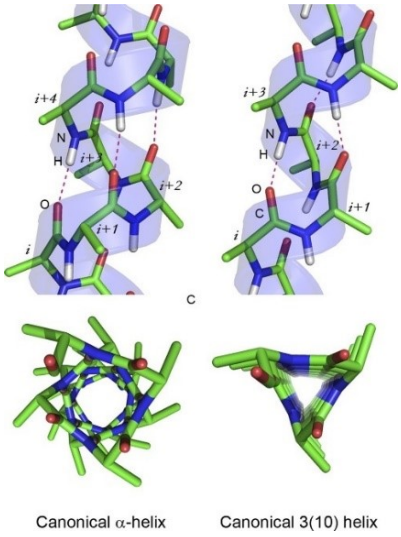

Figure 2.3 The α-helix and its basic unit and the 310-helix and its basic.

As a result, the latter is less tightly bound and less elongated than the first one. (*Figure 2.3 and Table 2.1)*

PARAMETER	A-HELIX	3_{10}-HELIX
RESIDUES PER TURN	3.63	3.24
C=O···H–N	$i \rightarrow i + 4$	$i \rightarrow i + 3$
PSEUDO-CYCLE	α-turn or C13-structure	β-turn or C10-structure
PITCH	5.67 Å	6.29 Å
Ψ	-42°	-30°
Φ	-63°	-57°

Table 2.1 Parameters for the α- and 310-helical conformations.

Looking at the ψ and ϕ dihedral angles in the Ramachandran map, you can see that they fall in the same region. *(Figure 2.4)*

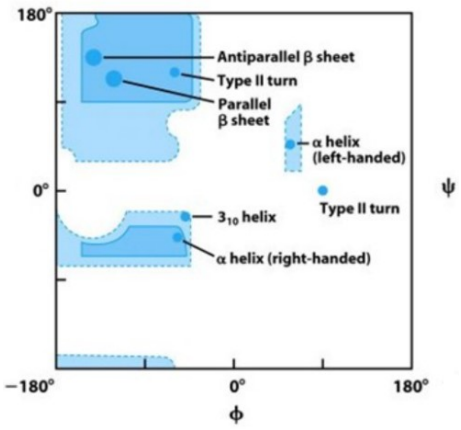

Figure 2.4 Ramachandran map

About 15-20% of all protein helix structures are 3_{10}-helices,[11] which are typically shorter (3-5 residues) than alpha-helices (10-12 residues).[12] These helices have been investigated as intermediates in the folding/unfolding of alpha-helices, so if one of the two conformations should prove impossible (e.g. due to side chain interactions) the main chain can switch to the other conformation.[13] In fact, for L amino acids, there is no unpermitted region between the alpha (angles) and 3_{10} (corners) conformations, allowing free interconversion between the two. The increased presence of alpha helices is due to the fact that the entropic penalty for ring closure required for $i \rightarrow i + 3$ formation, compared to $i \rightarrow i + 4$, is lower. In addition, C^{α}-tetrasubstituted α-amino acids have been shown to promote the occurrence of helices, specifically 3_{10}-helices. Tetrasubstituted amino acids have an alkyl or aryl group at the α-carbon atom, creating a steric obstruction that restricts φ and ψ dihedral angles. The simplest C^{α}-tetrasubstituted amino acid is α-aminoisobutyric acid (Aib) *(Figure 2.5)*, which has two methyl groups in alpha that limit its conformational freedom.

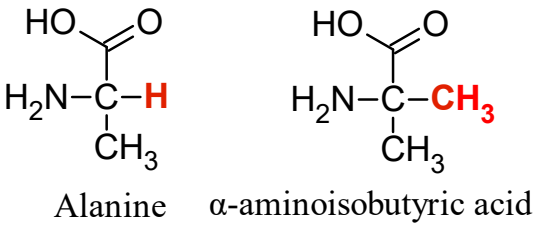

Figure 2.5 Chemical structures of Alanine (tri-substituted amino acids) and α-aminoisobutyric acid (tetra-substituted amino acids).

Crystallographic studies have shown peptides containing Aib and trisubstituted amino acids (such as Alanine) exhibit 3_{10}-helices, α-helices and mixed helices structures. This

behavior is due to the amount of Aib present (the higher the Aib the more 3_{10}-helix is formed), but also to the length (the longer the α-helix is formed).[14]

It is clear from these considerations, how important is the design of the amino acid sequence. Knowing the possible structure that the foldamer can have, it will be possible to insert the functional groups dedicated to catalysis in the right position of the helix. Moreover, knowing the geometry of the helices, it will be possible to put the reactive groups at the right distance. In this way you will have stable and well-organized structures capable of being selective for certain reactions and type of substrate.

2.3 Carbon-carbon bond chemistry

In synthetic organic chemistry, the cleavage and formation of carbon-carbon bonds is of considerable interest. For this reason, these types of reactions have also been explored in foldamer catalysis. The foldamers that have been used are of various types, showing once again the potential of the design strategies for these oligomers depending on the conditions and purpose for which they are intended. It will be seen that β-amino acids are often used instead of α-amino acids. These residues give a well-known secondary structure that is the 14-helix (*Figure 2.6*).

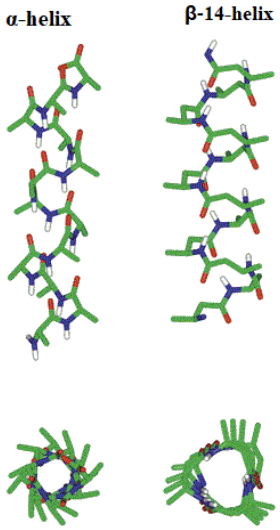

Figure 2.6 The α-helix and its basic unit and the 14-helix and its basic.

It is a β-peptide, characterized by 14-membered ring hydrogen bonds between C=O(*i*) ···H-N(*i*+*2*).[15] By using β^3 residues, which possess a side chain on the backbone carbon atom adjacent to the nitrogen atom, in parallel to having a narrow angular alignment, which allows the side chains to be brought closer together, it allows modifications that can improve some of its structural parameters. In fact, it has been seen that by incorporating subunit derived from trans-2-aminocyclohexanecarboxylic acid (ACHC) its stability is improved, allowing it to be entirely helical in aqueous solution.[16]

Taking example from a previous work using small helical α-peptides,[17] one of the first examples of foldamer catalysis using β-peptide, is on the retro-aldol reaction of 4-phenyl-4-hydroxy-2-oxobutyrate in aqueous buffer[18]. (*Figure 2.7 (a)*). The most efficient β-peptide features the ACHC-ACHC-β^3-hLys sequence repeat. The ACHC residues allow the formation of a stable, hydrophobic 14-helix (which aids self-assembly in aqueous solution), while the β^3-hLys residues generate a strip of amine/ammonium side chains (*Figure 2.7(b)*). The latter are crucial for the catalytic mechanism that seems to involve these residues that with the keto group of the substrate lead to the formation of imine. In addition, the proximity of the positive charges allows the lowering of the pK_a values of at least one ammonium group facilitating the catalysis in this reaction.

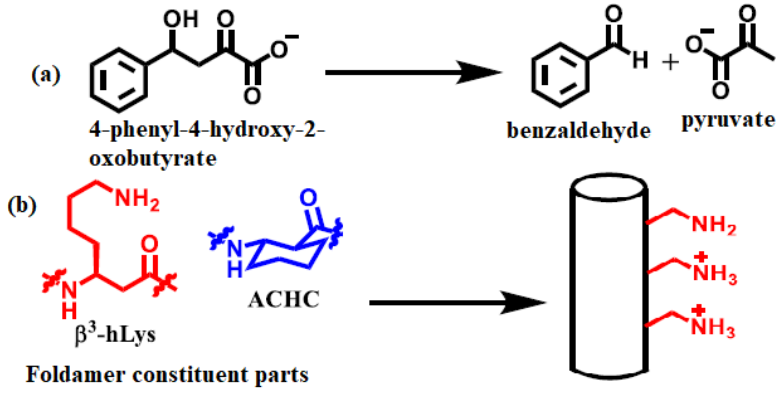

Figure 2.7 (a) retro-aldol reaction (b) Representation of foldamer with ACHC and β3-hLys residues clustered on the helical face.

Studies on enzymes have clarified that hydrogen bonds in the active sites are crucial for catalysis, for example in the stabilization of the transition states. In this regard, the use of hydrogen bonds for catalysis has also been explored in foldamers. In the last

decade Guichard er al. characterized urea-based foldamers, seeing their propensity to fold into a helix with 2.5 residues per turn. This is realized by a series of $C{=}O_i\cdots HN'_{i+2}$ and $C{=}O_i\cdots HN_{i+3}$ hydrogen bonds, which stabilize the structure[19] (*Figure 2.8*).

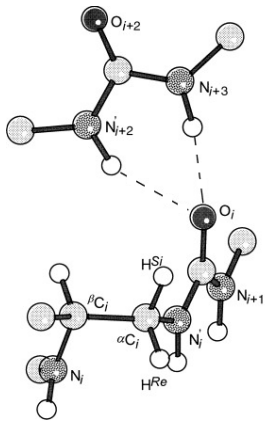

Figure 2.8 Schematic representation of the hydrogen-bonding pattern as found in the 2.5 helix of oligourea.

Studied in the context of enantioselective C-C bond formation reactions these oligomers have been shown to be efficient for the addition of malonates to nitro-olefins[20] (*Figure 2.9 (a)*), a synthetically interesting reaction due to the rich chemistry of nitro groups[21]. Working with a Brønsted base, this foldamer is particularly efficient, leading to high enantioselectivity at very low catalyst concentrations. In addition, the first two urea in the chain, not being employed in intramolecular hydrogen bonds, may act as hydrogen bond acceptors, probably becoming responsible for substrate activation and recognition (*Figure 2.9 (b)*).

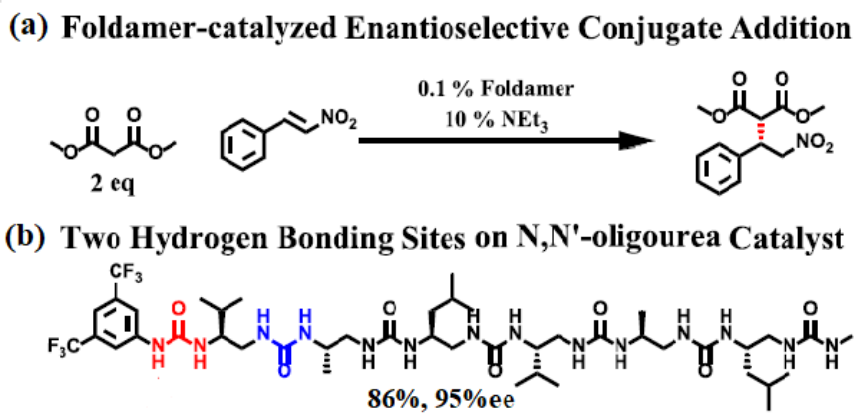

Figure 2.9 (a) Foldamer-catalyzed, enantioselective conjugate addition (b) N,N'-oligourea catalyst

This work is inspired by One of the earliest works uses poly-L-leucine for the epoxidation of Julia-Colonna, an epoxidation on unsaturated two- or three-phase ketones. In the mechanism all substrates bind to the catalyst generating a tertiary complex. In the helix, the 4 hydrogens not engaged in intramolecular H-bonds are available to accept H-bonds with the substrates[22].

Work by Price, Michaelis et al. involves the use of the amino acid Aib within the chain, here a bifunctional catalyst is developed for enantioselective Dies-Alder reactions and indole alkylation reactions[23]. The catalyst under consideration is an 11-residue alpha-peptide, in which the helical structure is promoted by Aib residues, while the catalytic sites are represented by an imidazolidinone and a thiourea, incorporated at position 2 and 6, which protrude from the side chains (*Figure 2.10 (a)*). The Dies-Alder reaction was tested between 2-butenal and a carbamate-functionalized diene, leading to good results (*Figure 2.10 (b)*).

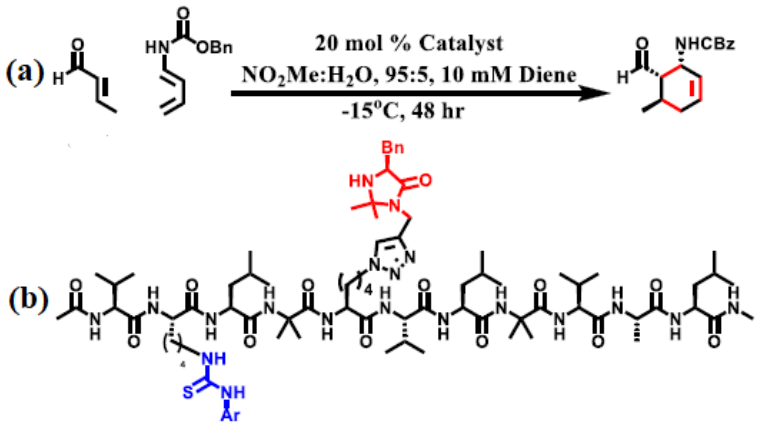

Figure 2.10 (a)Peptide-catalyzed Diels-Alder reaction (b) foldamer catalyst

By placing the two non-proteinogenic residues at the correct distance within the helical structure, the thiourea will be able to recruit the diene by aligning it with the imidazolidinone, while the latter will provide electrophilic activation for 2-butenal, through the formation of the iminium ion[24]. The results show excellent yield and enantioselectivity confirming the correct design of the foldamer. Control studies have been carried out to confirm the efficiency of this catalyst. One of these emphasized the selectivity of the catalyst, in fact it involved the competition between a diene with carbamate (able to bind to thiourea) and one without. Using the functionalized foldamer, a strong selectivity towards the diene with carbamate was found, which was not the case with a simple imidazolidinone catalyst (*Figure 1.11 (a)*). A second control

experiment instead highlighted the importance of the helical structure of the peptide, in fact, using a peptide in which proline residues were incorporated (*Figure 2.11 (b)*), interrupting the helical folding, catalysis was drastically decreased.

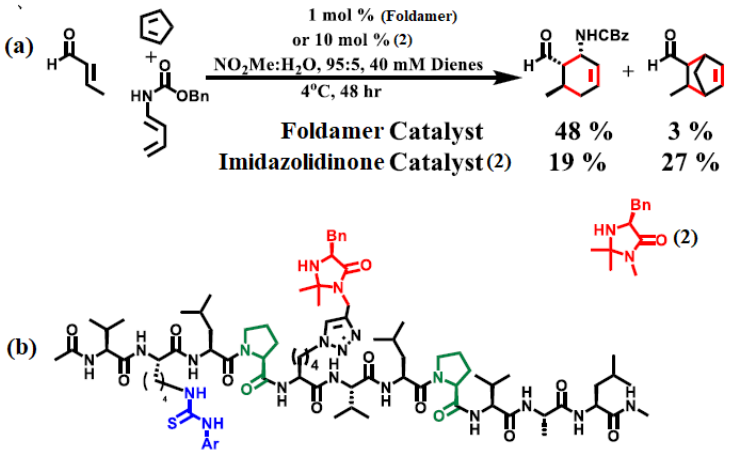

*Figure 2.11 Control experiments (a) comparison between bifunctional peptide catalyst and imidazolidinone (**2**) (b) Peptide catalyst with proline.*

Most enzymatic transformations have a synthetic counterpart. Often though, the mechanisms by which natural and synthetic catalysts operate differ markedly. The catalytic asymmetric aldol reaction as a fundamental C−C bond forming reaction in chemistry and biology is an interesting case in this respect. In this reaction an enolate is combined with an aldehyde or ketone to result in the formation of a beta-hydroxy carbolic compound.

Chemically, this enzyme-mediated reaction is dominated by approaches that utilize preformed enolate equivalents in combination with a chiral catalyst. Typically, a metal is involved in the reaction mechanism. Most enzymes, however, use a fundamentally different strategy and catalyze the direct aldolization of two unmodified carbonyl compounds. Class I aldolases utilize an enamine-based mechanism, while Class II aldolases mediate this process by using a zinc cofactor[25,26]. (*Figure 2.12*).

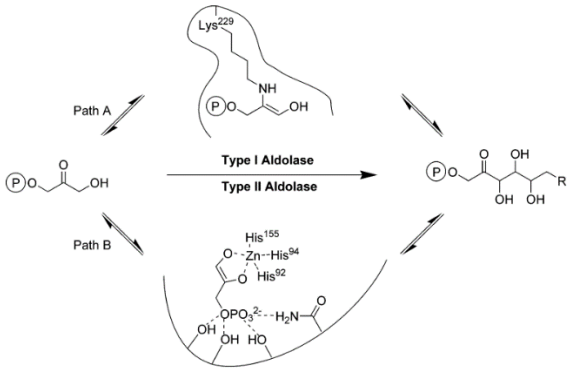

Figure 2.12 Mechanisms of Type I and Type II aldolases.

In 1998 it was discovered the first small-molecule asymmetric class II aldolase mimics have been described in the form of zinc, lanthanum, and barium complexes[27,28].

However, amine-based asymmetric class I aldolase mimics have not been described in the literature. Importantly, in 2000 it was proposed that the amino acid proline is an effective asymmetric catalyst for the direct aldol reaction between unmodified acetone and a variety of aldehydes[29].

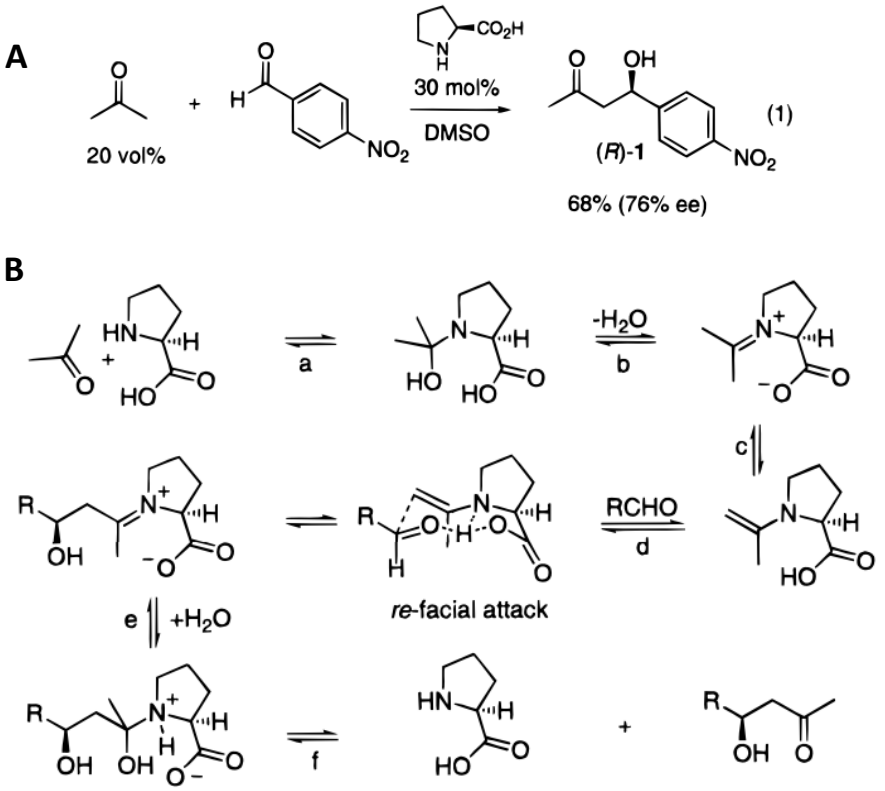

Scheme 2.1 Proposed enamine mechanism of the Proline-catalyzed asymmetric aldol reaction.

Currently, it is still assumed that this aldol reaction occurs via an enamine mechanism (*Scheme 2.1*). Proline, functions as a "micro-aldolase" that provides both the nucleophilic amino group and an acid/base cocatalyst in the form of the carboxylate. This co-catalyst may facilitate each individual step of the mechanism, including the nucleophilic attack of the amino group (a), the dehydration of the carbinol amine intermediate (b), the deprotonation of the iminium species (c), the carbon−carbon bond forming step (d), and both steps of the hydrolysis of the iminium-aldol intermediate (e and f). The tricyclic hydrogen bonded framework provides for enantiofacial selectivity.

2.4 Macrocyclic compounds

It is well known that many molecules of pharmacological interest are derived from natural products. Among these, macrocyclic complexes have developed a certain interest because of their great efficacy. Moreover, they are a good starting point to understand how to design molecules with properties necessary to produce new therapies. For these reasons the synthesis of macrocyclic complexes attracts synthetic chemists.[30] Cyclic compounds containing a ring with 12 or more atoms have already been synthesized for therapeutic strategies, such as the treatment of hepatitis C[31], but also for the development of new technologies in the application as optoelectronic, liquid-crystalline, and sensing materials[32]. The need to search for efficient synthesis strategies for this category of compounds is due to the competition of the ring closure reaction, which has an entropic penalty to pay, with collateral intermolecular reactions, which reduce the yield leading to undesirable products[33,34].

In this regard, strategies to facilitate the synthesis of macrocyclic compounds have been devised.

One such strategy involves the preorganization of linear precursors. Widely used in supramolecular chemistry, since by appropriately organizing the substrate, it is possible to "pay" for the conformational rearrangement cost earlier in terms of ΔG. This technique for cyclization involves multipoint coordination between a cation, anion, or neutral partner to thus facilitate macrocycle synthesis[33] (*Figure 2.13*).

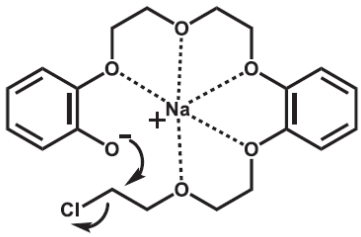

Figure 2.13 Guest-mediated cyclization. Prior approaches to macrocyclization.

Obviously, this technique depends on the pre-existing non-covalent interactions in the linear precursor. It is widely used for the preparation of crown ethers or azacrown ethers by placing a heteroatom such as oxygen or sulfur, which acting as a nucleophile allows the ring closure step[35].

Another quite effective approach for the synthesis of macrocycles is the catalytic method called ring closed metathesis (RCM)[36] (*Figure 2.14*).

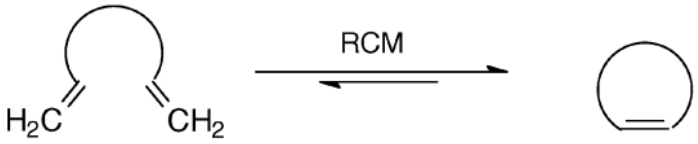

Figure 2.14 Ring Closed Metathesis (RCM) cyclization

The products of this reaction are unsaturated rings resulting from the intramolecular metathesis of two terminal alkynes. In addition, this process involves the use of metal catalysts. Obviously, it is necessary for the metal center to coordinate between the internal functionalities (*Figure 2.15)*[37,38].

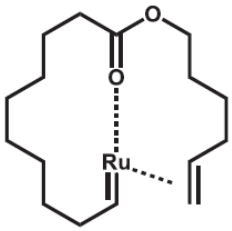

Figure 2.15 Ring Closed Metathesis (RCM) cyclization.

Finally, one method to mention for the purposes of this paper is one that takes inspiration from biological systems[39]. These biosynthetic systems don't have the problem of entropic cost because they place the linear precursors in the right

conformation and position for ring closure. In this way, in addition to catalyzing the reaction, they avoid the occurrence of competing intermolecular reactions[40].

An example of the use of this approach is from Gellman et al. in which, inspired by biological systems, the authors developed a foldamer-catalyst, which thanks to the active sites arranged in the right position activates the ends of a linear precursor and by orienting them in the right way ensures ring closure through the formation of C-C bonds[10] (*Figures 2.16*).

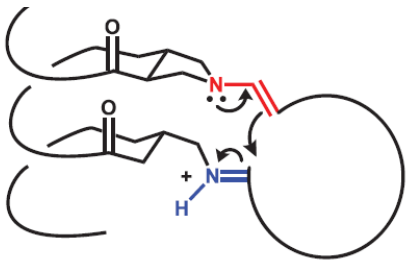

Figure 2.16 Foldamer-catalyst designed by Gellman et al.

3. RESULT AND DISUSSION

3.1 Foldamers synthesis strategy

We speculated that if one of the functionalities of the catalytic diad can be placed directly into the backbone of a helical foldamer rather than at a side-chain position, then the versatility of the system could be expanded, possibly opening the way to catalytic triads. (*Figure 3.1*)

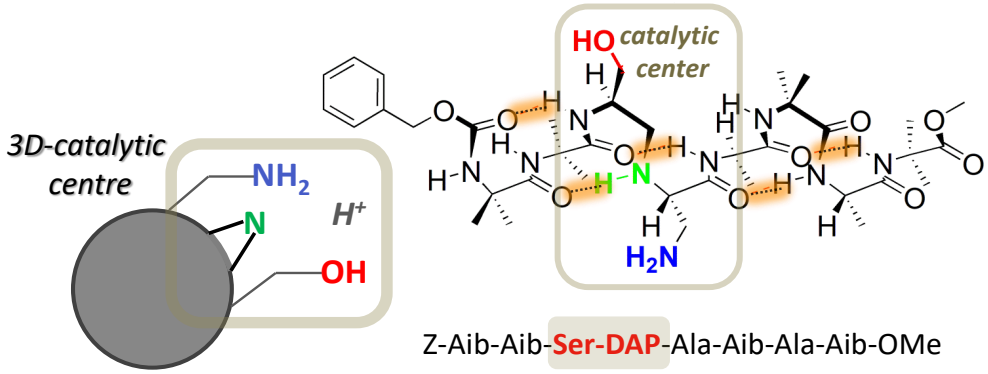

Figure 3.1 Scheme and sketch of a hypothetical catalytic triad inside the foldamer

To this aim, peptide-based foldamers containing a -CH_2-NH- moiety as replacement of one peptide bond (Ψ[CH_2NH] in the notation for peptide bond surrogates) represent suitable candidates. Concerning the helical foldameric scaffold, we relied on the well documented ability of α-aminoisobutyric acid (Aib), to promote stable and highly populated α-/3_{10}-helical conformations when combined with protein amino acids in α-peptides even of limited main-chain length.[14]

As a preliminary step, we explored the conformational effects of the Ψ[CH_2NH] backbone modification in selected model compounds.

First, Boc-Aib-OH was converted in its Weinreb amide derivative [Boc-Aib-N(OMe)Me], and then chemically transformed in Boc-Aib-H (**1**) by a selective reduction, which is run by the addition of 1 eq of $LiAlH_4$ in THF. *(Figure 3.2)*

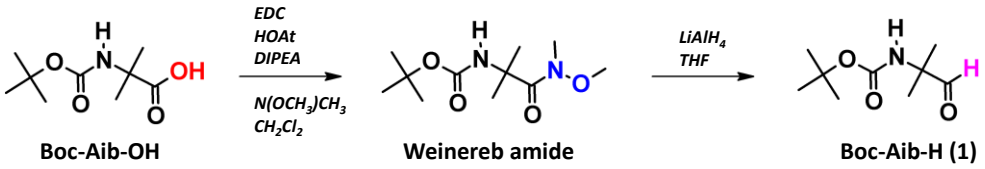

Figure 3.2 Synthesis strategy for obtaining Boc-Aib-H

In the Weinreb amide, the oxygen atom adjacent to the nitrogen atom decreases the electron density on nitrogen, so that the attack from the nitrogen atom becomes unfavorable. The reaction intermediate enclosed in the grey highlighted box in *Figure 3.3* is stable due to the oxygen atom of the methoxy-amide coordinating to the aluminum atom. After hydrolysis, the methoxy-amide anion becomes a much better leaving group, due to the oxygen atom stabilizing the negative charge, affording the aldehyde functional group rather than an amine functional group as described by the red mechanism depicted in *Figure 3.3*.

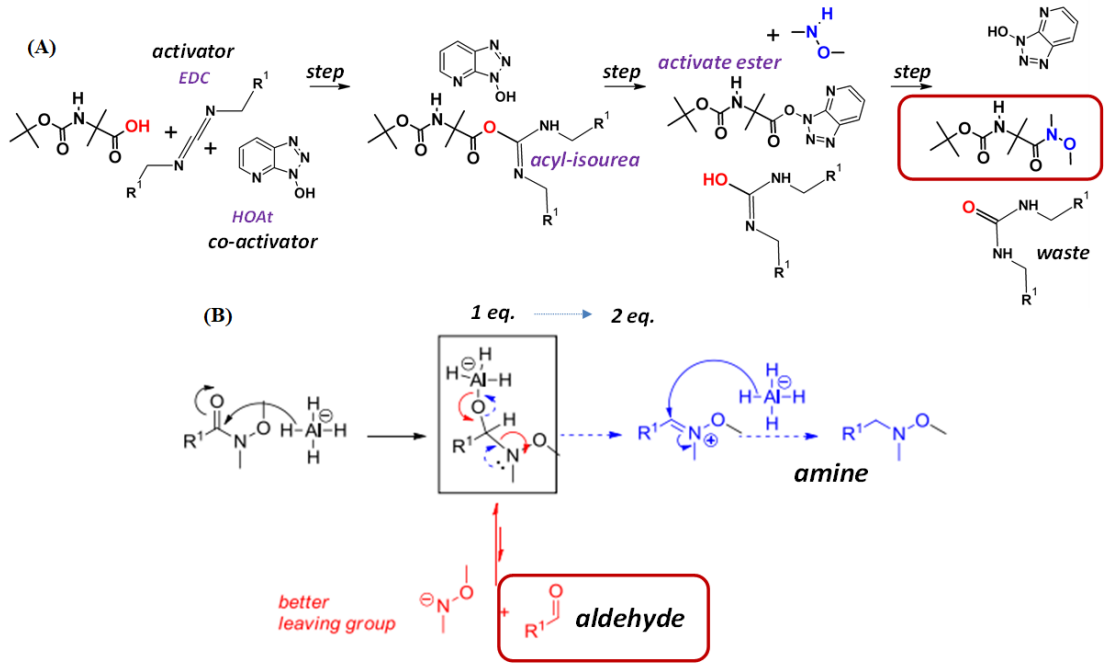

Figure 3.3 (A) Weinreb amide synthesis mechanism (B) Aldehyde synthesis mechanism

Importantly, Boc-Aib-H was obtained as a single crystal suitable for X-ray diffraction analyses. X-Ray diffraction data collection, structure solution and refinement were performed by Dr. Marco Crisma (ICB-CNR, Padova). (*Figure 3.4*)

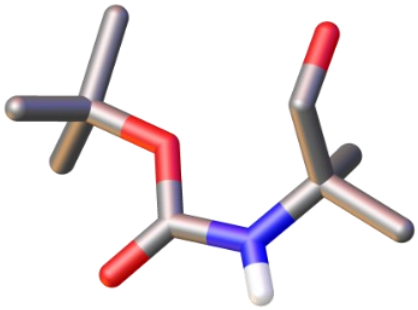

Figure 3.4. X-ray diffraction structure of Boc-Aib-H.

The molecular structure of Boc-Aib-H at the solid state displayed is *cis* conformation of the urethane amide bond.

The reaction between Boc-Aib-H (**1**) and H-L-Val-CO-NH-*p*ClBn (**2**) (Boc, *tert*-butyloxycarbonyl; NH-*p*ClBn, *para*-chlorobenzylamino) resulted in the formation of the corresponding stable Shiff-base product Boc-AibΨ[CH=N]-L-Val-NH-*p*ClBn (**3**). Moreover, the subsequent reduction with $NaBH_4$ afforded the Ψ[CH_2NH] bond modification as highlighted in compound (**4**). *(Figure 3.4)*

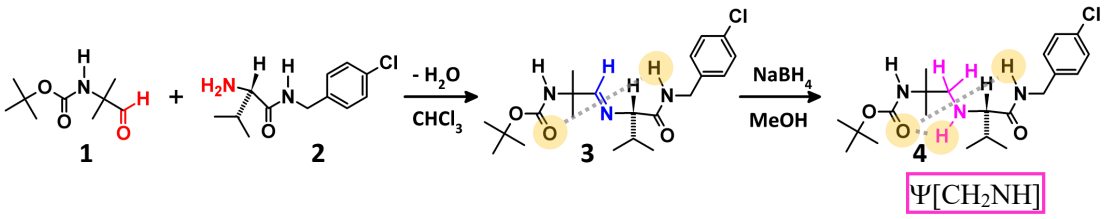

*Figure 3.5 Synthesis of Boc-Aib Ψ[CH_2N]-L-Val-NH-pClBn (**4**) via Shiff-base*

The NMR analysis shown in *Figure 3.6* confirms the occurrence of the two reactions. Following the formation of imine, we see the characteristic peak at about 7.5 ppm of imine (**3**), which disappears upon reduction giving way to the aliphatic peaks at about 2.5 and 2.9 ppm.

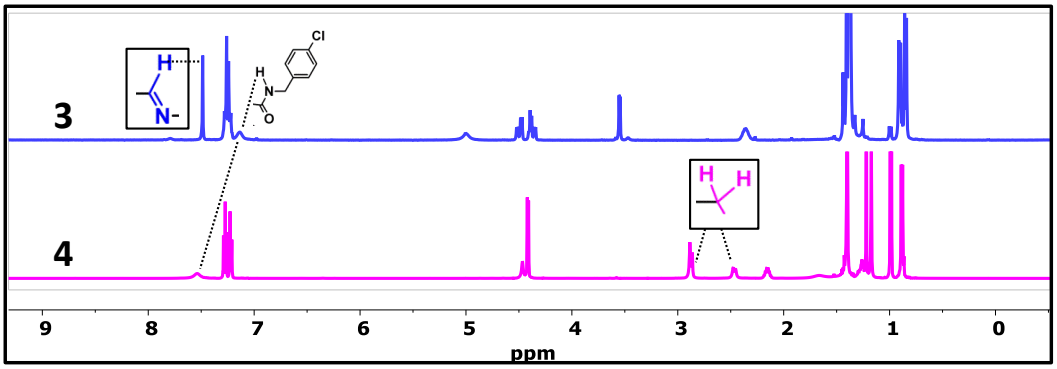

*Figure 3.6 NMR comparison of Boc-Aib Ψ[CH=N]-L-Val-NH-pClBn (**3**) and Boc-Aib Ψ[CH_2N]-L-Val-NH-pClBn (**4**)*

Crystals of Boc-AibΨ[CH=N]-L-Val-NH-*p*ClBn were grown from ethyl acetate / *n*-hexane through the vapor diffusion technique. Relevant crystal data and structure refinement parameters are listed in Table 4.1 in Experimental Section.

The molecular structure of Boc-AibΨ[CH=N]-L-Val-NH-*p*ClBn, determined by single-crystal X-ray diffraction analysis, is illustrated in *Figure 3.7*, while its packing mode is illustrated in *Figure 3.8*.

X-Ray diffraction data collection, structure solution and refinement were performed by Dr. Marco Crisma (ICB-CNR, Padova).

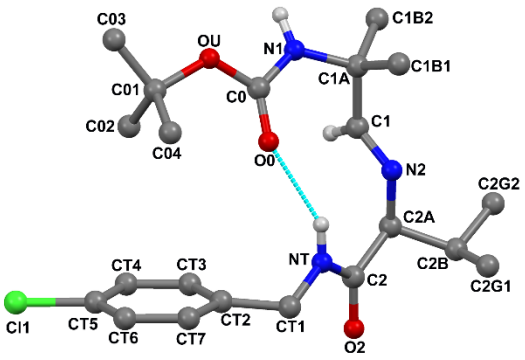

Figure 3.7 X-Ray diffraction structure of Boc-AibΨ[CH=N]-L-Val-NH-pClBn with atom numbering. Most of the H-atoms are omitted for clarity. The intramolecular hydrogen bond is indicated by dashed line.

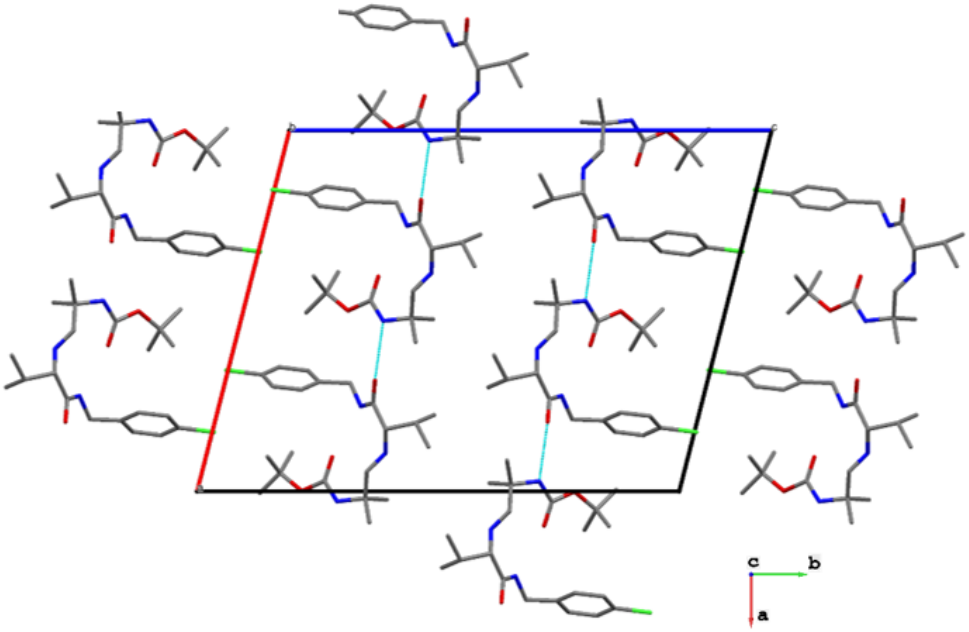

Figure 3.8 Packing mode of Boc-AibΨ[CH=N]-L-Val-NH-pClBn as viewed down the b axis. Intermolecular hydrogen bonds are indicated by dashed lines.

The C1=N2 bond length is 1.257(4) Å. For comparison, the peptidic C-N bond, owing to its partial double bond character, is slightly longer, 1.32 Å. The values of the bond angles at C1 and N2 are 122.9(3)° and 117.8(3)°, respectively. The imino moiety is found in the *E* configuration without significant deviation from the ideal *trans* planarity, the value of the C1A-C1-N2-C2A torsion angle being -176.4(3)°. The C1A···C2A distance, 3.77 Å, compares well with that between consecutive C^{α} atoms in a polypeptide chain, 3.80 Å.

The *pseudo*peptide backbone is folded in a β-turn conformation stabilized by an intramolecular N-H···O=C hydrogen bond between the *p*-Cl-benzylamide N-H group and the urethane carbonyl oxygen atom [N···O and H···O distances 2.968(3) Å and 2.19 Å, respectively; N-H···O angle 149.7°]. The values of the ϕ,ψ, backbone torsion angles adopted by the (*pseudo*) Aib and L-Val residues [ϕ_1,ψ_1 = 51.7(4)°, -128.2(3)°; ϕ_2,ψ_2 = -101.8(3)°, 8.0(4)°] are close to those typical for the *i*+1 and *i*+2 corner positions of a regular type-II′ β-turn conformation (60°, -120° and -80°, 0°, respectively)[41]. It is worth noting that the overwhelmingly preferred conformation of the regular Aib residue in peptides is 3_{10}-/α-helical[42], whereas *semi*-extended (or polyproline II) conformations, which include the *i*+1 corner position of type-II (II′) β-turns, are scarcely populated[43]. Conceivably, lack of the C=O group in the *pseudo*-Aib residue might modify the energetic profile of the conformational map with respect to

that of the parent compound, particularly along the ψ coordinate. In the packing mode, an intermolecular hydrogen bond is observed between the (urethane) N1-H1 group and a (x-1/2, y+1/2, z) symmetry equivalent of the (amide) O2 carbonyl oxygen atom, generating rows of molecules along the *a* direction (*Figure 3.8*).

To the best of our knowledge, there is no precedent of crystallographic characterization of an imino surrogate for a peptide bond between two amino acids.

3.2 Effect of introducing modification into the backbone

As discussed before, the reduction of the imino group of (**3**) allows the formation of its amino (secondary amine, Ψ[CH_2NH]) surrogate (**4**). To explore the effect of the introduction of the secondary amine backbone modification in more structured foldamers, a set of Boc-(L-Ala-Aib)$_n$-H (*n* = **1**, **2**, **4**; **6'-8'**) and H-(L-Ala-Aib)$_n$-OMe (*n* = **1**, **2**, **4**; **6''-8''**) were synthesized and combined under reductive conditions (General Procedure in *Figure 3.9 (A)*) to form the amino surrogate foldamers Boc-(L-Ala-Aib)$_n$Ψ[CH_2NH]-(L-Ala-Aib)$_n$-OMe (*n* = **1**, **2**, **4**; **6-8**) illustrated in *Figure 3.9 (B)*.

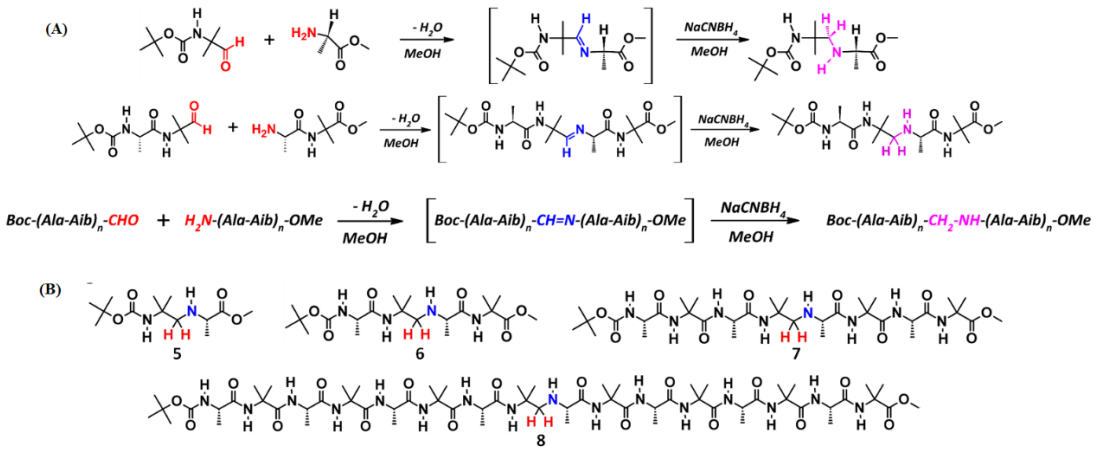

Figure 3.9 (A) Synthesis of Boc-(L-Ala-Aib)$_n$ Ψ[CH_2NH]-(L-Ala-Aib)$_n$-OMe under reductive condition (B) foldamers Boc-(L-Ala-Aib)$_n$ Ψ[CH_2NH]-(L-Ala-Aib)$_n$-OMe (n = ***1***, ***2***, ***4***; ***6-8***)

Attempts were made to grow single crystals, suitable for an X-ray diffraction analysis, from most of the synthesized compounds. Success was achieved so far for the peptide aldehydes Boc-(L-Ala-Aib)$_2$-H and Boc-(L-Ala-Aib)$_4$-H. X-Ray diffraction data collection, structure solution and refinement were performed by Dr. Marzio Rancan

(ICMATE-CNR, Padova). In the following, the most relevant conformational features of the two structures are briefly outlined.

The X-ray diffraction structure of Boc-(L-Ala-Aib)$_2$-H is illustrated in *Figure 3.10*. The peptide backbone is folded and stabilized by two intramolecular N-H···O=C intramolecular H-bonds, namely between the N-H group of Aib(3) and the Boc urethane carbonyl oxygen, and between the N-H group of Aib(4) and the C=O group of Aib(1). As a result, two consecutive β-turns (intramolecularly H-bonded C_{10} structures) are formed. The values of the backbone torsion angles adopted by residues 1-3 are: ϕ_1,ψ_1 = -56.1°, -29.6°; ϕ_2,ψ_2 = -56.9°, -23.5°; ϕ_3,ψ_3 = -64.5°, -30.2°. On these bases, both consecutive β-turns belong to type-III, the building unit of the 3_{10}-helix. As a consequence, the conformation adopted by the peptide aldehyde Boc-(Aib)$_4$-H can be described as an incipient 3_{10}-helix. The C-terminal α-amino aldehyde residue is characterized by a positive value for the ϕ backbone torsion angle (ϕ_4 = 48.9°). In peptides and proteins, the ψ torsion angle is defined as involving the bond sequence N(*i*)-C$^{\alpha}$(*i*)-C(*i*)-N(*i*+*1*). For a C-terminal α-amino aldehyde residue, the equivalent "ψ" torsion angle has to be measured by taking the aldehyde H atom as a replacement for the N(*i*+*1*) atom. In our case, the value of "ψ_4" is 33.3°. Being both ϕ_4 and "ψ_4" positive, the C-terminal α-amino aldehyde residue displays in this structure a screw sense reversal with respect to the preceding residues, a rather common observation for helical peptides carrying an Aib ester at their C-terminus.

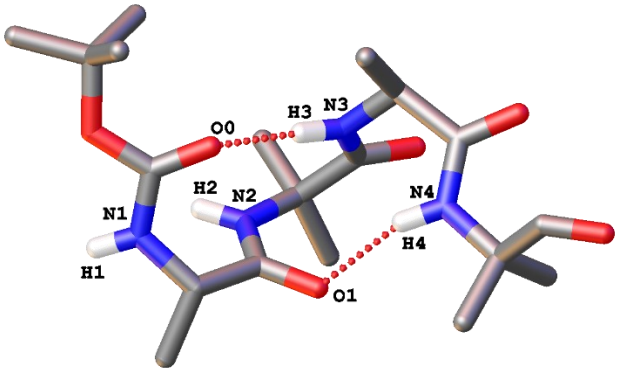

Figure 3.10 X-ray diffraction structure of Boc-(L-Ala-Aib)$_2$-H. Most of these H-atoms are omitted for clarity. Intramolecular H-bonds are indicated by dotted lines.

The crystal-state conformation of the octapeptide aldehyde Boc-(L-Ala-Aib)$_4$-H (*Figure 3.11*) is fully α-helical, featuring five consecutive N-H···O=C intramolecular

H-bonds of the *i+4* → *i* type (α-turn or C_{13} structure). The C-terminal C_{13} structure, characterized by a rather elongated H-bond, encompasses a C_{10} structure, in that the N8-H8 group is H-bonded to both the O4 and O5 carbonyl oxygen atoms. The values of the sets of ϕ,ψ backbone torsion angles for residues 1-7 (*Table 3.1*) do not differ much from those averaged the values obtained from a statistical analysis of high-resolution crystal structures of α-helical peptides (ϕ = –63°, ψ = –42°). The C-terminal Aib(8)-H residue is also helical, with retention of the right-handed screw sense of the preceding residues.

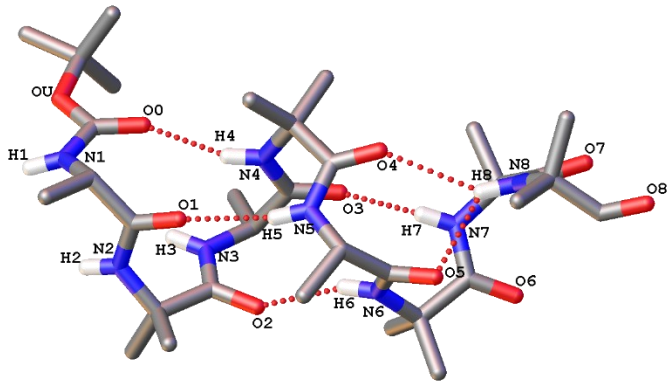

Figure 3.11 X-ray diffraction structure of Boc-(L-Ala-Aib)$_4$-H. Most of H-atoms are omitted for clarity. Intramolecular H-Bonds are indicated by dotted lines.

	L-ALA(1)	AIB(2)	L-ALA(3)	AIB(4)	L-ALA(5)	AIB(6)	L-ALA(7)	AIB(8)
ϕ	-72.8	-56.2	-71.3	-59.2	-64.4	-58.1	-68.7	**-48.9**
ψ	-49.2	-41.6	-38.3	-46.3	-47.4	-37.5	-31.7	**-33.6**^{A}

Table 3.1 Values of the φ,ψ backbone torsione angle (°) for the X-ray diffraction structure of Boc-(L-Ala-Aib)$_4$-H

The *pseudo*dipeptide Boc-AibΨ[CH_2NH]-L-Ala-OMe **5**, too short to give rise to an intramolecularly H-bonded conformation, was also prepared. When the -CH_2NH- peptide bond surrogate is within a chiral molecule, the two methylene protons are diasterotopic. *Figure 3.12* reports the methylene region of the ^{1}H NMR spectra of compound **5**-**8**. In the flexible *pseudo*dipeptide **5** the separation between the proton signals of the two methylene protons (Δδ) is 0.17 ppm, whereas it increases to 0.41 ppm in the case of the *pseudo*tripeptide **4**, long enough to populate a β-turn

conformation. In the series of foldamers **6-8**, Δδ increases from 0.46 ppm to 1.3 ppm and 1.5 ppm as the total main-chain length increases from four to eight and sixteen residues, respectively. These results support the view that a high population of folded conformation is achieved at the level of the longest oligomer investigated.

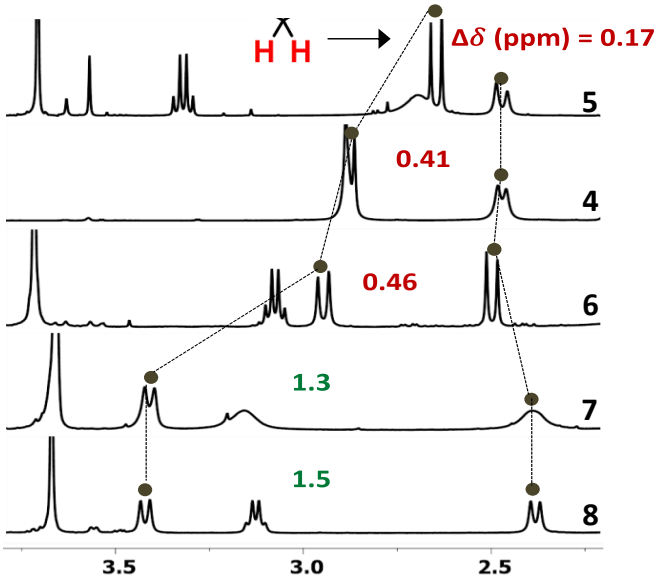

*Figure 3.12 Methylene region of the ^{1}H NMR spectra of compound **5-8.***

The X-ray diffraction structure of Boc-(L-Ala-Aib)$_4$Ψ[CH$_2$NH] -(L-Ala-Aib)$_4$-OMe **8** is illustrated in *Figure 3.13*.

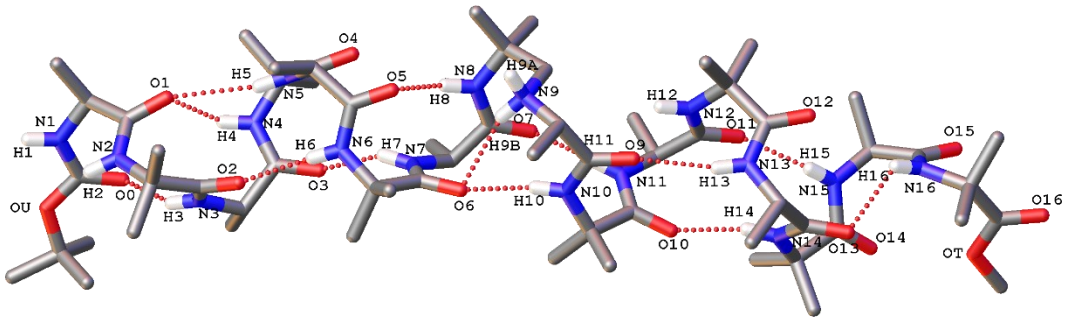

*Figure 3.13 X-ray diffraction structure of Boc-(L-Ala-Aib)$_4$Ψ[CH$_2$NH] -(L-Ala-Aib)$_4$-OMe. Intramolecular H-bonds in Foldamer **8** are indicated by dotted lines.*

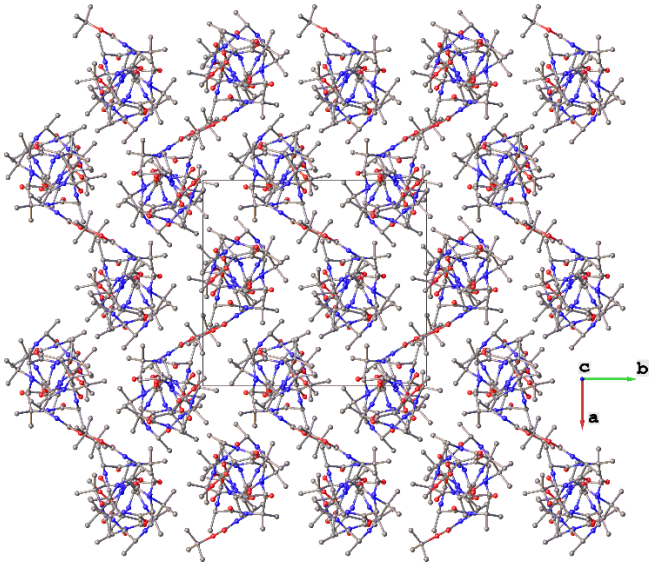

Figure 3.14 Packing mode of Boc-(L-Ala-Aib)$_4$Ψ[CH$_2$NH] -(L-Ala-Aib)$_4$-OMe. Intermolecular hydrogen bonds are indicated by dashed lines.

According to our analysis, the secondary amine N9 atom carries two H-atoms. In addition to the cationic foldamer, one hydroxide anion and two co-crystallized water molecules (not shown) compose the asymmetric unit. The conformation adopted by foldamer **8** is largely α-helical in its C-terminal half, whereas the N-terminal half shows a mixed 3_{10}-/α-helical character. Specifically, starting from the N-terminus, two intramolecularly H-bonded C_{10} structures, having the NH groups of residues 3 and 4 as the donors and the urethane carbonyl oxygen O0 and the peptide carbonyl oxygen O1 as the acceptors, are observed. The orientation of the N5-H5 group toward O1 would be appropriate for the formation of a C_{13} structure as well. However, the H5···O1 separation, 2.70 Å, exceed the commonly accepted limit for the occurrence of an N-H···O=C H-bond.[10] Then, two consecutive C_{13} structures (N6-H6···O2 and N7-H7···O3) are followed by two C_{10} structures, N8-H8···O5 and N9-H9B···O6. This latter interaction involves as the donor one of the two H-atoms of the protonated secondary amine. The second H-atom on N9 is intermolecularly H-bonded to the co-crystallized hydroxide anion. The intramolecular H-bonding scheme continues with two C_{13} structures (N10-H10···O6 and N11-H11···O7). There is no possibility for the N12-H12 group to form a C_{13} structure because the *pseudo* Aib residue at position 8 lacks the carbonyl group. Conversely, N12-H12 is involved in a C_{10} structure of which O9 is the acceptor, although the interaction is rather elongated and distorted. The α-helical pattern is restored with three additional C_{13} structures (N13-H13···O9, N14-

H14···O10, and N15-H15···O11), and terminates with a N16-H16···O13 C_{10} structure. The average values of the backbone torsion angles for residues 1–7 are ϕ = –59.2°, ψ = –39.1°, and those averaged over residues 9–15 are ϕ = –60.1°, ψ = –42.7°, quite close to the values obtained from a statistical analysis of high-resolution crystal structures of α-helical peptides (ϕ = –63°, ψ = –42°). At the -Aib(8)Ψ[CH_2NH]-L-Ala(9)- junction, the values of the backbone torsion angles are ϕ_8 = –59.9(5)°, ψ_8 = –57.7(5)°, "ω"$_8$ = 169.3(3)°, ϕ_9 = –52.6(5)°, ψ_9 = –56.0(5)°. Overall, the Ψ[CH_2NH] modification seems to be tolerated within a helical backbone. In particular, the torsion angle about the C8–N9 single bond deviates by less than 10° from the *trans* planarity typical for a regular peptide bond. However, the ψ_8 and ψ_9 values are significantly larger than those in a peptide α-helix, inducing a bending in the molecular shape. Indeed, angle between the two lines connecting the C^α atoms of residues 1 and 7 on one side, and of residues 7 and 15 on the other side (which can be considered as an approximation of the axis of the respective helical segment) is 33°.

3.3 Catalytic Foldamers

Based on the X-ray structure of foldamer **8** (sketched in *Figure 3.15 (A)*), we decided to build up a tridimensional catalytic center around the secondary amine as highlighted in *Figure 3.15 (B)*. For this propose we planned to develop a general synthetic strategy where series of fragments with appropriate functional side chain (in the way to eventually assists the catalytic function of the novel secondary amine), will be combined directly to readily form the desired catalytic center.

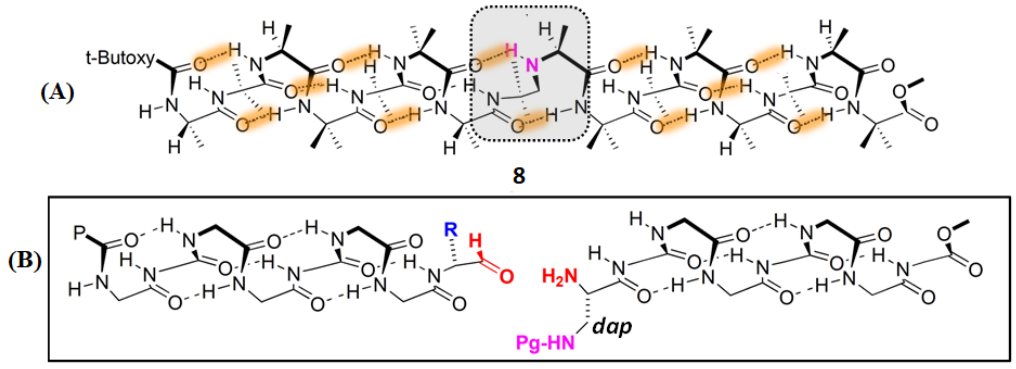

*Figure 3.15 (A) Sketched of foldamer **8** (B) Sketched of the tridimensional catalytic center around the secondary amine*

Foldamer **9** (*Figure 3.16*) was synthetized starting Z-(L-Ala-Aib)$_2$-H which was combined under reductive conditions with H_2N-Dap $^{(Boc)}$-(L-Ala-Aib)$_2$-OMe. The final foldamer was obtained after removal of the Dap side chain Boc protection group.

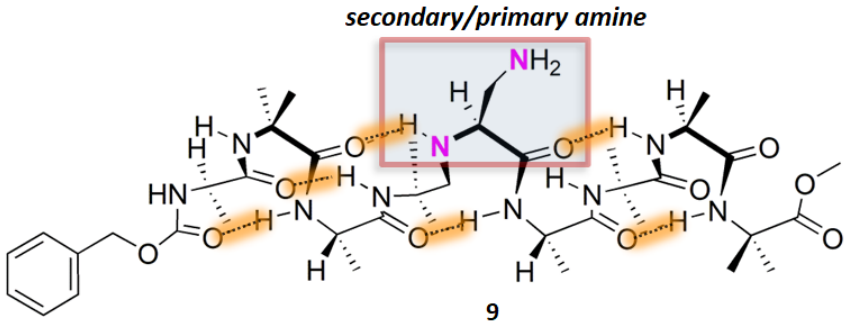

*Figure 3.16 Z-(L-Ala-Aib)$_2$ Ψ[CH$_2$NH]-Dap-(L-Ala-Aib)$_2$-Ome. Foldamer **9**.*

In this foldamer primary and secondary amines are spaced by two carbon atoms and reciprocally oriented according to the secondary structure.

To expand the general strategy to form a variety of 3D centers, Z-Aib-Aib-(Aaa)-H (Aaa= Val, Asp and Ser) were combined with H_2N-Dap$^{(Boc)}$-(L-Ala-Aib)$_2$-OMe to form foldamers **10-12** (*Figure 3.17*).

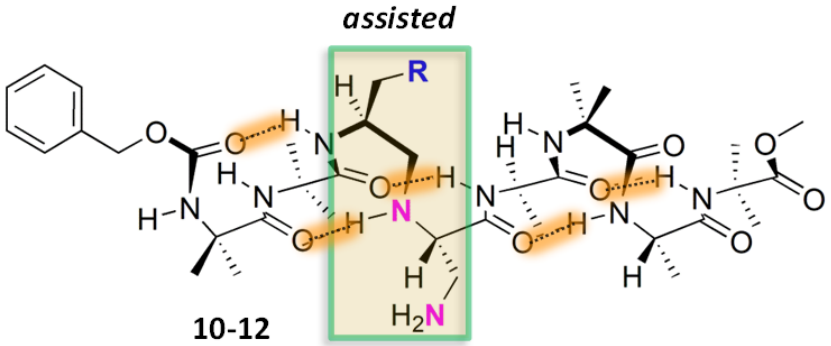

*Figure 3.17 Foldamers **10-12** with a variety of 3D catalytic centers. In addition to the primary and secondary amine, they also possess a R centre.*

These three foldamers are characterized by an identical length, an identical 3D-folding, while they differ each other for the chemical nature of the assisted chemical functionality introduced nearby the primary/secondary amines catalytic center *Figure 3.17* (See Experimental Section for its synthesis)

As a first example of chemical reactivity, we compared our foldamer performances to those recently published by Gellman and co-workers[10]. In their studies, well-folded foldamers were able to activate both ends of a linear dialdehyde precursor thus to oriented the reaction (via imine/enamine intermediate), therefore acting as a powerfully template for a ring closure through carbon-carbon bond formation.

We selected the linear dialdehydes showed in *Figure 3.18* (See Experimental section for details), as a precursor for cyclization.

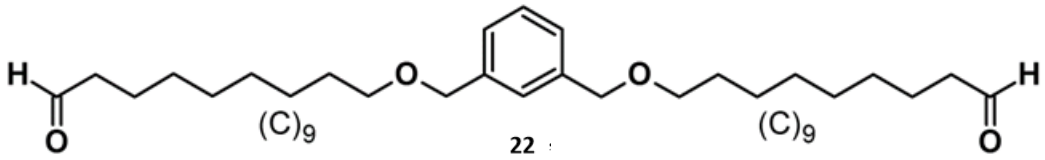

Figure 3.18 9-((3-(((9-oxononyl)oxy)methyl)benzyl)oxy)nonanal. Aldehyde chosen as a substrate for intramolecular aldol condensation reactions.

For its synthesis (**22**), we started with a nucleophilic substitution reaction (S_N1) to attach two nonane-1,9-diol (**18**) residues to a 1,3-bis(bromomethyl)benzene residue (*Figure 3.19(A)*). This first step already had complications due to the fact that we obtained the monosubstituted product preferentially, despite the fact that the reactions went for 48 hours and furthermore no efficient syntheses for this compound were reported in the literature. Having isolated the desired diol (**21**), through chromatographic column, we used DMP to selectively oxidize the two alcohols to aldehydes and obtain the desired product (**22**). (*Figures 3.19(B)*). DMP is a widely used oxidant since it is able to selectively oxidize alcohols to corresponding carbonic compound under neutral conditions[45].

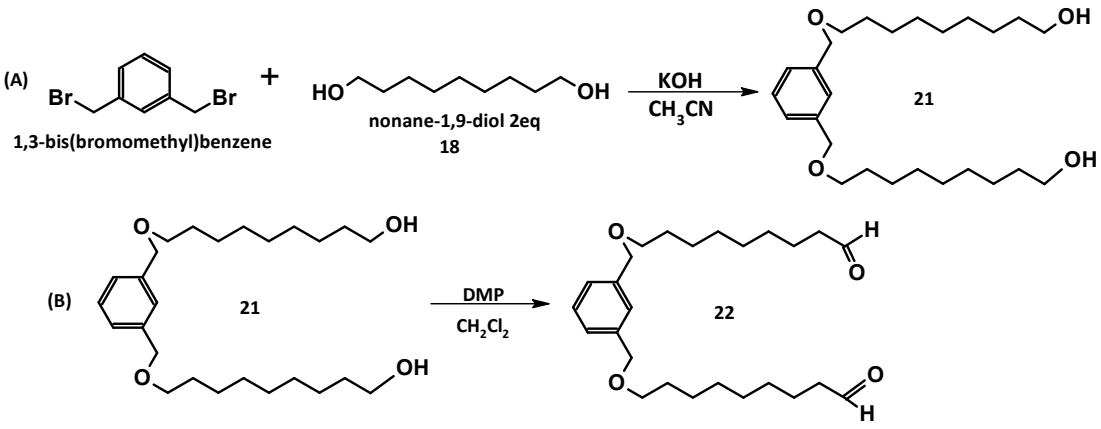

Figure 3.19 (A) Synthesis of diol (21) (B) Synthesis of aldehydes (22) with DMP oxidant

Having obtained the aldehyde, the aim was to do the cyclization reaction with the catalysts (**9-10-11-12**), so following the same conditions used by Gellman (See Experimental Section for more details) we performed the reaction with this substrate (**22**). (*Figure 3.20*)

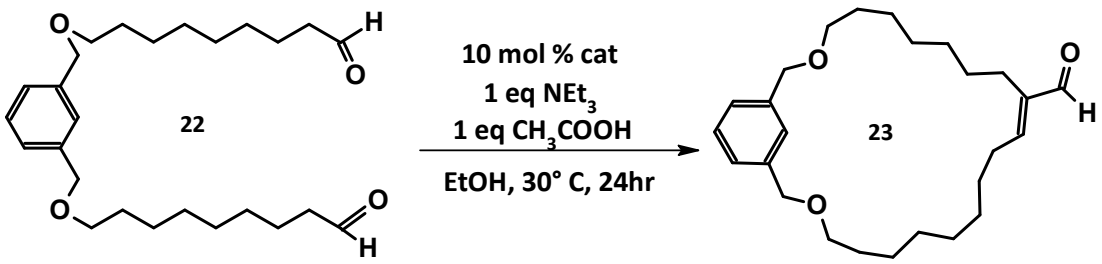

*Figure 3.20 Synthesis of compound (**23**) with Z-Aib-CH_2-NH-$(CH_2)_2$-NH_2 catalysts (**9-10-11-12**).*

All the reactions were run in ethanol, at 30 °C, 10 mM of substrate and 10% mol of each foldamer (See Experimental section for details). Reactions were checked by HPLC after 12 hours of reaction. Foldamer **9** and **10** which are different only for length (and contained an aliphatic side chain) displayed the same reactivity by archiving respectively 55 and 53% yield in the cyclic condensate product (*Figure 3.21*). Interestingly, foldamers **11** and **12** in the same reaction condition improved the yields up to 90 and 95 % respectively. Thus, the presence of a carboxylic group (Asp) or a hydroxyl group (Ser) seem to assist both the catalytic center to achieve a faster chemical conversion of the substrate.

In our opinion the two groups could participate to the catalysis, or stabilize the transition state by lowering its energy, or they could somehow stabilize the foldamer in the secondary structure more suitable for the catalysis.

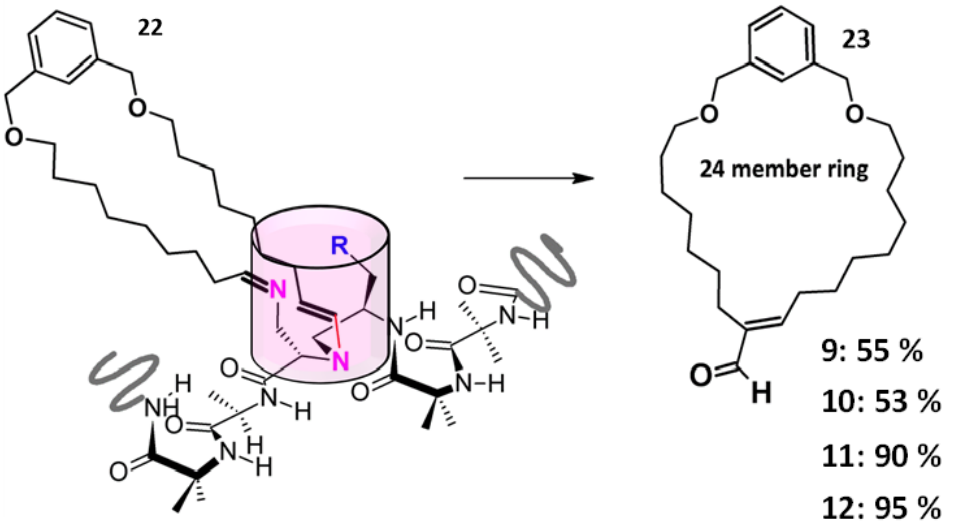

Figure 3.21 Intramolecular aldol reaction between aldehyde and foldamers ***9-10-11-12***

The reaction gave the desired cycle, an indication that the design performed until now was proper. The NMR analysis in *Figure 3.22* confirms these results. In fact, it is possible to see the triplet, corresponding to the proton of the double bond around 6.5 ppm, a typical zone where the protons of unsaturated aliphatic bonds (C=C) fall. Besides, the peak of the proton of the aldehyde and that of the proton of the double bond are 1:1, confirming once again that aldehyde has cyclized.

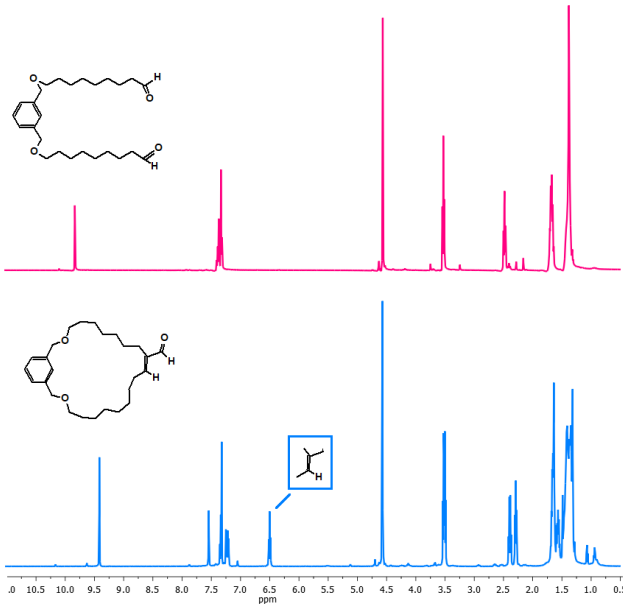

*Figure 3.22 NMR comparison of aldehyde (**22**) and its condensation product (**23**)*

The distance of the reaction centers was correct so that the aldehydes are at the optimal distance to have the cycle. The foldamer, since the structure is rigid, holds the aldehydes in a "blocked" position in order to condense in the desired cycle.

Thus, as a direct comparison with Gellman work, we can state that helical foldamer discussed in this work are much efficient and in the same time much easy to achieve.

3.4 Study on shorter catalytic system

After investigating the previously described foldamers, we used the same synthesis methods to produce smaller molecules, with the same catalytic centers, to see if they were able to do the same intramolecular reaction described above. In this way we were able to study the catalytic system itself with a less complex system.

Before proceeding with the cyclization reaction, we studied a generic aldol condensation reaction between an aromatic aldehyde, 4-nitrobenzaldehyde, and a ketone, cyclohexanone. The product (2,6-bis[(4-nitrophenyl)methylidene]cyclohexan-1-one), which served as a reference, was initially synthesized by basic catalysis using KOH (See Experimental section for its synthesis). (*Figure 3.23*)

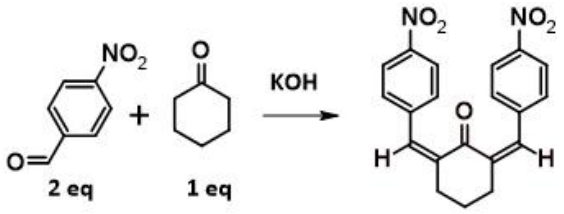

Figure 3.23 Aldol condensation reaction between 4-nitrobenzaldehyde and cyclohexanone via basic catalysis.

At this point we designed the first catalyst, to see if the reaction centers formed by the two amines, primary and secondary, were able to proceed in the above reaction. The new catalyst (**14**) is formed from a valine residue, whose amine is protected by a Boc, and ethylenediamine. The synthesis to obtain this catalyst follows the same procedure as that to obtain the catalytic center within foldamers: synthesis of Boc-Val-H (*Figure 3.24 (A)*) and coupling of Boc-Val-H with ethylenediamine (*Figure 3.24 (B)*).

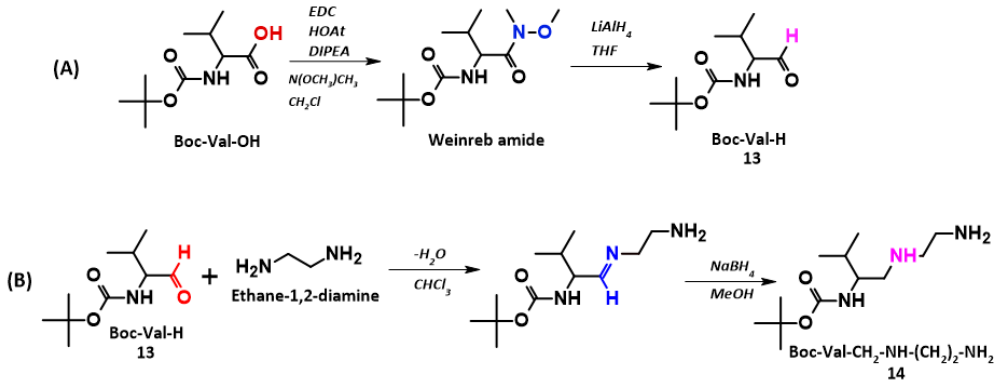

Figure 3.24 (A) synthesis of Boc-Val-H via Weinreb amide (B) synthesis of Boc-Val-CH_2-NH-$(CH_2)_2$-NH_2 via Shiff-base intermediate.

Boc-Val-CH_2-NH-$(CH_2)_2$-NH_2 (**14**) has the primary terminal amine two carbons away from the secondary, directly linked to Valine, and together they represent the reactive center of this molecule. The aldol condensation reaction between 4-nitrobenzaldines and cyclohexanone with this catalyst run in ethanol, at 30 °C, 10% mol of catalyst and in the presence of acetic acid and triethylamine (84 µl and 194 µl respectively) [44]. (*Figure 3.25*)

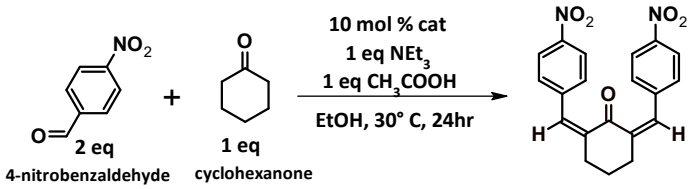

Figure 3.25 Generic conditions chosen for the aldol reaction

A hypothetical mechanism of the reaction with the catalyst (**14**) is presented in *Scheme 3.1.* The primary amine reacts as a nucleophile against the first aldehyde giving the corresponding imine (b). The ketone, on the other hand, reacts with the secondary amine forming the enamine (c). At this point we can have the nucleophilic attack of the enamine on the imine carbon forming a 7 cycle that will easily go to elimination (e). The hydrolysis of the charged imine will finally lead to restore the ketone and the catalytic sites, which will be able to perform a new catalytic cycle for the other aldehyde and the remaining free site of the ketone (f-g).

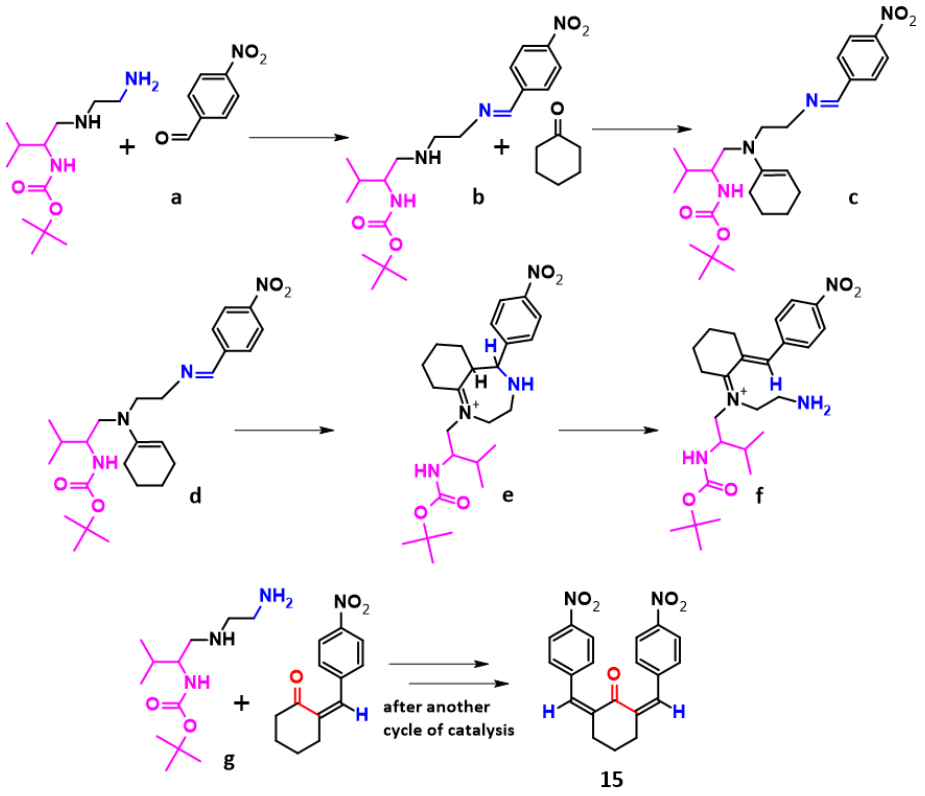

Scheme 3.1 Proposed mechanism of the Boc-Val-CH_2-NH-$(CH_2)_2$-NH_2-catalyzed aldol reaction.

We wondered whether the distance between the two amines was critical to the occurrence of the reaction. Therefore, we synthesized a new catalyst, Pro-NH-$(CH_2)_2$-NH_2 (**16**), composed this time of Proline and ethylenediamine (*Figure 3.26*). The synthesis was carried out by protecting the proline secondary amine with a Boc which, following coupling with ethylenediamine was then removed.

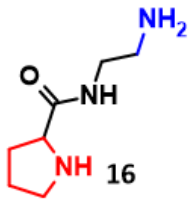

Figure 3.26 Pro-NH-$(CH_2)_2$-NH_2

In this case, compared to (**14**), the primary amine is not only two carbons away, but, in addition to these, there is also an amide group separating it from the secondary amine.

We performed the aldol condensation reaction under the same conditions as the previous one, but this time the conversion to product (**15**) was zero.

First of all, the distance between the two sites could affect the positioning of the aldehyde and ketone around the catalyst. Then, since the two sites are far apart and the number of bonds is high and the substrates are not rigid, they could be much free to rotate, making their approach unlikely.

Understanding which was the best distance between the two amines, we decided to proceed with intramolecular aldol condensation reaction, always taking example from those performed by Gellman et al.[10]

First, we synthesized a new catalyst (**17**). This time, after protecting the ethylenediamine with a Boc, we reacted it with a Z-Aib-H residue, following the usual procedures seen before with foldamers and catalyst (**14**) (see Experimental Section for more details). Finally, we unblocked the compound from the Boc and obtained the desired catalyst (**17**). (*Figure 3.27*)

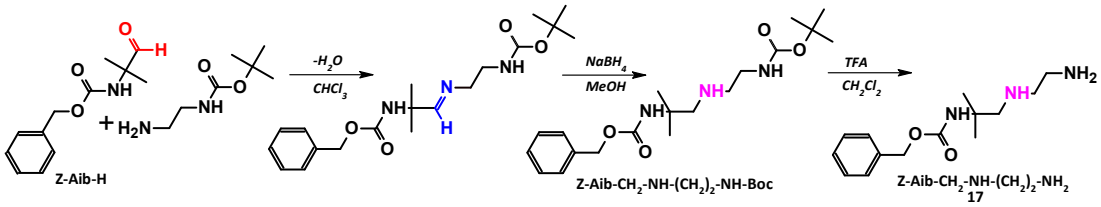

Figure 3.27 Synthesis of Z-Aib-CH_2-NH-$(CH_2)_2$-NH_2 via Shiff-base intermediate.

Once the catalyst was prepared, it was necessary to synthesize the substrate that would undergo the cyclization. For this reaction, nonanedial (**19**) was chosen which should have condensed leading to a macrocycle of 16 atoms. For its synthesis we started from its diol (**18**) (1,9-nonediol), which was converted to aldehyde thanks to Dess Martin periodinane (DMP) (*Figure 3.28*). (See Experimental Section for more details)

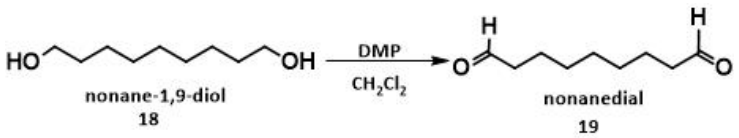

*Figure 3.28 Synthesis of nonanedial (**19**) with Dess Martin periodinane.*

After synthesizing all the components necessary for the condensation reaction, we performed it in ethanol, a 30° C, 10% mol of catalyst and in the presence of acetic acid and triethylamine.

There were two products that could be expected from this reaction. A first product is the cyclization one, in which two aldehydes should have condensed leading to a macro cycle of 16 atoms. A second reaction could have been the intermolecular reaction which would have led to the "polymerization" of aldehydes.

After 48 hours, the reaction was turned off and the product was isolated by chromatographic column. Unexpectedly, the reaction product was none of those expected. In fact, thanks to the mass spectrum we were able to deduce that three aldehydes had cyclized together leading to a macrocycle of 24 atoms (**20**). (*Figure 3.29*)

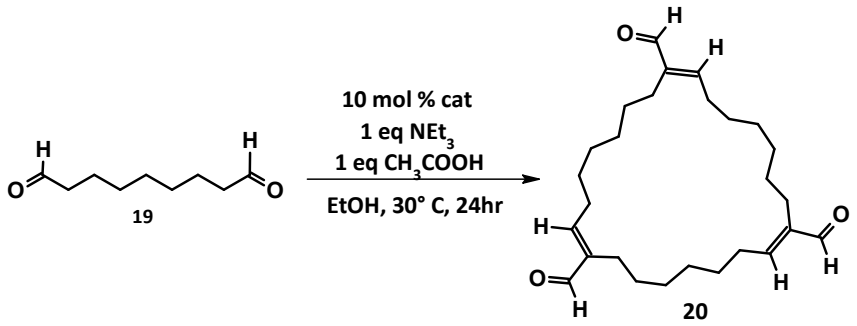

*Figure 3.29 Synthesis of compound (**20**) with Z-Aib-CH_2-NH-$(CH_2)_2$-NH_2 catalyst (**17**).*

The NMR analysis in *Figure 3.30* highlights the above results. First of all, it is possible to see the appearance of a multiplet corresponding to the proton of the double bond around 6.5 ppm, a typical zone where the protons of unsaturated aliphatic bonds (C=C) fall. Moreover, it can be deduced from this spectrum that the aldehyde has cyclized because the peak of the proton of the aldehyde and that of the proton of the double bond are 1:1, on the contrary if they had linear structure (*Figure 3.31*), they would be in 2:1 ratio.

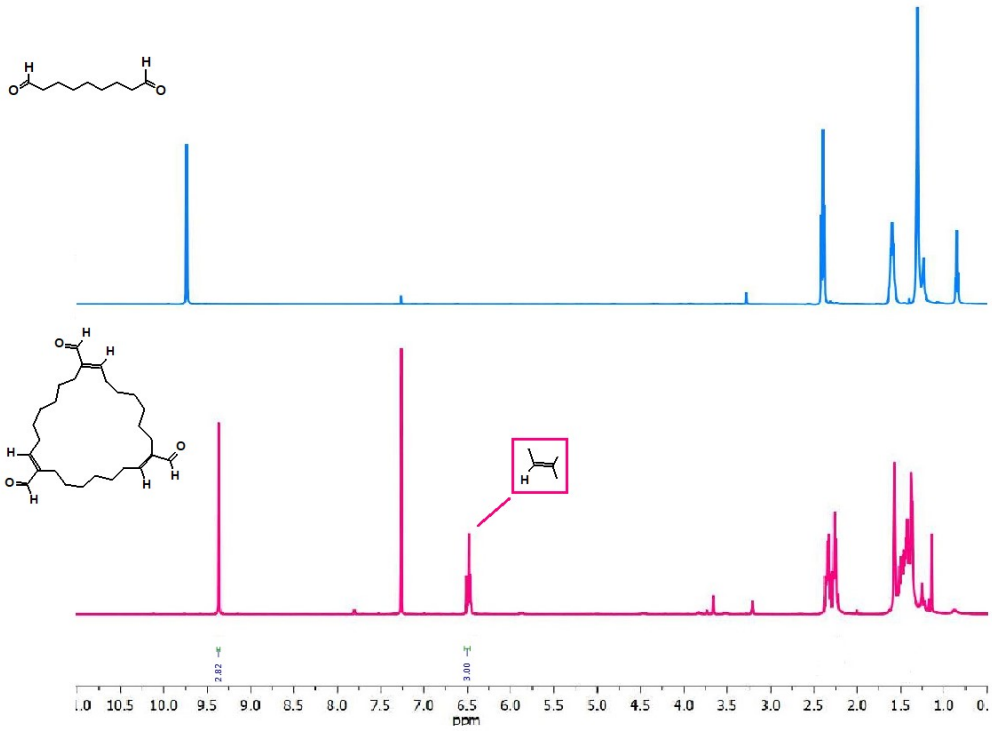

*Figure 3.30 NMR comparison of nonanedial (**19**) and its condensation product (**20**)*

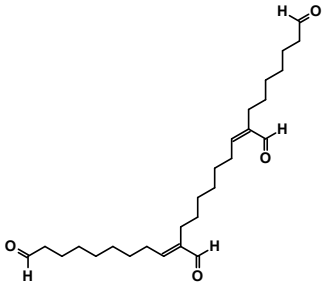

Figure 3.31 intermolecular aldol tri-adduct

4. EXPERIMENTAL SECTION

4.1 Materials and Methods

4.1.1. Reagents and solvents

Producer	Chemical
Merck (Darmstadt, Germania)	N,N-diisopropylethylamine (DIPEA)
	trifluoroacetic acid (TFA)
	triethylamine (TEA)
	L-amino acids methyl ester hydrochloride
	N-(3-Dimethylaminopropyl)-N′-ethylcarbodiimide hydrochloride (EDC·HCl)
	N,O-dimethylhydroxylamine hydrochloride
	lithium aluminum hydride ($LiAlH_4$)
	sodium cyanoborohydride ($NaCNBH_4$)
	4-chlorobenzylamine
	Boc-L-amino acids
	cyclohexanone
	4-nitrobenzaldehyde
	nonane-1,9-diol
	Dess-Martin periodinane

	bis(bromomethyl)benzene
	anthracene-9-carbaldehyde
	Potassium hydroxide (KOH)
GL Biochem (Shanghai)	1-hydroxy-7-aza-1,2,3-benzotriazole (HOAt)
Euriso-Top (St. Aubin, Francia)	DMSO-d_6
	$CDCl_3$
	$CDCN_3$

4.1.2. General Methods

Thin Layer Chromatography

The progress of the reactions is monitored with Thin Layer Chromatography (TLC), using silica gel 60 F254 plates (Merck). The separation of the different substances that make up the reaction mixture is possible thanks to the use of various eluents, or mixtures of several solvents (usually two) which suitably combined lead to the obtainment of solutions with different values of polarity. The plate, once eluted, may already show the stains of the compound if the latter presents a coloration. In case it is colorless, the compounds are highlighted by oxidation with an alcoholic solution of Phosphomolybdic Acid (PMA): for alcohols, phenols, alkenes, and many carbonyl compounds. Or, if unprotected amino groups are contained the detection can be done by developing the plate with a solution of ninhydrin in ethanol.

Flash chromatography

This technique was applied in the product purification steps. The stationary phase is constituted by a 60 Macherey-Nagel silica gel (particle size 40-63m); the eluent must be chosen carefully, so that it presents the right polarity; this feature allows to obtain a good separation of the chemical species present in the sample. The compound to be

1. Direct loading at the head of the column of the solubilized product in the minimum quantity of eluent;
2. Direct loading at the head of the column of the product solubilized in the minimum amount of solvent, other than the quantity of solvent, different from the eluent;
3. The product is solubilized in the minimum possible quantity of solvent and some silica is added to the solution thus obtained. Then the solvent is removed with the rotavapor, so that the product to be purified the product to be purified is adsorbed by the silica itself, which will then be loaded at the head of the column.

Mass Spectrometry

Mass spectra by electrospray ionization (ESI), collected in the positive mode, were performed on Perseptive Biosystem Mariner ESI-ToF5220 spectrometer (Foster City, CA).

Nuclear Magnetic Resonance

^{1}H NMR, ^{13}C NMR, and 2D-NMR spectra were recorded at 25°C on Bruker Avance400 or 500 MHz instruments. ^{1}H and ^{13}C spectra were referenced relative to the solvent residual peaks and chemical shifts (δ) reported in ppm downfield of tetramethylsilane ($CDCl_3$ δ H: 7.26 ppm, δ C: 77.16 ppm; CD_3CN δ H: 1.94 ppm; DMSO δ H: 2.50 ppm). The multiplicity of a signal is indicated as br, broad; s, singlet; d, doublet; t, triplet; m, multiplet.

High-Performance Liquid Chromatography.

The HPLC measurements were performed using an Agilent 1200 apparatus (Palo Alto, CA), equipped with a UV detector at various wavelength and a column Agilent extend-C18 (stationary phase). Eluants: A= 9:1 H_2O/CH_3CN, 0.05 % TFA; B= 1:9 H_2O/CH_3CN, 0.05 % TFA.

Melting point

Melting point of the compounds were determined using a Leitz Laborlux 12 microscope equipped with a Mavotherm 32 thermometer (sensor: NiCr-Ni thermocouple; resolution: 0.1 K; inherent deviation: 199°C ± 0.5% meas. val.).

4.2 Synthesis and Characterization of compounds

4.2.1 Synthesis of catalysts for the study of the catalytic system

Synthesis of Boc-Val-N(OCH_3)CH_3

Boc-Val-OH (3 g, 13.8 mmol) was dissolved in dry acetonitrile and HOAt (2.09 g, 15.1 mmol) and EDC·HCl (2.95 g, 15.1 mmol) were added. Then N,O-dimethylhydroxylamine hydrochloride (1.68 g, 17.2 mmol) was added to the reaction and DIPEA was used to reach basic pH. The reaction was allowed to stir at room temperature for 12 hours, then the solvent was removed under reduced pressure. The residue was dissolved in ethyl acetate, washed with $KHSO_4$ (5% aqueous solution) and $NaHCO_3$ (5% aqueous solution), dried over Na_2SO_4, filtered and concentrated.

Colorless solid, 72% yield, 2.58 g,

Synthesis of Boc-Val-CHO

Boc-Val-N(OCH_3)CH_3 (2.2 g, 8.45 mmol) was dissolved in dry tetrahydrofuran and $LiAlH_4$ (0.64 g, 16.8 mmol) was added. The reaction was followed by TLC. Once the reaction was over, $KHSO_4$ 5% was added dropwise to the reaction mixture, and ethyl acetate and brine were used to dilute the solution. The organic phase was separated, dried over Na_2SO_4, filtered and concentrated under reduced pressure. The crude aldehyde was obtained as a colorless oil.

Colorless Oil, 1.7 g, the product with impurities, has not been purified for this intermediate stage.

Synthesis of Boc-Val-CH_2-NH-$(CH_2)_2$-NH_2

Boc-Val-CHO (1.65 g, 8.21 mmol) was dissolved in dry MeOH. To this solution, ethylenediamine (5.48 ml, 82.1 mmol) and acetic acid (0.47 ml, 8.21 mmol) were added. After 30 minutes, $NaCNBH_3$ (0.77 g, 12.3 mmol) was dissolved in dry MeOH and added to the reaction. The mixture was stirred overnight at room temperature, then the solvent was removed under reduced pressure. The residue was dissolved in EtOAc and washed with Na_2CO_3 (5%) and brine, dried over anhydrous Na_2SO_4, filtered and concentrated. The compound was purified *via* flash chromatography using DCM/MeOH 8:2 as eluant.

Colorless solid, 48% yield, 0.96 g

^1H NMR (400 MHz, $CDCl_3$) δ 4.73 (d, 1H), 3.48 (s, 1H), 2.83-2.60 (m, 5H), 1.73 (s, 2H), 1.4 (s, 9H), 0.87 (t, 6H).

Synthesis of *tert*-butyl (2-aminoethyl) carbamate

Ethylenediamine (3.35 ml, 50 mmol) was dissolved in a solution 1:1 H_20/acetonitrile, in vigorous stirring and cooling with an ice bath. When the solution has cooled, drip a solution of Boc2O (3.5 g, 16 mmol) dissolved in acetonitrile. The mixture was stirred overnight at room temperature. The solution was separated in EtOAc, dried over anhydrous Na_2SO_4, filtered and concentrated. The compound was purified *via* flash chromatography using DCM/MeOH 95:5 as eluant.

Colorless solid, 51% yield, 1.29 g

^{1}H NMR (400 MHz, $CDCl_3$) δ 5.02 (s, 1H), 3.12 (q, 2H), 2.75 (t, 2H), 1.40 (s, 9H), 1.32 (s, 2H).

Synthesis of Z-Aib-N(OCH_3)CH_3

Z-Aib-OH (3 g, 12.6 mmol) was dissolved in dry dichloromethane and HOAt (1.71 g, 12.6 mmol) and EDC·HCl (2.4 g, 12.6 mmol) were added. Then N,O-dimethylhydroxylamine hydrochloride (2.45 g, 25.2 mmol) was added to the reaction and DIPEA was used to reach basic pH. The reaction was allowed to stir at room temperature overnight, then the solvent was removed under reduced pressure. The residue was dissolved in EtOAc, washed with $KHSO_4$ (5% aqueous solution) and $NaHCO_3$ (5% aqueous solution), dried over Na_2SO_4, filtered and concentrated.

Colorless solid, 66% yield, 7.13 mmol, 2.31 g

^{1}H NMR (400 MHz, $CDCl_3$) δ 7-36-7.30 (m, 5H), 5.78 (s, 1H), 5.09 (s, 2H), 3.61 (s, 3H), 3.19 (s, 3H), 1.61 (s, 6H)

Synthesis of Z-Aib-CHO

Z-Aib-N(OCH_3)CH_3 (1.5 g, 5.3 mmol) was dissolved in dry tetrahydrofuran and $LiAlH_4$ (0.40 g, 10.6 mmol) was added. The reaction was followed by TLC. Once the reaction was over, $KHSO_4$ 5% was added dropwise to the reaction mixture, and ethyl acetate and brine were used to dilute the solution. The organic phase was separated, dried over Na_2SO_4, filtered and concentrated under reduced pressure. The crude aldehyde was obtained as a colorless oil. The compound was purified *via* flash chromatography using DCM/MeOH 95:5 as eluant.

Colorless oil, 72% yield, 0.85 g, 3.8 mmol

^{1}H NMR (400 MHz, $CDCl_3$) δ 9.43 (s, 1H), 7-39-7.31 (m, 5H), 5.32 (s, 1H), 5.10 (s, 2H), 3.61 (s, 3H), 1.39 (s, 6H)

Synthesis of Z-Aib-CH_2-NH-$(CH_2)_2$-NH-Boc

Z-Aib-CHO (0.35 g, 1.58 mmol) was dissolved in dry MeOH. To this solution, *tert*-butyl (2-aminoethyl) carbamate (0.25 g, 1.58 mmol) and acetic acid (900 µl, 1.58 mmol) were added. After 30 minutes, $NaCNBH_3$ (0.2 g, 3.2 mmol) was dissolved in dry MeOH and added to the reaction. The mixture was stirred overnight at room temperature, then the solvent was removed under reduced pressure. The residue was dissolved in EtOAc and washed with Na_2CO_3 (5%) and brine, dried over anhydrous Na_2SO_4, filtered and concentrated. The compound was purified *via* flash chromatography using DCM/MeOH 95:5 as eluant.

Colorless solid, 39% yield, 0.22 g

^{1}H NMR (400 MHz, $CDCl_3$) δ 7-35-7.29 (m, 5H), 5.32 (s, 1H), 5.04 (s, 2H), 4.87 (s, 1H), 3.20-3.19 (d, 2H), 2.71 (t, 2H), 5.64(s, 2H), 1.42 (s, 9H),1.30 (s, 6H)

Synthesis of Z-Aib-CH_2-NH-$(CH_2)_2$-NH_2

The protected compound was dissolved in a TFA/DCM 1:1 (v/v) mixture and the removal of protecting groups was followed by TLC. At the end of the reaction, the solution was evaporated to dryness, the crude residue was dissolved in milliQ water and lyophilized.

4.2.2 Synthesis of aldehydes

Synthesis of nonanedial

nonane-1,9-diol (1.8 mmol, 0.288 g), was dissolved in 18 mL dichloromethane. Dess-Martin periodinane (4.7 mmol, 2 g) was then added all at once. The reaction mixture was stirred under N2 for 3 hours, at which point 20 mL diethyl ether was then added. The entire contents of the flask were combined with 30 mL saturated aqueous sodium bicarbonate containing 7.5 g sodium thiosulfate pentahydrate. The mixture was stirred vigorously for 1 hour at room temperature. The mixture was transferred to a separatory funnel and the organic layer was removed. The aqueous layer was extracted 2 times with 100 mL diethyl ether. All the organic layers were then combined and washed with

100 mL saturated aqueous sodium bicarbonate (2X), and brine (1X). The organic layers were then dried with sodium sulfate, filtered, and concentrated under vacuum. The light yellow oil obtained was purified *via* flash chromatography using hexane/ EtOAc 8:2 as eluant.

Colorless oil, 56% yield, 0.156 g

^{1}H NMR (400 MHz, $CDCl_3$) δ 9.73 (t, 1H), 2.42-2.38 (m, 4H), 1.60 (t, 4H), 1.30 (s, 6H).

Synthesis of 9-((3-(((9-hydroxynonyl)oxy)methyl)benzyl)oxy)nonan-1-o

Nonane-1,9-diol (3.8 mmol, 0.607 g), was dissolved in 20 mL of acetonitrile, then KOH was added (1.9 mmol, 0.106 g). In a beaker has been dissolved 1,3-bis(bromomethyl)benzene (1.9 mmol, 0.5 g) in 10 mL acetonitrile and the solution was then dripped into the reaction flask. The mixture was stirred for two days at room temperature, then the solvent was removed under reduced pressure.

The compound was purified *via* flash chromatography using DCM/MeOH 8:2 as eluant.

Colorless solid, 25% yield, 0.2 g

^{1}H NMR (400 MHz, $CDCl_3$) δ 7.36-7.26 (m, 4H), 4.58 (s, 4H), 3.36 (t, 4H), 3.49 (t, 4H), 1.67-1.56 (m, 8H), 1.55-1.36 (m, 22H)

Synthesis of 9-((3-(((9-oxononyl)oxy)methyl)benzyl)oxy)nonanal

9-((3-(((9-hydroxynonyl)oxy)methyl)benzyl)oxy)nonan-1-o (0.3 mmol, 0.128 g), was dissolved in 3 mL dichloromethane. Dess-Martin periodinane (0.75 mmol, 0.318 g) was then added all at once. The reaction mixture was stirred under N2 for 3 hours, at which point 3.5 mL diethyl ether was then added. The entire contents of the flask were combined with 5 mL saturated aqueous sodium bicarbonate containing 1.25 g sodium thiosulfate pentahydrate. The mixture was stirred vigorously for 1 hour at room temperature. The mixture was transferred to a separatory funnel and the organic layer was removed. The aqueous layer was extracted 2 times with 1 mL diethyl ether. All the organic layers were then combined and washed with saturated aqueous sodium bicarbonate (2X), and brine (1X). The organic layers were then dried with sodium sulfate, filtered, and concentrated under vacuum. The light-yellow oil obtained was purified *via* flash chromatography using hexane/ EtOAc 8:2 as eluant.

Colorless oil, 60% yield, 0.076 g

^{1}H NMR (400 MHz, $CDCl_3$) δ 9.78 (s, 2H), 7.36-7.27 (m, 4H), 4.52 (s, 4H), 3.48 (t, 4H), 2.44 (t,4H), 1.66-1.60 (m, 8H), 1.34 (s, 17H)

4.2.3 Synthesis of control substrate

Synthesis of 2,6-bis[(4-nitrophenyl)methylidene]cyclohexan-1-one

To a stirring solution of the cyclohexanone (0.5 g 5.1 mmol) and 4-nitrobenzaldehyde (1.54 g 10.2 mmol) in minimum amount of ethanol, solid KOH (0.014 g 0.25 mmol) was added. The reaction mixture was stirred at ambient temperature till the disappearance of the starting materials (TLC). The solid separated was filtered and washed with water and dried. The product, so-obtained, was crystallized with ethanol to give the desired compounds.

Yellow solid, 95% yield, 1.76 g,

4.2.4 Synthesis of foldamers

Synthesis of Boc-Val-NH-CH_2-Ph-Cl

Boc-Val-OH (1 g, 4.6 mmol) was dissolved in dry dichloromethane and HOAt (0.626 g, 4.6 mmol) and EDC·HCl (0.882 g, 4.6 mmol) were added. Then 4-chlorobenzylamine (1.303 g, 9.2 mmol) was added to the reaction and DIPEA was used to reach basic pH. The reaction was allowed to stir at room temperature for 12 hours, then the solvent was removed under reduced pressure. The residue was dissolved in ethyl acetate, washed with $KHSO_4$ (5% aqueous solution) and $NaHCO_3$ (5% aqueous solution), dried over Na_2SO_4, filtered and concentrated.

Colorless solid, 69% yield, 1.081 g, m.p. 96-98°C.

^{1}H NMR (400 MHz, $CDCl_3$) δ 7.21 (dd, J = 33.1, 8.3 Hz, 4H), 6.94 (s, 1H), 5.27 (d, J = 8.8 Hz, 1H), 4.36 (qd, J = 15.1, 5.9 Hz, 2H), 3.96 (t, J = 7.8 Hz, 1H), 2.17 – 2.05 (m, 1H), 1.40 (s, 9H), 0.94 (dd, J = 10.1, 6.9 Hz, 6H).

Synthesis of NH_2-Val-NH-CH_2-Ph-Cl

Boc-Val-NH-CH_2-Ph-Cl (1 g, 2.93 mmol) was dissolved in a TFA/dichloromethane (1:1) solution and removal of Boc- group was followed by TLC. After evaporation of

the solvent, the residue was dissolved in dichloromethane and washed with $NaHCO_3$ (5% aqueous solution), dried over Na_2SO_4, filtered and concentrated. The product was purified *via* flash chromatography (eluants: CH_2Cl_2/MeOH 9:1).

Colourless solid, 92% yield, 0.649 g, m.p. 96-98°C.

^{1}H NMR (400 MHz, $CDCl_3$) δ 7.73 (br, 1H), 7.31 (d, *J* = 8.4 Hz, 2H), 7.24 (d, *J* = 8.3 Hz, 2H), 4.44 (qd, *J* = 14.9, 6.1 Hz, 2H), 3.31 (d, *J* = 3.6 Hz, 1H), 2.45 – 2.31 (m, 1H), 1.43 (br, 2H), 1.01 (d, *J* = 7.0 Hz, 3H), 0.84 (d, *J* = 6.9 Hz, 3H).

^{13}C{^{1}H} NMR (101 MHz, $CDCl_3$) δ 174.4, 137.3, 133.1, 129.1, 128.7, 60.1, 42.4, 30.8, 19.7, 16.0.

General synthesis of Boc-(Ala-Aib)$_x$-COOH

2-Chlorotrityl chloride resin (1.6 mmol/g) was added to a vessel. The resin was swelled in DMF and then the first Fmoc-amino acid (2 eq. relative to the resin) was dissolved in DMF and DIPEA (4 eq. relative to the carboxylic acid) was added. This mixture was added to the resin and stirred for 2 h. At the end of this time, the mixture was filtered and the resin was washed with DMF, DCM and DMF. For successive couplings, a solution of the amino acid Fmoc-AA-OH (3 eq.), HATU (3 eq.), HOAt (2.7 eq) and DIPEA (6 eq.) in DMF was added to the resin and stirred for 1h and 30 minutes. The resin was filtered, and washed with DMF, DCM and DMF. Iterative cycles of Fmoc deprotection and coupling were carried out with 20% piperidine solution in DMF. Unreacted sites were capped by treatment with an 18:4:1 DMF/Ac_2O/DIPEA mixture for 20 minutes. For the last coupling, Boc-Ala-OH was used. Cleavage of the peptide sequence from the resin was performed with a mixture of hexafluoroisopropanol/DCM 1:4 (v/v); the filtrated was collected and evaporated under reduced pressure. The residue was triturated in cold Et_2O, centrifuged and lyophilized.

Boc-(Ala-Aib)$_2$-COOH

^{1}H NMR (400 MHz, $CDCl_3$) δ 8.00 (br, 1H), 7.65 (s, 1H), 7.63 (s, 1H), 7.40 (s, 1H), 5.96 (s, 1H), 4.40 – 4.26 (m, 1H), 4.00 – 3.84 (m, 1H), 1.55 (d, J = 9.8 Hz, 12H), 1.45 (s, 9H), 1.39 (dd, J = 17.5, 7.2 Hz, 6H).

Boc-(Ala-Aib)$_4$-COOH

^{1}H NMR (400 MHz, $CDCl_3$) δ 7.80 (d, 1H), 7.75 (s, 1H), 7.68 (d, 1H), 7.58 (t, 3H), 7.49 (d, 1H), 7.26 (s, 1H), 6.47 (s, 1H), 4.53(m, 1H), 3.39 (m, 2H), 3.83 (m, 1H), 1.62 (d, 6H), 1.57 (s, 3H), 1.52-1.42 (m, 34H), 1.35 (d, 3H)

$^{13}C\{^{1}H\}$ NMR (101 MHz, $CDCl_3$) δ 177.8 177.0, 175.8, 175.6, 175.0, 174.8, 173.8, 157.5, 90.9, 77.1, 87.4, 56.8, 56.5, 56.3, 53.4, 53.2, 52.9, 49.0, 28.4, 27.6, 27.0, 26.9, 25.4, 24.4, 23.0, 22.9, 22.7, 16.7, 16.6, 16.5.

MS (ESI-TOF): $[M+H]^+$ calc. for $C_{33}H_{58}N_8O_{11}$ = 743.8686 m/z; found = 743.4815 m/z.

General synthesis of Boc-(Ala-Aib)$_2$-N(OCH$_3$)CH$_3$

Boc-(Ala-Aib)$_2$-OH (1 eq.) was dissolved in dry dichloromethane and HOAt (1 eq.) and EDC·HCl (1eq) were added. Then N,O-dimethylhydroxylamine hydrochloride (2 eq.) was added to the reaction and DIPEA was used to reach basic pH. The reaction was allowed to stir at room temperature for 12 hours, then the solvent was removed under reduced pressure. The residue was dissolved in ethyl acetate, washed with $KHSO_4$ (5% aqueous solution) and $NaHCO_3$ (5% aqueous solution), dried over Na_2SO_4, filtered and concentrated.

Boc-(Ala-Aib)-N(OCH$_3$)CH$_3$

^{1}H NMR (400 MHz, $CDCl_3$) δ 7.2 (s, 1H), 5.16 (s, 1H), 4.12 (s, 1H), 3.67 (s, 3H), 3.19 (s, 3H), 1.41 (s, 9H), 1.31 (d, 3H)

$^{13}C\{^{1}H\}$ NMR (101 MHz, $CDCl_3$) δ 174.3, 171.2, 155.5, 77.2, 60.8, 57.5, 50.5, 34.0, 28.4, 23.3, 18.8

Boc-(Ala-Aib)$_2$-N(OCH$_3$)CH$_3$

Colorless solid, 87% yield, 0.478 g

^{1}H NMR (400 MHz, $CDCl_3$) δ 7.37 (s, 1H), 7.32 (d, J = 8.1 Hz, 1H), 6.70 (s, 1H), 5.39 (br, 1H), 4.55 – 4.41 (m, J = 7.3 Hz, 1H), 3.93 (dd, J = 7.1, 3.4 Hz, 1H), 3.68 (s, 3H), 3.23 (s, 3H), 1.59 (d, J = 3.7 Hz, 6H), 1.56 (s, 3H), 1.47 (s, 9H), 1.46 (s, 3H), 1.41 (t, J = 7.4 Hz, 6H).

$^{13}C\{^{1}H\}$ NMR (101 MHz, $CDCl_3$) δ 173.4, 173.2, 171.4, 156.6, 81.3, 60.6, 56.8, 56.6, 52.7, 49.3, 31.6, 28.2, 27.4, 25.0, 24.7, 23.8, 22.7, 17.8, 17.1, 14.1.

MS (ESI-TOF): $[M+Na]^+$ calc. for $C_{21}H_{39}N_5O_7$= 496.5534 m/z; found = 496.2739 m/z.

Boc-(Ala-Aib)$_4$-N(OCH$_3$)CH$_3$

Colorless solid, 92% yield, 0.97 g

^{1}H NMR (400 MHz, $CDCl_3$) δ 7.79 (s, 1H), 7.64 (s, 1H), 7.58 (s, 1H), 7.52-7.46 (m, 3H), 7.40 (d, 1H), 7.26 (s, 1H), 6.66 (s, 1H), 4.35 (t, 1H), 3.95 (m, 2H), 3.84 (d, 1H), 3.65 (s, 3H), 3.23 (s, 3H), 1.62-1.55 (m, 10H), 1.50-1.44 (m, 39H), 1.38 (d, 4H)

$^{13}C\{^{1}H\}$ NMR (101 MHz, $CDCl_3$) δ 176.7, 176.6, 176.5, 175.0, 174.7, 174.5, 172.5, 157.4, 80.6, 77.0, 60.5, 60.4, 56.8, 56.5, 56.3, 56.1, 55.5, 55.4, 52.8, 52.7, 49.9, 49.6, 31.5, 28.3, 27.3, 25.2, 23.2, 22.9, 17.5, 16.5, 14.2, 14.1.

General synthesis of Boc-(Ala-Aib)$_x$-CHO

Boc-(Ala-Aib)$_2$-N(OCH_3)CH_3 (1eq) was dissolved in dry tetrahydrofuran and $LiAlH_4$ (2eq) was added. The reaction was followed by TLC. Once the reaction was over, $KHSO_4$ 5% was added dropwise to the reaction mixture, and ethyl acetate and brine were used to dilute the solution. The organic phase was separated, dried over Na_2SO_4, filtered and concentrated under reduced pressure. The crude aldehyde was obtained as a colorless oil. The product was purified *via* flash chromatography (eluant: chloroform/methanol 97/3).

Boc-(Ala-Aib)-CHO

^{1}H NMR (400 MHz, $CDCl_3$) δ 9.36 (s, 1H), 6.84 (s, 1H), 5.06 (s,1H), 4.16 (s,1H), 1.44 (s, 9H), 1.35 (m, 9H)

Boc-(Ala-Aib)$_2$-CHO

Colorless solid, 96% yield, 0.334 g

^{1}H NMR (400 MHz, $CDCl_3$) δ 9.40 (s, 1H), 7.68 (s, 1H), 7.52 (d, J = 7.5 Hz, 1H), 6.93 (s, 1H), 5.88 (s, 1H), 4.63 – 4.20 (m, J = 7.4 Hz, 1H), 3.94 – 3.77 (m, 1H), 1.59 (s, 3H), 1.48 – 1.41 (m, 15H), 1.38 (d, J = 7.3 Hz, 3H), 1.36 (s, 3H), 1.33 (s, 3H).

$^{13}C\{^{1}H\}$ NMR (101 MHz, $CDCl_3$) δ 201.6, 174.0, 173.3, 156.9, 81.1, 59.2, 56.7, 53.2, 49.4, 28.4, 28.2, 27.7, 23.4, 21.4, 21.3, 17.3, 16.8.

MS (ESI-TOF): $[M+H]^+$ calc. for $C_{19}H_{34}N_4O_6$ = 415.5045m/z; found = 415.2534 m/z

Boc-(Ala-Aib)$_4$-CHO

Colorless solid, 90% yield, 0.382 g

^{1}H NMR (400 MHz, $CDCl_3$) δ 9.42 (s, 1H), 7.78 (d, 1H), 7.70 (s, 1H), 7.58 (m, 3H), 7.47 (d, 1H), 7.15 (s, 1H), 6.16 (s, 1H), 4.37 (m, 1H), 3.98 (m, 2H), 3.86 (m, 1H), 1.59 (s, 3H), 1.48 (m, 32H), 1.37 (9H)

$^{13}C\{^{1}H\}$ NMR (101 MHz, $CDCl_3$) δ 202.23, 176.9, 176.4, 175.3, 174.9, 174.5, 174.4, 174.0, 157.3, 81.2, 77.1, 59.3, 56.9, 56.6, 56.4, 53.4, 52.9, 52.8, 49.6, 28.4, 28.3, 27.7, 27.4, 27.2, 23.3, 23.0, 22.9, 21.5, 21.4, 17.3, 16.9, 16.6, 16.5.

MS (ESI-TOF): $[M+H]^+$ calc. for $C_{33}H_{58}N_8O_{10}$ = 727.8692 m/z; found = 727.4382 m/z.

Synthesis of Boc-(Ala-Aib)$_2$-COOMe

The peptide was synthetized following 2-Chlorotrityl chloride resin (1.6 mmol/g) was added to a vessel. The resin was swelled in DMF and then the first Fmoc-amino acid (2 eq. relative to the resin) was dissolved in DMF and DIPEA (4 eq. relative to the carboxylic acid) was added. This mixture was added to the resin and stirred for 2 h. At the end of this time, the mixture was filtered and the resin was washed with DMF, DCM and DMF. For successive couplings, a solution of the amino acid Fmoc-AA-OH (3 eq.), HATU (3 eq.), HOAt (2.7 eq) and DIPEA (6 eq.) in DMF was added to the resin and stirred for 1h and 30 minutes. The resin was filtered, and washed with DMF, DCM and DMF. Iterative cycles of Fmoc deprotection and coupling were carried out with 20% piperidine solution in DMF. Unreacted sites were capped by treatment with an 18:4:1 DMF/Ac_2O/DIPEA mixture for 20 minutes. For the last coupling, Boc-Ala-OH was used. Cleavage of the peptide sequence from the resin was performed with a mixture of DIPEA/MeOH/DMF 1:5:5 (v/v) stirring overnight; the filtrated was collected and evaporated under reduced pressure. The residue was triturated in cold Et_2O, centrifuged and lyophilized.

Synthesis of NH$_2$-(Ala-Aib)$_2$-COOMe

Boc-(Ala-Aib)$_2$-COOMe was dissolved in a TFA/DCM 1:1 (v/v) mixture and the removal of Boc- protecting group was followed by TLC. At the end of the reaction, the solution was evaporated to dryness, the crude residue was dissolved in DCM and washed with $NaHCO_3$ 5%. The organic phase was dried over Na_2SO_4, filtered and concentrated. The product was purified *via* flash chromatography (eluants: CH_2Cl_2/MeOH 9:1).

^{1}H NMR (400 MHz, $CDCl_3$) δ 7.85 (s, 1H), 7.26 (s, 1H), 6.76 (d, *J* = 8.0 Hz, 1H), 4.55 – 4.43 (m, *J* = 7.2 Hz, 1H), 3.73 (s, 3H), 3.50 (q, *J* = 6.9 Hz, 1H), 1.95 (br, 2H), 1.51 (s, 3H), 1.39 – 1.25 (m, 15H).

Synthesis of Boc-(Ala-Aib)$_4$-COOMe

Peptide Boc-(Ala-Aib)$_4$-COOMe was synthesized using standard solid phase 9-fluorenylmethoxycarbonyl (Fmoc) chemistry on a 2-chlorotrityl chloride resin. For each step, Fmoc deprotection was performed by mixing the resin in a piperidine/N,N-dimethylformamide (DMF) (2:8, *v/v*) solution for 10 minutes (2x), then washing with

DMF, MeOH and DCM. For all of the amino acid couplings we used the following protocol: 5.0 eq. (relative to the resin loading) of Fmoc-protected amino acid were activated externally with 4.9 eq. of O-Benzotriazole-N,N,N',N'-tetramethyluronium hexafluorophosphate (HBTU) and 10 eq. of diisopropylethylamine (DIPEA) in DMF (2.5 ml/mmol of amino acid). This mixture was then added to a peptide chamber containing the resin and mixed for 3 hours. The resin was then drained and rinsed with MeOH, and DCM, then allowed to dry. As a last coupling, Boc-Ala-OH (5.0 eq.) was used instead of Fmoc-amino acid residue. Cleavage of the peptide sequence from the resin was performed with a mixture of DIPEA/MeOH/DMF 1:5:5 (v/v) stirring overnight; the filtrated was collected and evaporated under reduced pressure. The residue was triturated in cold Et_2O, centrifuged and lyophilized.

^{1}H NMR (400 MHz, DMSO) δ 8.35 (s, 1H), 7.91 (d, *J* = 4.6 Hz, 1H), 7.73 (s, 1H), 7.61 (d, *J* = 5.7 Hz, 1H), 7.56 (s, 1H), 7.53 (s, 1H), 7.29 (d, *J* = 7.7 Hz, 1H), 7.16 (d, *J* = 4.9 Hz, 1H), 4.13 – 4.03 (m, 1H), 4.00 – 3.84 (m, 3H), 3.55 (s, *J* = 15.8 Hz, 3H), 1.44 – 1.33 (m, 33H), 1.30 (d, *J* = 7.2 Hz, 6H), 1.23 (d, *J* = 7.3 Hz, 6H).

^{13}C{^{1}H} NMR (101 MHz, DMSO) δ 176.2, 175.7, 174.7, 174.3, 174.2, 174.0, 173.7, 172.0, 156.4, 79.1, 56.4, 56.3, 56.1, 55.3, 52.2, 51.7, 51.2, 48.9, 28.6, 26.5, 26.3, 26.0, 25.2, 25.2, 24.6, 24.4, 24.0, 17.7, 17.6, 17.4, 17.2, 16.9.
MS (ESI-TOF): $[M+H]^+$ calc. for $C_{34}H_{60}N_8O_{11}$ = 757.8952 m/z; found = 757.4417 m/z

Synthesis of NH_2-(Ala-Aib)$_4$-COOMe

Boc-(Ala-Aib)$_4$-COOMe was dissolved in a TFA/DCM 1:1 (v/v) mixture and the removal of Boc- protecting group was followed by TLC. At the end of the reaction, the solution was evaporated to dryness, the crude residue was dissolved in DCM and washed with $NaHCO_3$ 5%. The organic phase was dried over Na_2SO_4, filtered and concentrated. The product was purified *via* flash chromatography (eluants: CH_2Cl_2/MeOH 9:1).

^{1}H NMR (400 MHz, DMSO) δ 8.15 (s, 1H), 7.77 (s 1H), 7.60 (m, 3H), 7.48 (s, 2H), 4.24 (t, 1H), 3.92 (m, 1H), 3.63 (s, 3H), 3.48 (t, 1H), 1.46-1.25 (m, 36H)

^{13}C{^{1}H} NMR (101 MHz, DMSO) δ 177.1, 176.9, 176.5, 175.5, 174.7, 174.4, 173.0, 56.8, 56.5, 56.2, 56.0, 55.9, 53.5, 52.9, 52.6, 52.2, 50.6, 49.9, 27.3, 27.0, 26.9, 25.1, 25.0, 23.5, 23.3, 22.9, 21.1, 17.2, 16.8, 16.5.
MS (ESI-TOF): $[M+H]^+$ calc. for $C_{34}H_{60}N_8O_{11}$ = 657.7794 m/z; found = 657.3962 m/z

General procedure for reductive amination

Peptide aldehyde (1 mmol) was dissolved in dry MeOH (15mL). The peptide with the amino component (1.5 eq) and $NaCNBH_3$ (2 eq.) dissolved in the minimum amount of MeOH were added to the solution sequentially. Acetic acid (2 eq.) was added to the reaction and the mixture was stirred for 2h at room temperature. Then, the solvent was removed under reduced pressure. The residue was dissolved in EtOAc and washed with Na_2CO_3 (5%) and brine, dried over anhydrous Na_2SO_4, filtered and concentrated. The peptide were purified *via* flash chromatography using DCM/MeOH as eluant.

Boc-(Ala-Aib)-CH_2-NH-(Ala-Aib)-COOMe

^{1}H NMR (400 MHz, $CDCl_3$) δ 7.66 (s, 1H), 6.33 (s, 1H), 5.09 (d, 1H), 4.01 (t, 1H), 3.72 (s, 3H), 3.10-3.05 (m, 1H) 2.95 (d, 1H), 2.50 (d, 1H), 1.54 (d, 6H), 1.43 (s, 10 H), 1.34-1.27 (m, 13H)

Boc-(Ala-Aib)$_2$-CH_2-NH-(Ala-Aib)$_2$-COOMe

^{1}H NMR (400 MHz, $CDCl_3$) δ 7.28 (s, 1H), 7.75 (d, 2H), 7.46 (s, 1H), 6.72 (d,2H), 5.5 (s, 1H), 4.48 (t, 1H), 3.93 (m, 2H), 3.94 (s, 3H), 3.41 (d, 1H), 2.38 (s, 1H), 1.53-1.34 (m, 47 H)

Boc-(Ala-Aib)$_4$-CH_2-NH-(Ala-Aib)$_4$-COOMe

White solid, 81 %, g 0.174

^{1}H NMR (400 MHz, $CDCl_3$) δ 8.69 (s,1H), 8.30 (s,1H), 7.73 (d, 2H), 7.64 (d, 1H), 7.57-7.44 (m, 8H), 6.99 (s.1H), 6.8 (s, 1H), 5.84 (s, 1H), 4.02-3.99 (m, 6H), 3.68 (s,3H), 3.51-3.47 (m, 2H), 3.13 (d,1H), 2.38 (d,1H), 1.55-1.34 (m, 83H)

Synthesis of Z-Aib$_2$-Ser$^{(tBu)}$-CHO

Peptide Z-Aib$_2$-Ser$^{(tBu)}$-CHO was synthesized using standard solid phase 9-fluorenylmethoxycarbonyl (Fmoc) chemistry on a Weinreb AM (N-Fmoc- N-methoxy-β-alanine) resin. Following removal of the Fmoc- group with 20% piperidine in DMF, the addition of the first amino acid (5 eq. relative to the resin loading) was achieved with HATU (5 eq. relative to resin loading) in DMF. DIPEA (10 eq. relative to the resin loading) was added immediately and the mixture was stirred for 3 hr. The resin was then drained and rinsed with MeOH, and DCM, then allowed to dry. For all of the amino acid couplings the following protocol was used: 5.0 eq. (relative to the resin loading) of Fmoc-protected amino acid activated externally with 4.9 eq. of

HATU and 10 eq. of DIPEA in DMF (2.5 ml/mmol of amino acid). This mixture was then added to a peptide chamber containing the resin and mixed for 3 hours. The resin was then drained and rinsed with MeOH, and DCM, then allowed to dry. Removal of the Fmoc- group was performed with 20% piperidine in DMF. As a last coupling, Z-Aib-OH (5.0 eq.) was used instead of Fmoc-amino acid residue. For the reductive cleavage of the peptide sequence, the resin was swollen in THF, flushed with nitrogen and cooled to 0 °C. LiAlH4 (11 eq.) was added portion wise, and the mixture was allowed to stir for 3 h. The mixture was again cooled to 0 °C and diluted with EtOAc. The mixture was then quenched with saturated Rochelle's salt solution and allowed to stir for 15 min to ensure quenching. The mixture was then filtered and the resulting filtrate was extracted three times using EtOAc. The combined EtOAc fractions were concentrated in vacuo to yield the desired peptide aldehyde.

Synthesis of Z-Aib$_2$-Asp$^{(OtBu)}$-CHO

Peptide Z-Aib$_2$-Asp$^{(OtBu)}$-CHO was synthesized using standard solid phase 9-fluorenylmethoxycarbonyl (Fmoc) chemistry on a Weinreb AM (N-Fmoc- N-methoxy-β-alanine) resin. Following removal of the Fmoc- group with 20% piperidine in DMF, the addition of the first amino acid (5 eq. relative to the resin loading) was achieved with HATU (5 eq. relative to resin loading) in DMF. DIPEA (10 eq. relative to the resin loading) was added immediately and the mixture was stirred for 3 hr. The resin was then drained and rinsed with MeOH, and DCM, then allowed to dry. For all of the amino acid couplings the following protocol was used: 5.0 eq. (relative to the resin loading) of Fmoc-protected amino acid activated externally with 4.9 eq. of HATU and 10 eq. of DIPEA in DMF (2.5 ml/mmol of amino acid). This mixture was then added to a peptide chamber containing the resin and mixed for 3 hours. The resin was then drained and rinsed with MeOH, and DCM, then allowed to dry. Removal of the Fmoc- group was performed with 20% piperidine in DMF. As a last coupling, Z-Aib-OH (5.0 eq.) was used instead of Fmoc-amino acid residue. For the reductive cleavage of the peptide sequence, the resin was swollen in THF, flushed with nitrogen and cooled to 0 °C. LiAlH4 (11 eq.) was added portion wise, and the mixture was allowed to stir for 3 h. The mixture was again cooled to 0 °C and diluted with EtOAc. The mixture was then quenched with saturated Rochelle's salt solution and allowed to stir for 15 min to ensure quenching. The mixture was then filtered and the resulting

filtrate was extracted three times using EtOAc. The combined EtOAc fractions were concentrated in vacuo to yield the desired peptide aldehyde.

Synthesis of Z-DAP$^{(Boc)}$-(Ala-Aib)$_2$-COOMe

Boc-(Ala-Aib)$_2$-COOMe (0.5 g, 1.12 mmol) was dissolved in a TFA/DCM 1:1 (v/v) mixture and the removal of Boc- protecting group was followed by TLC. At the end of the reaction, the solution was evaporated to dryness, the crude residue was dissolved in DCM and washed with $NaHCO_3$ 5%. The organic phase was dried over Na_2SO_4, filtered and concentrated. The product was used for the coupling reaction with Z-DAP$^{(Boc)}$-OH (N_α-Z-N_β-Boc-L-2,3-diaminopropionic acid, 0.57 g, 1.7 mmol), previously activated by means of HOAt (0.23 g, 1.7 mmol) and EDC·HCl (0.32 g, 1.7 mmol) in dry DCM. NH_2-(Ala-Aib)$_2$-COOMe in dry DCM was added to the active ester and DIPEA was used to reach basic pH. The reaction was allowed to stir at room temperature for 12 hours, then the solvent was removed under reduced pressure. The residue was dissolved in ethyl acetate, washed with $KHSO_4$ (5% aqueous solution) and $NaHCO_3$ (5% aqueous solution), dried over Na_2SO_4, filtered and concentrated.

Synthesis of NH$_2$-DAP$^{(Boc)}$-(Ala-Aib)$_2$-COOMe

Z-DAP$^{(Boc)}$-(Ala-Aib)$_2$-COOMe (1 g, 1.5 mmol) was dissolved in MeOH (30 ml, 0.05 M) under nitrogen atmosphere. Palladium on carbon (0.016 g, 0.15 mmol) was added and the reaction was stirred for 1 hr under nitrogen atmosphere. The reaction was followed by TLC. The solution was filtered on celite and the solvent was evaporated under reduced pressure to give the free amino-peptide as a colourless oil.

Synthesis of Z-Aib$_2$-Ser$^{(tBu)}$-CH$_2$-NH-DAP$^{(Boc)}$-(Ala-Aib)$_2$-COOMe

Z-Aib$_2$-Ser$^{(tBu)}$-CHO (0.254 g, 0.56 mmol) was dissolved in dry MeOH. To this solution, NH_2-DAP$^{(Boc)}$-(Ala-Aib)$_2$-COOMe (0.3 g, 0.56 mmol) and acetic acid (33 μl, 0.56 mmol) were added. After 30 minutes, $NaCNBH_3$ (0.071 g, 1.12 mmol) was dissolved in dry MeOH and added to the reaction. The mixture was stirred overnight at room temperature, then the solvent was removed under reduced pressure. The residue was dissolved in EtOAc and washed with Na_2CO_3 (5%) and brine, dried over anhydrous Na_2SO_4, filtered and concentrated. The peptide was purified *via* flash chromatography using DCM/MeOH 95:5 as eluant.

Synthesis of Z-Aib$_2$-Asp$^{(tBu)}$-CH$_2$-NH-DAP$^{(Boc)}$-(Ala-Aib)$_2$-COOMe

Z-Aib$_2$-Asp$^{(OtBu)}$-CHO (0.27 g, 0.56 mmol) was dissolved in dry MeOH. To this solution, NH$_2$-DAP$^{(Boc)}$-(Ala-Aib)$_2$-COOMe (0.3 g, 0.56 mmol) and acetic acid (33 µl, 0.56 mmol) were added. After 30 minutes, $NaCNBH_3$ (0.071 g, 1.12 mmol) was dissolved in dry MeOH and added to the reaction. The mixture was stirred overnight at room temperature, then the solvent was removed under reduced pressure. The residue was dissolved in EtOAc and washed with Na_2CO_3 (5%) and brine, dried over anhydrous Na_2SO_4, filtered and concentrated. The peptide was purified *via* flash chromatography using DCM/MeOH 95:5 as eluant.

General procedure for reductive amination

Peptide aldehyde (1 mmol) was dissolved in dry MeOH (15mL). The amino component (1.5 eq) and $NaCNBH_3$ (2 eq.) dissolved in the minimum amount of MeOH were added to the solution sequentially. Acetic acid (2 eq.) was added to the reaction and the mixture was stirred for 2h at room temperature. Then, the solvent was removed under reduced pressure. The residue was dissolved in EtOAc and washed with Na_2CO_3 (5%) and brine, dried over anhydrous Na_2SO_4, filtered and concentrated. The peptide were purified *via* flash chromatography using DCM/MeOH as eluant.

Z-Aib$_2$-Ser$^{(tBu)}$-CH$_2$-NH-DAP$^{(Boc)}$-(Ala-Aib)$_2$-COOMe

Z-Aib$_2$-Asp$^{(tBu)}$-CH$_2$-NH-DAP$^{(Boc)}$-(Ala-Aib)$_2$-COOMe

Z-Aib$_2$-Val-CH$_2$-NH-DAP$^{(Boc)}$-(Ala-Aib)$_2$-COOMe

Z-(AlaAib)$_2$-CH$_2$-NH-DAP$^{(Boc)}$-(Ala-Aib)$_2$-COOMe

General procedure for foldamer deprotection

The protected peptide was dissolved in a TFA/DCM 1:1 (v/v) mixture and the removal of protecting groups was followed by HPLC. At the end of the reaction, the solution was evaporated to dryness, the crude residue was dissolved in milliQ water and lyophilized.

Z-Aib$_2$-Ser-CH$_2$-NH-DAP-(Ala-Aib)$_2$-COOMe

Z-Aib$_2$-Asp-CH$_2$-NH-DAP-(Ala-Aib)$_2$-COOMe

Z-Aib$_2$-Val-CH$_2$-NH-DAP-(Ala-Aib)$_2$-COOMe

Z-(AlaAib)$_2$-CH$_2$-NH-DAP-(Ala-Aib)$_2$-COOMe

4.2.5 Synthesis products of aldol condensation reaction

General Procedure for aldol reaction

Di-aldehyde (1mmol) was dissolved EtOH (or if it use aldehyde and ketone 2mmol e 1mmol respectively). To this solution, catalyst (10%mol) acetic acid (2mmol) and triethylamine (2mmol) were added. The mixture was stirred for 48 hours at 30°C, then the solvent was removed under reduced pressure. The compound was purified *via* flash chromatography.

Cyclohexanone and **4-nitrobenzaldehyde** with **Boc-Val-CH_2-NH-$(CH_2)_2$-NH_2**
Yellow solid, 76%, 0.19 g

^{1}H NMR (400 MHz, $CDCl_3$) δ 8.27 (d, 4H), 7.80 (s, 2H), 7.59 (d, 4H), 2.94 (t, 4H), (m, 2H).

Nonanedial with **Z-Aib-CH_2-NH-$(CH_2)_2$-NH_2**

Colorless oil, 66% yield, 0.105g

^{1}H NMR (400 MHz, $CDCl_3$) δ 9.37 (s, 3H), 6.50-6.45 (m, 3H), 2.38-2.33 (m, 6H), 2.31-2.23 (m, 6H), 1.53-1.27 (m, 24H).

The mass spectrum is of the oxidized aldehyde

MS (ESI-TOF): $[M+H]^+$ calc. for $C_{27}H_{42}O_6$ = 463.6268 m/z; found = 463.3541 m/z

9-((3-(((9-oxononyl)oxy)methyl)benzyl)oxy)nonanal with **Z-Aib-CH_2-NH-$(CH_2)_2$-NH_2**

Colorless oil, 83% yield, 0.052g

^{1}H NMR (400 MHz, $CDCl_3$) δ 9.38 (s, 1H), 7.51-7.17 (m, 4H), 6.46 (t, 4H), 3.48(q, 4H), 2.36 (q, 2H), 2.25 (t, 2H), 1.64-1.60 (m,7H), 1.45-1.28 (m, 21H)

4.2.6 Compound Spectra

Boc-Val-CH_2-NH-$(CH_2)_2$-NH_2

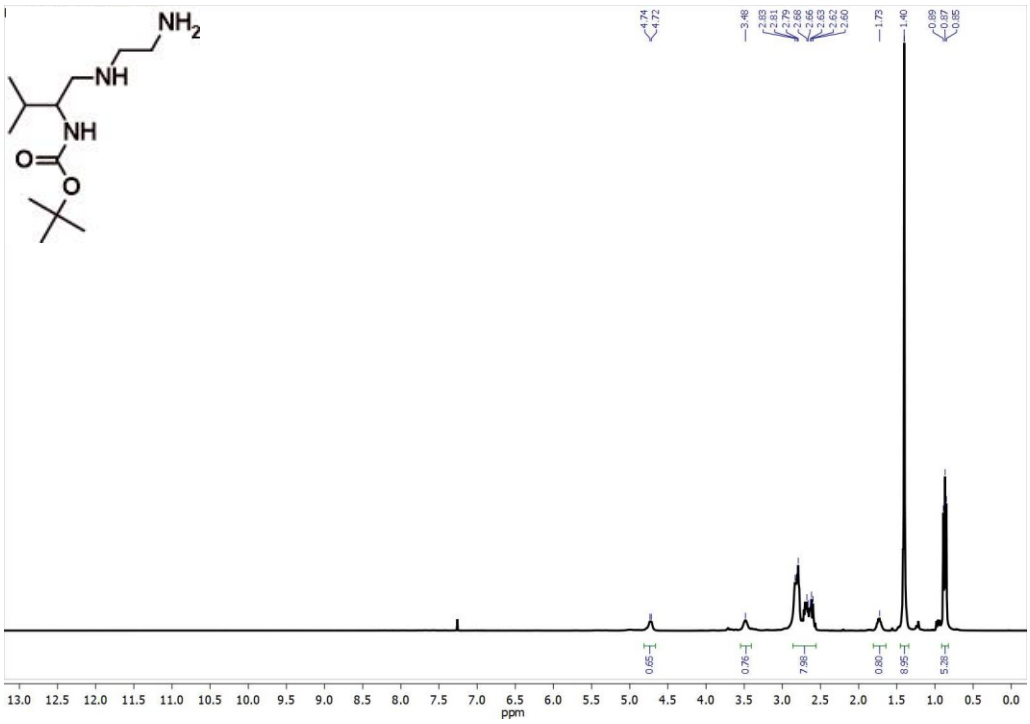

Figure 4.1 ^1H NMR (400 MHz, $CDCl_3$) of Boc-Val-CH_2-NH-$(CH_2)_2$-NH_2

***tert*-butyl (2-aminoethyl) carbamate**

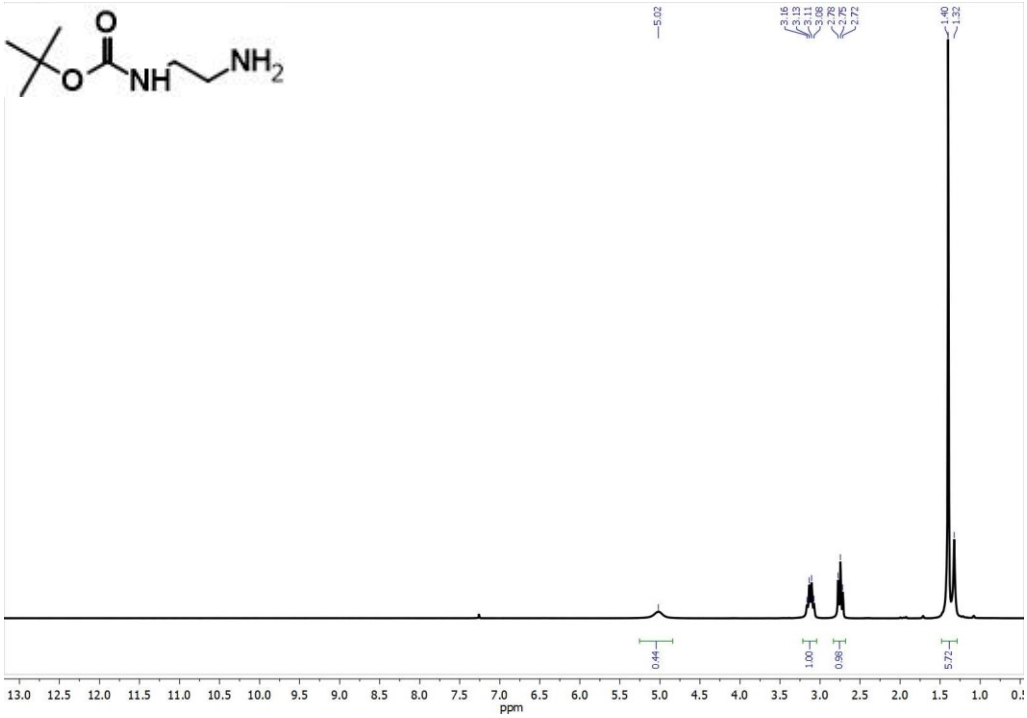

Figure 4.2 ^1H NMR (400 MHz, $CDCl_3$) of tert-butyl (2-aminoethyl) carbamate

Z-Aib-N(OCH₃)CH₃

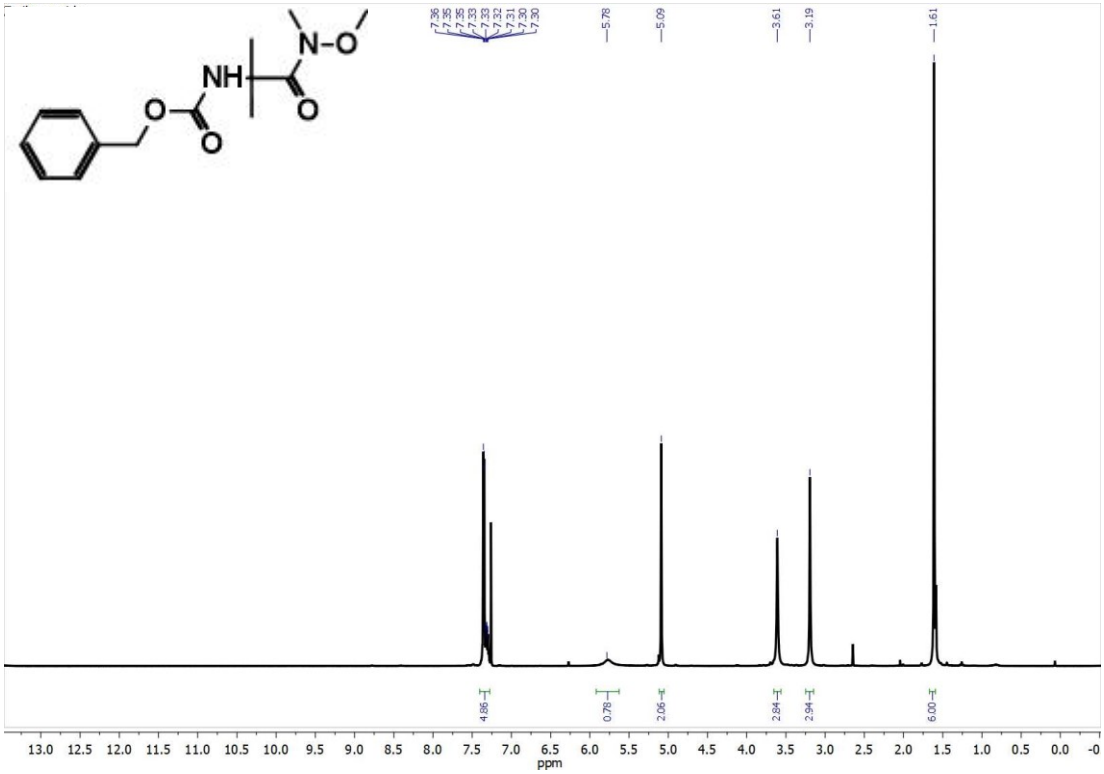

Figure 4.3 ^{1}H NMR (400 MHz, $CDCl_3$) of Z -Aib-N(OCH₃)CH₃

Z -Aib-CHO

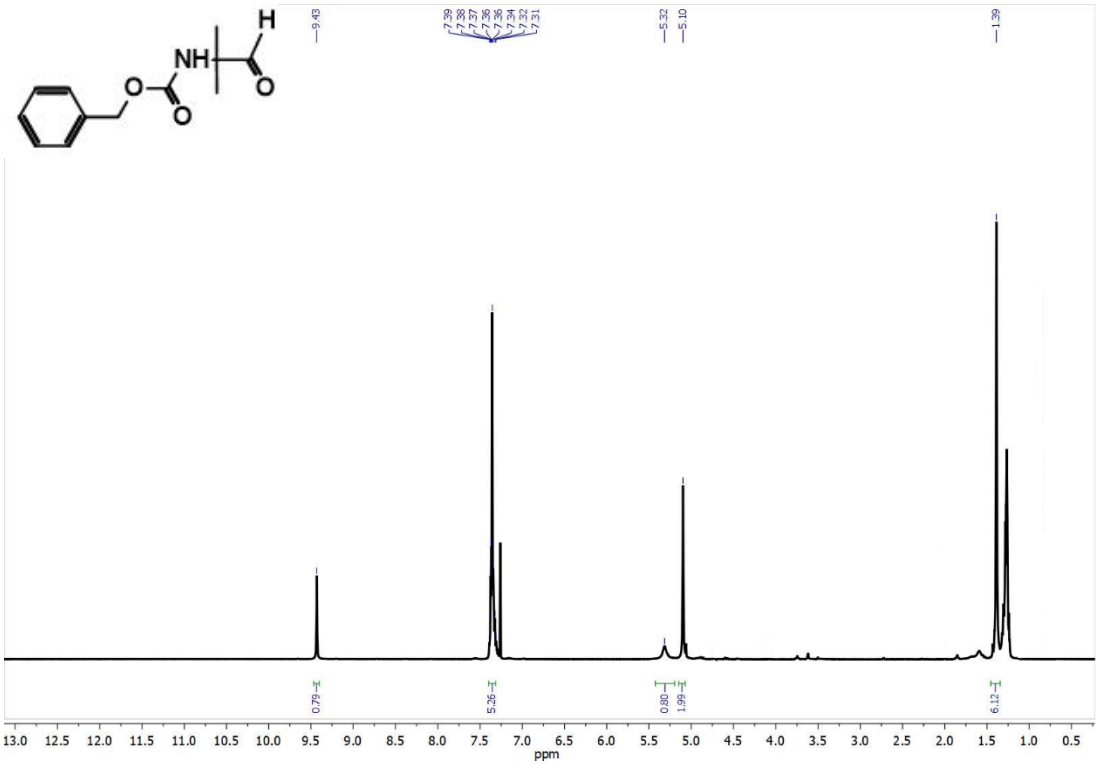

Figure 4.4 ^{1}H NMR (400 MHz, $CDCl_3$) of Z -Aib-CHO

Z-Aib-CH_2-NH-$(CH_2)_2$-NH-Boc

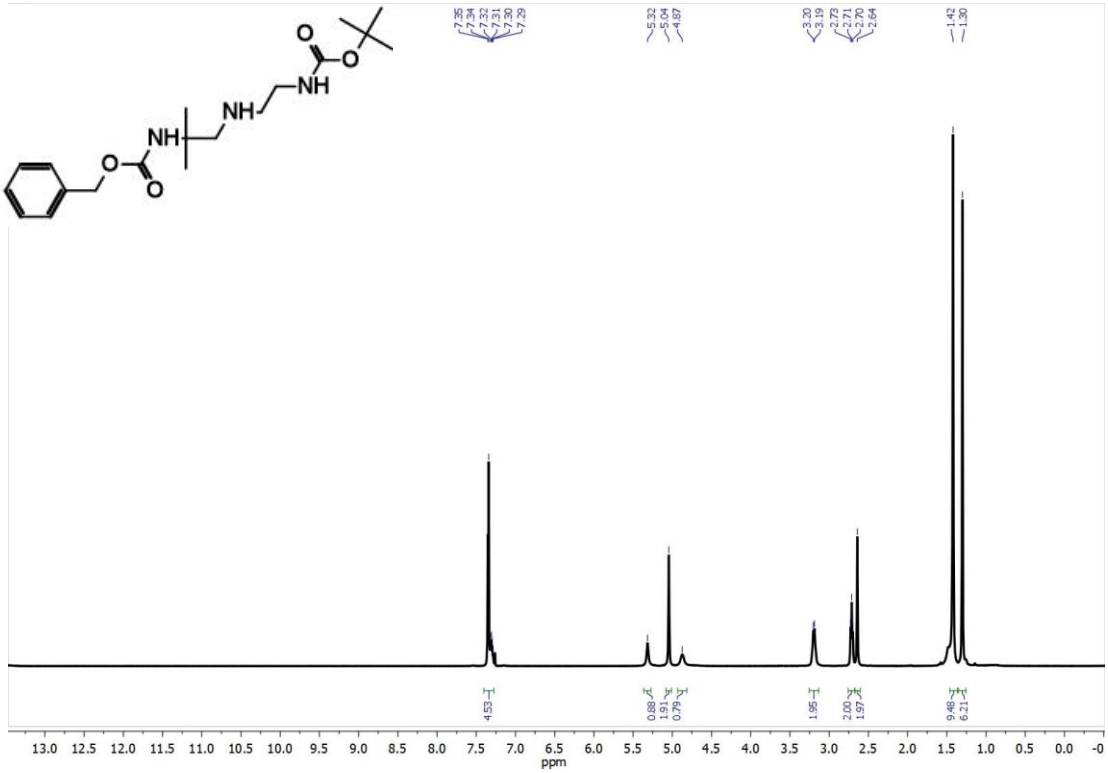

Figure 4.5 ^1H NMR (400 MHz, $CDCl_3$) of Z -Aib-monoboc

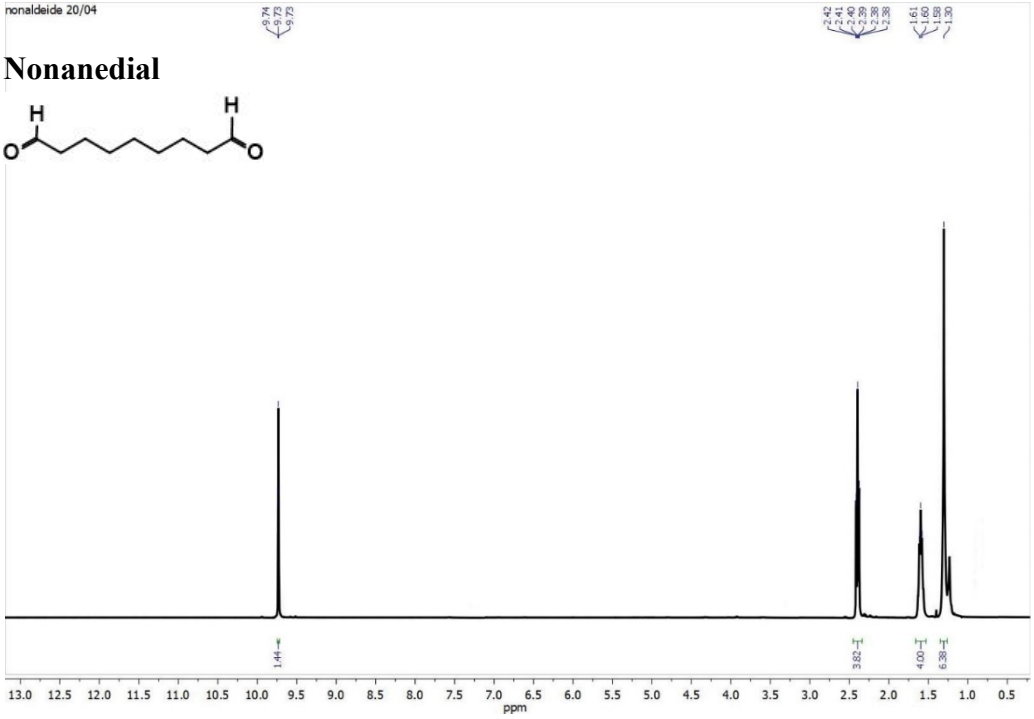

Figure 4.6 ^1H NMR (400 MHz, $CDCl_3$) of Nonanedial

9-((3-(((9-hydroxynonyl)oxy)methyl)benzyl)oxy)nonan-1-o

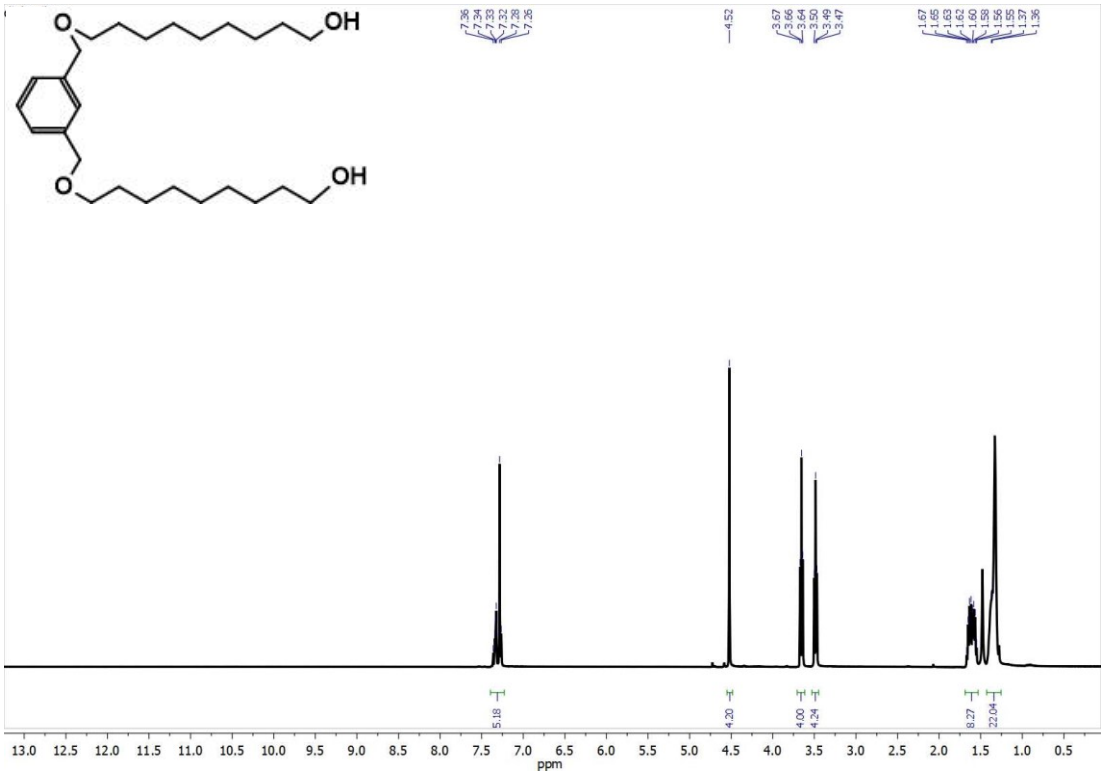

Figure 4.7 ^{1}H NMR (400 MHz, $CDCl_3$) of 9-((3-(((9-hydroxynonyl)oxy)methyl)benzyl)oxy)nonan-1-o

Synthesis of 9-((3-(((9-oxononyl)oxy)methyl)benzyl)oxy)nonanal

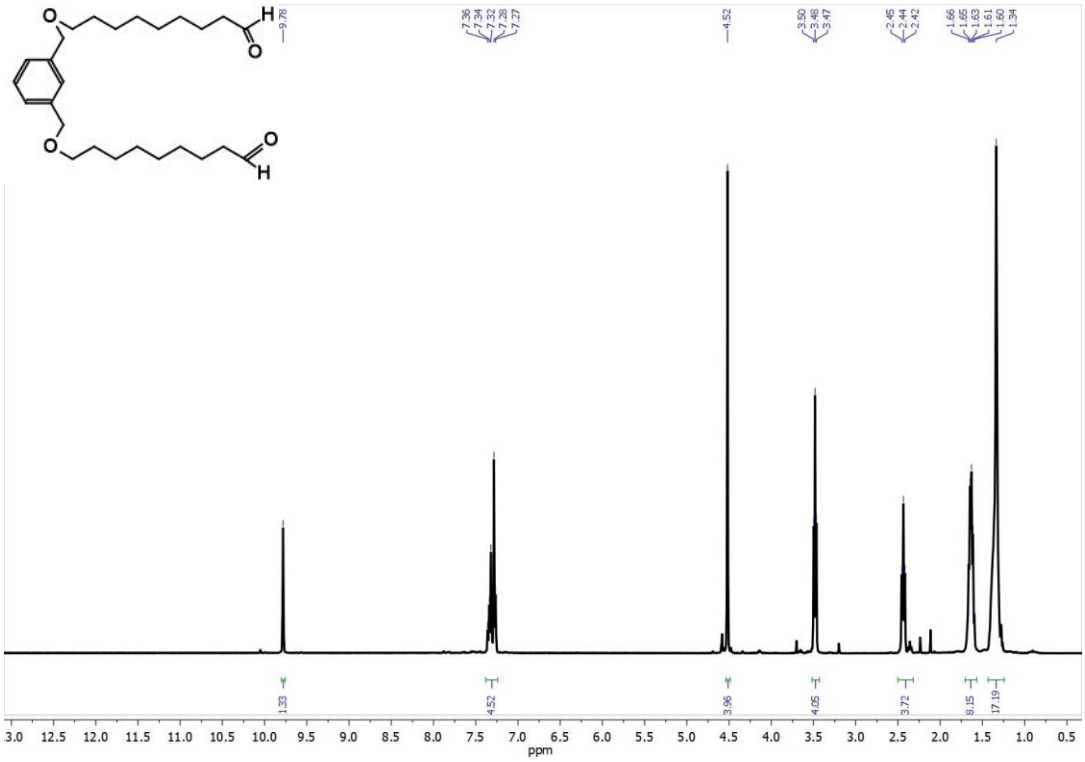

Figure 4.7 ^{1}H NMR (400 MHz, $CDCl_3$) of 9-((3-(((9-oxononyl)oxy)methyl)benzyl)oxy)nonanal

2,6-bis[(4-nitrophenyl)methylidene]cyclohexan-1-one

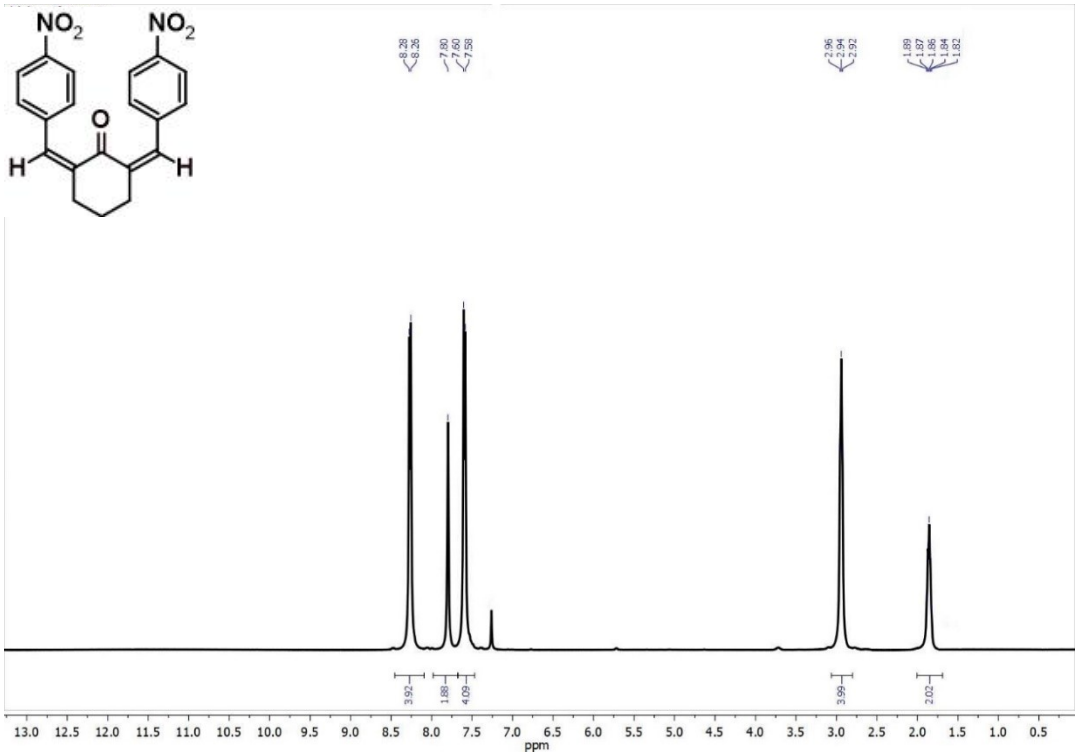

Figure 4.8 ^{1}H NMR (400 MHz, $CDCl_3$) of 2,6-bis[(4-nitrophenyl)methylidene]cyclohexan-1-one

Boc-(Ala-Aib)-N(OCH_3)CH_3

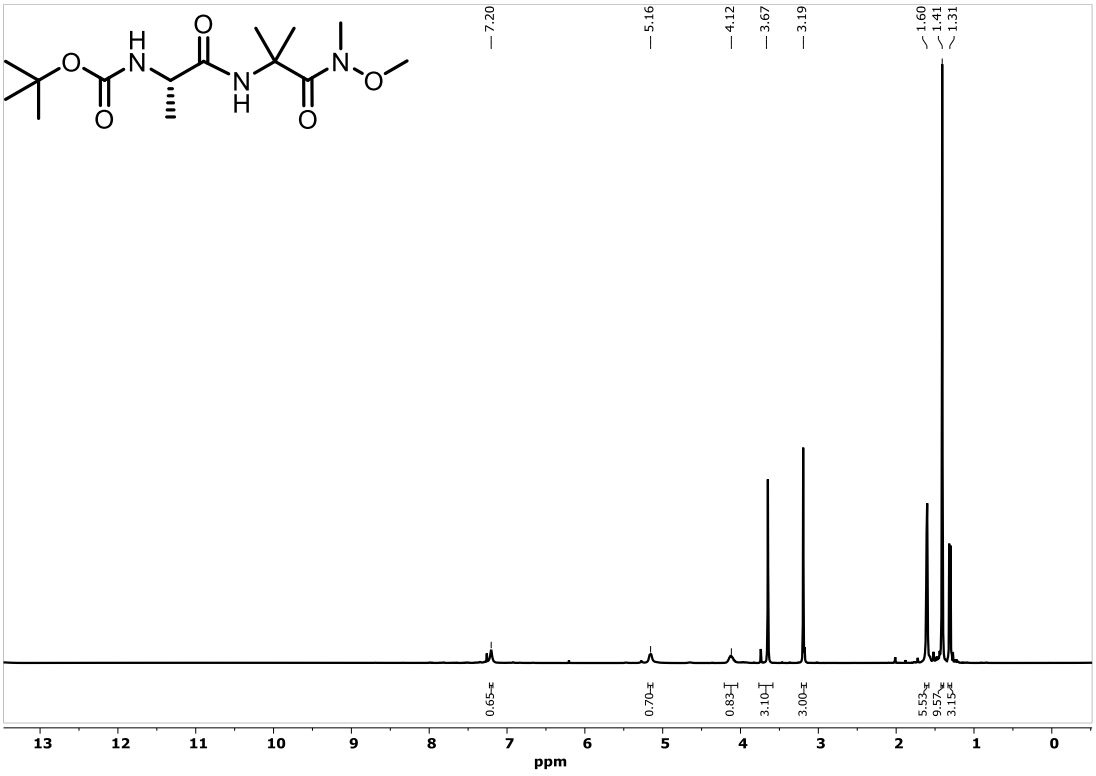

Figure 4.9 ^{1}H NMR (400 MHz, $CDCl_3$) of Boc-Ala-Aib-N(OCH_3)CH_3

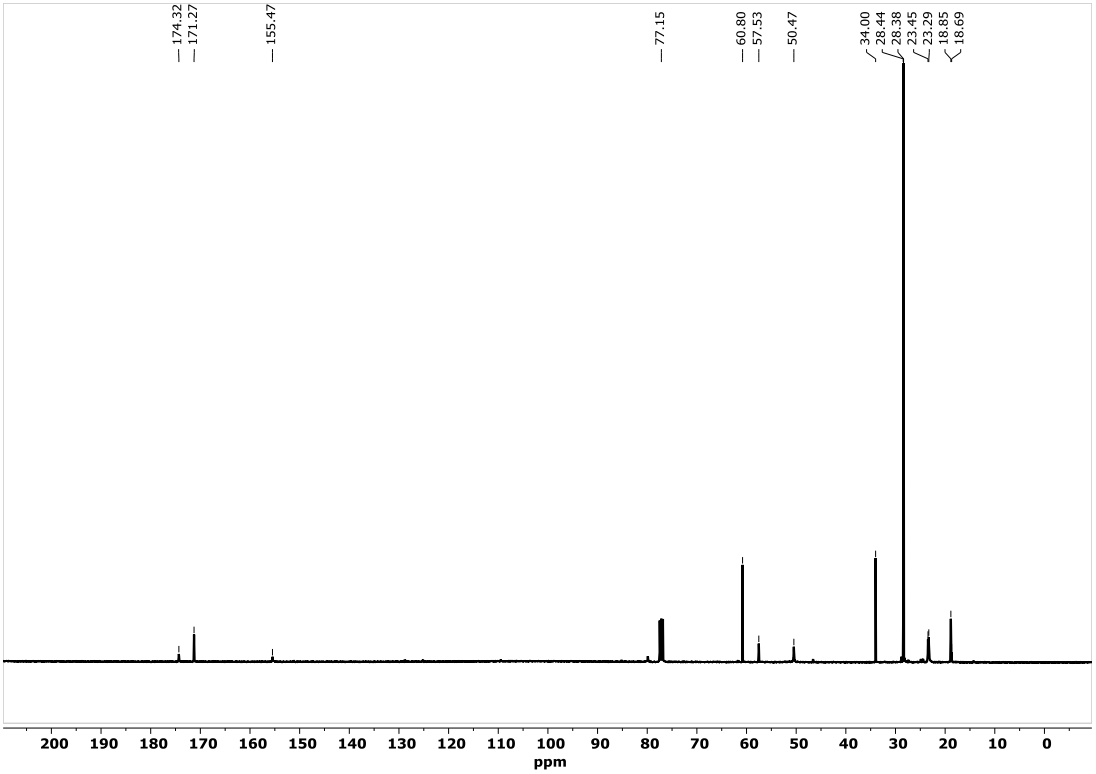

Figure 4.10 ^{13}C NMR (101 MHz, $CDCl_3$) of Boc-Ala-Aib-N(OCH_3)CH_3

Boc-(Ala-Aib)-CHO

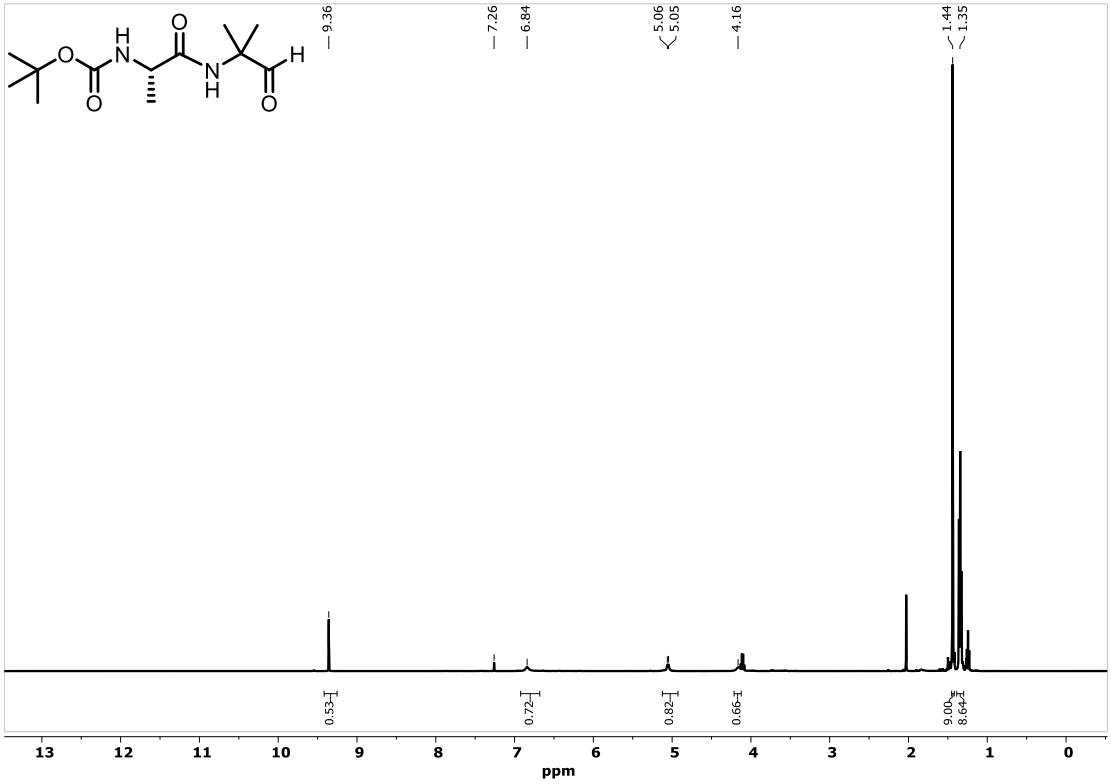

Figure 4.11 ^{1}H NMR (400 MHz, $CDCl_3$) of Boc-Ala-Aib-CHO

Boc-(Ala-Aib)$_2$-COOH

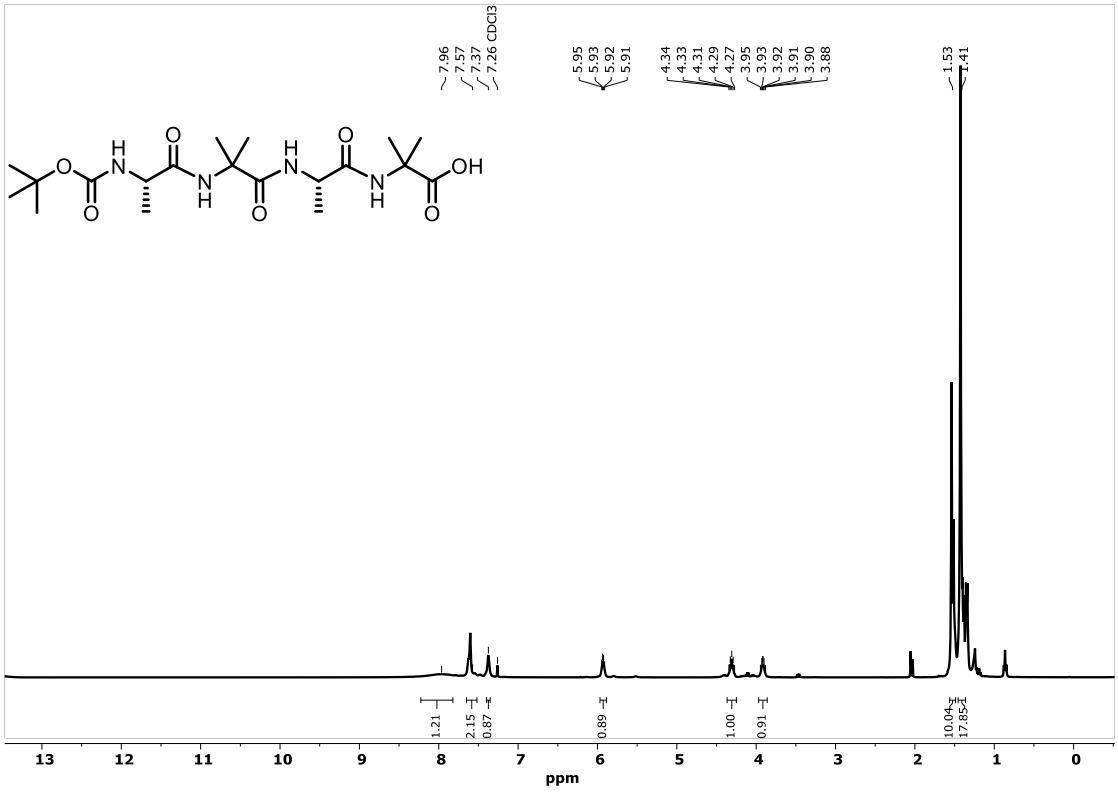

Figure 4.12 ^{1}H NMR (400 MHz, $CDCl_3$) of (Boc-Ala-Aib)$_2$-COOH

Boc-(Ala-Aib)$_2$-N(OCH$_3$)CH$_3$

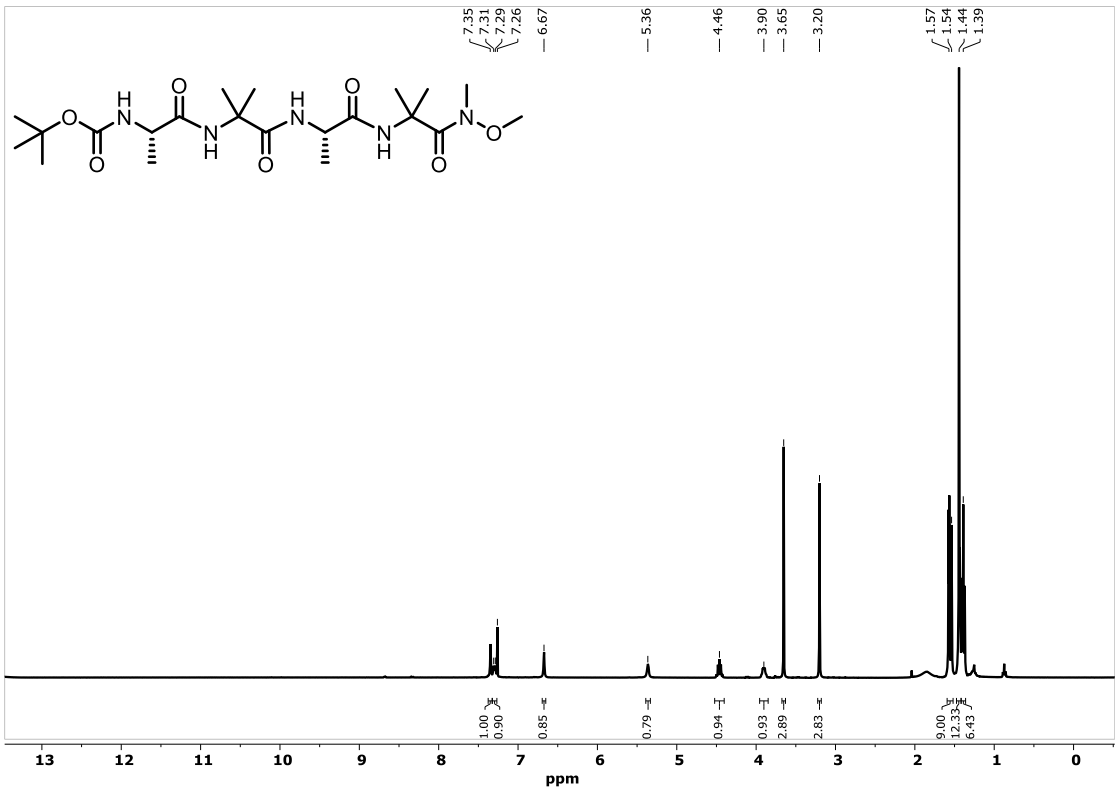

Figure 4.13 ^{1}H NMR (400 MHz, $CDCl_3$) of (Boc-Ala-Aib)$_2$-N(OCH$_3$)CH$_3$

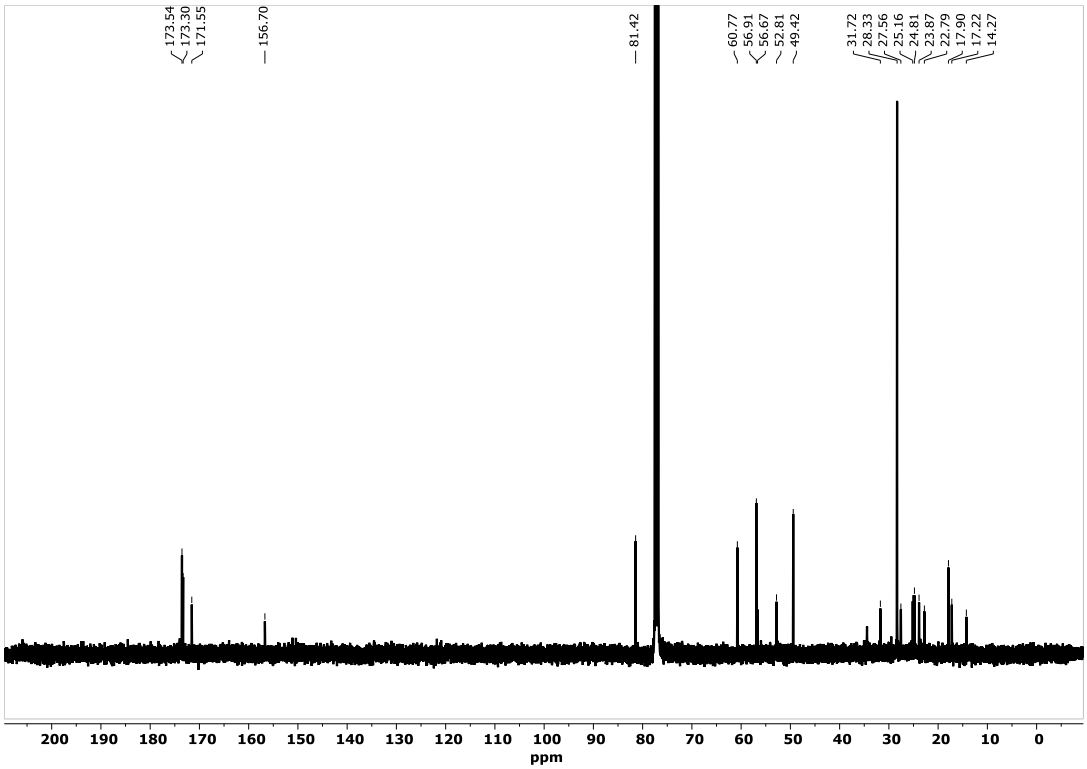

Figure 4.14 ^{13}C NMR (101 MHz, $CDCl_3$) of Boc-(Ala-Aib)$_2$-N(OCH$_3$)CH$_3$

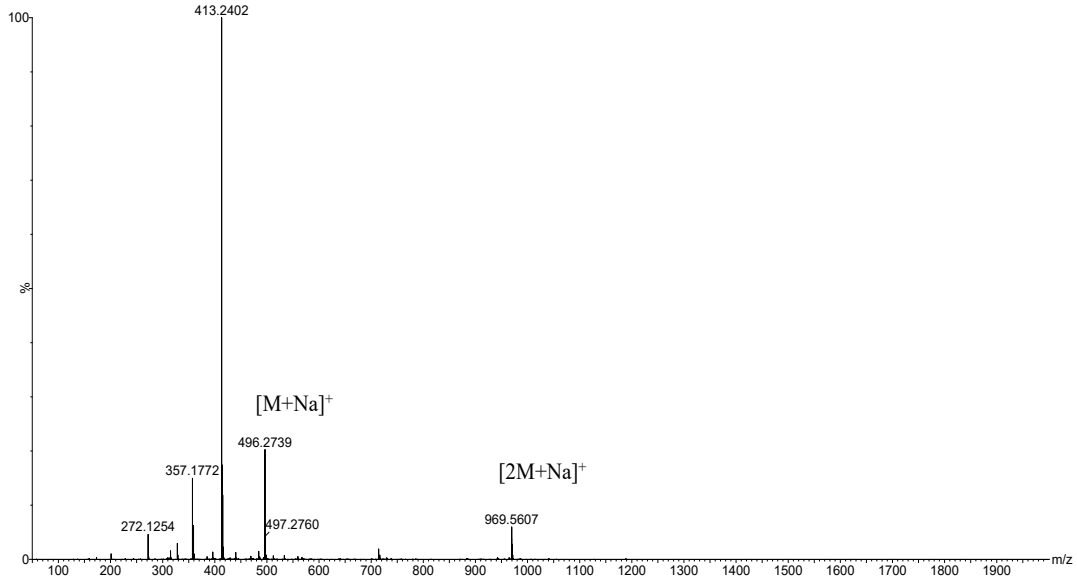

Figure 4.15 MS spectra Boc-(Ala-Aib)$_2$-N(OCH$_3$)CH$_3$

Boc-(Ala-Aib)$_2$-CHO

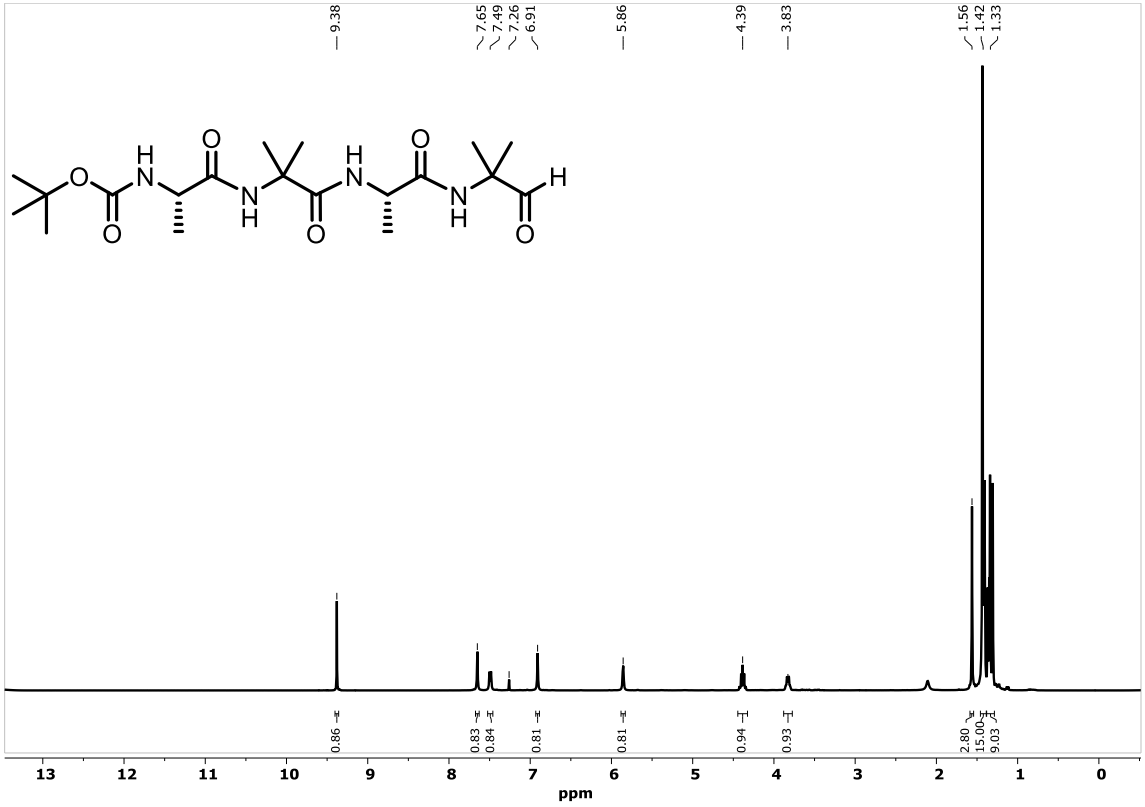

Figure 4.16 ^{1}H NMR (400 MHz, $CDCl_3$) of Boc-(Ala-Aib)$_2$-CHO

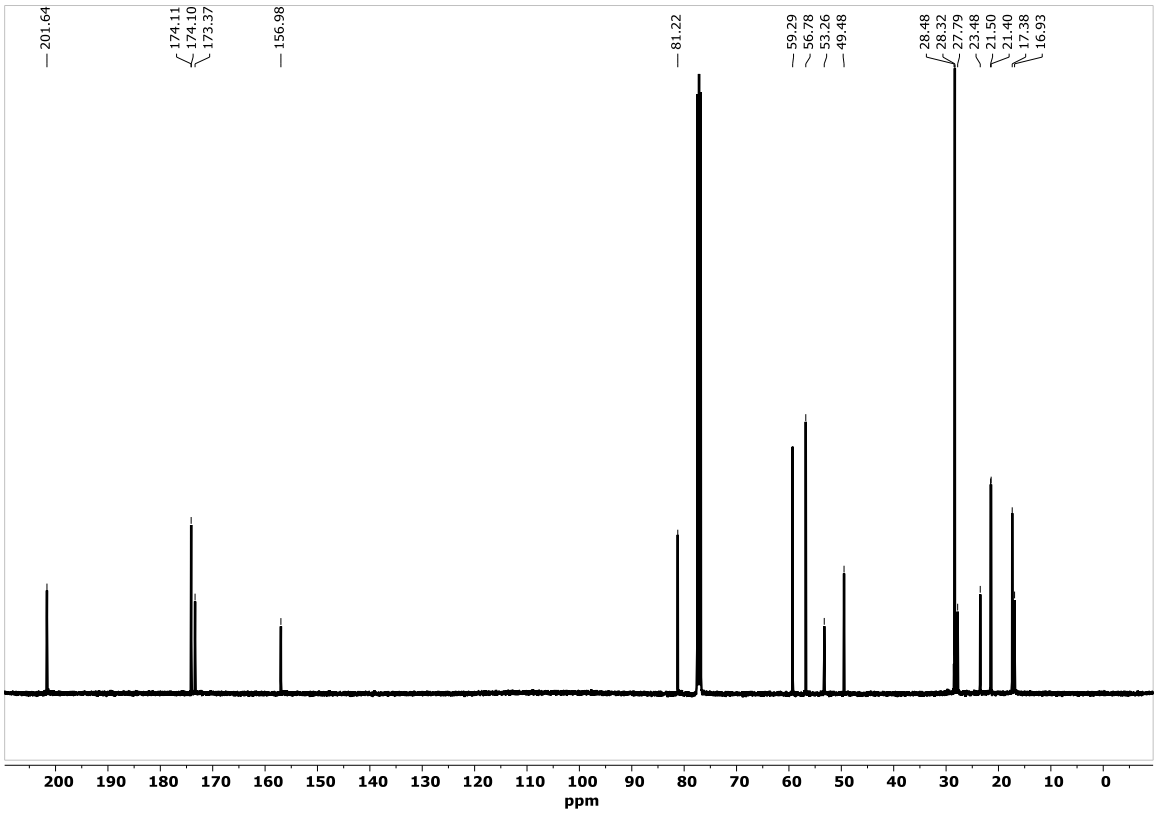

Figure 4.17 ^{13}C NMR (101 MHz, $CDCl_3$) of Boc-(Ala-Aib)$_2$-CHO

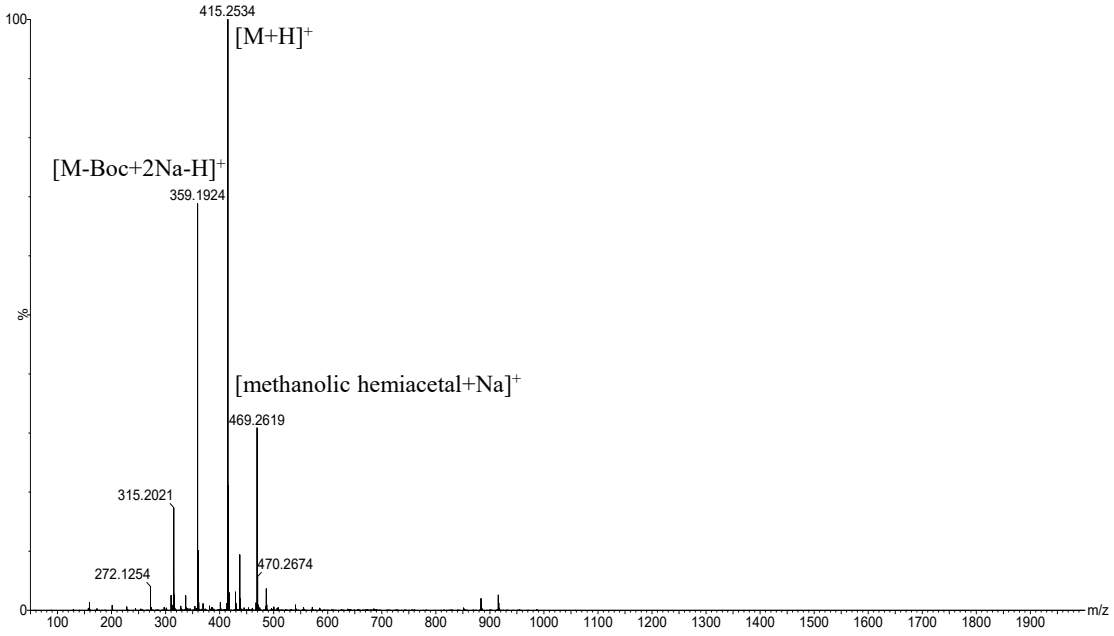

Figure 4.18 MS spectra Boc-(Ala-Aib)$_2$-CHO

NH$_2$-(Ala-Aib)$_2$-COOMe

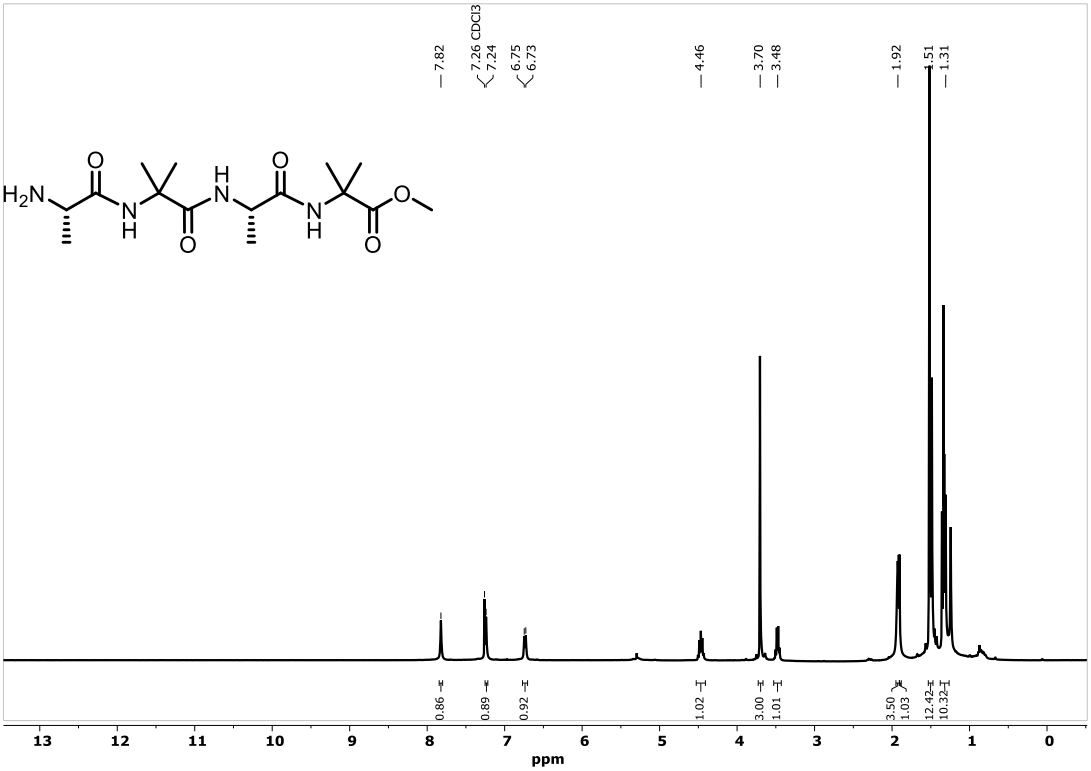

Figure 4.19 ^{1}H NMR (400 MHz, CDCl$_3$) of NH$_2$-(Ala-Aib)$_2$-COOMe

Boc-(Ala-Aib)$_4$-COOMe

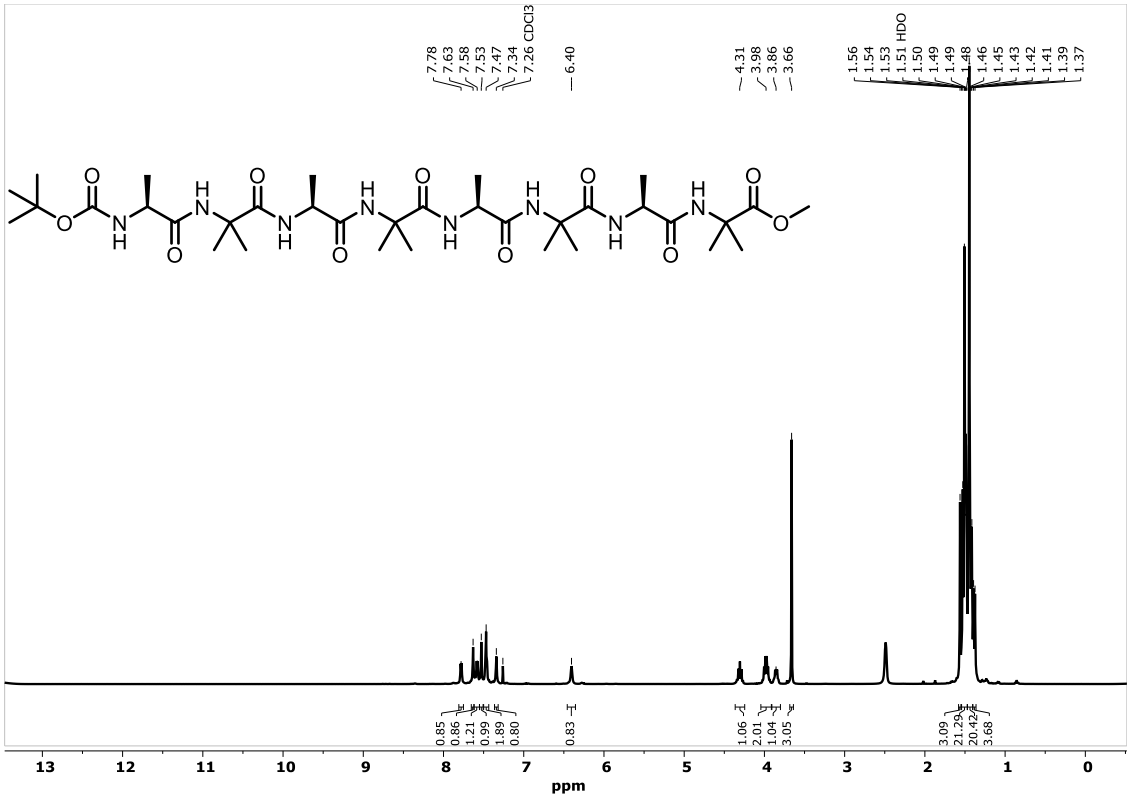

Figure 4.20 ^{1}H NMR (400 MHz, $CDCl_3$) of Boc-(Ala-Aib)$_4$-COOMe

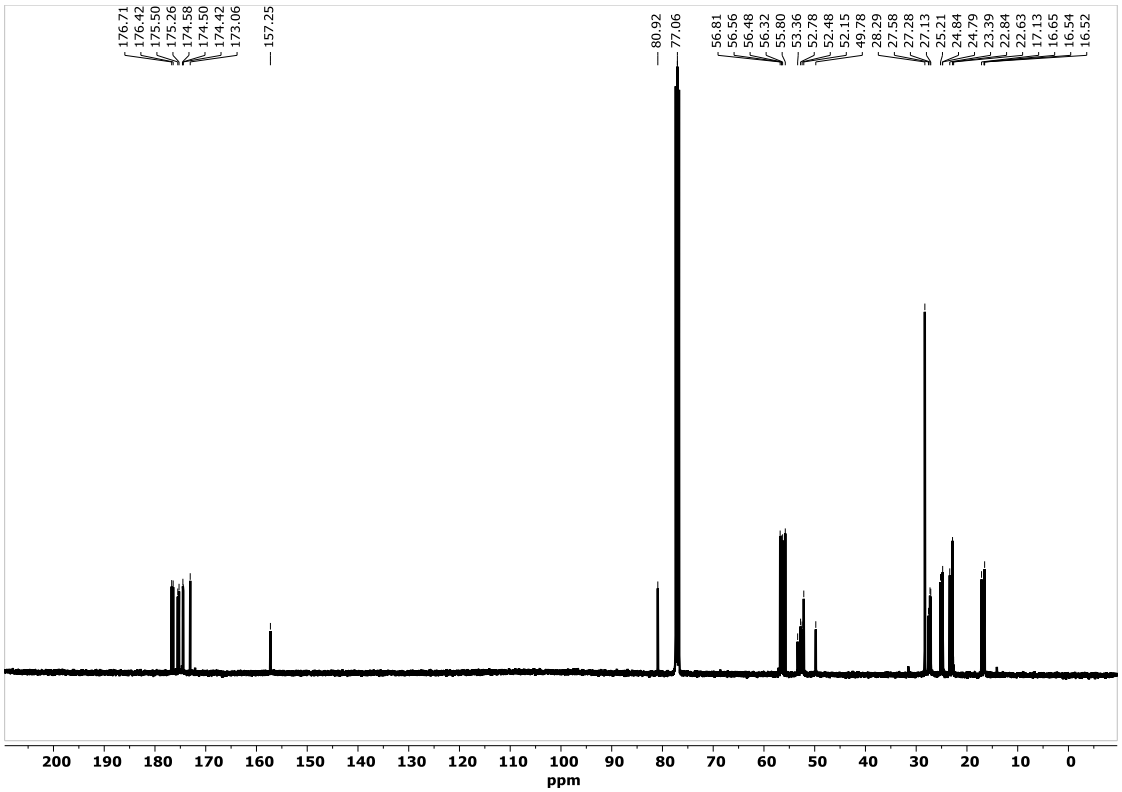

Figure 4.21 ^{13}C NMR (101 MHz, $CDCl_3$) of Boc-(Ala-Aib)$_4$-COOMe

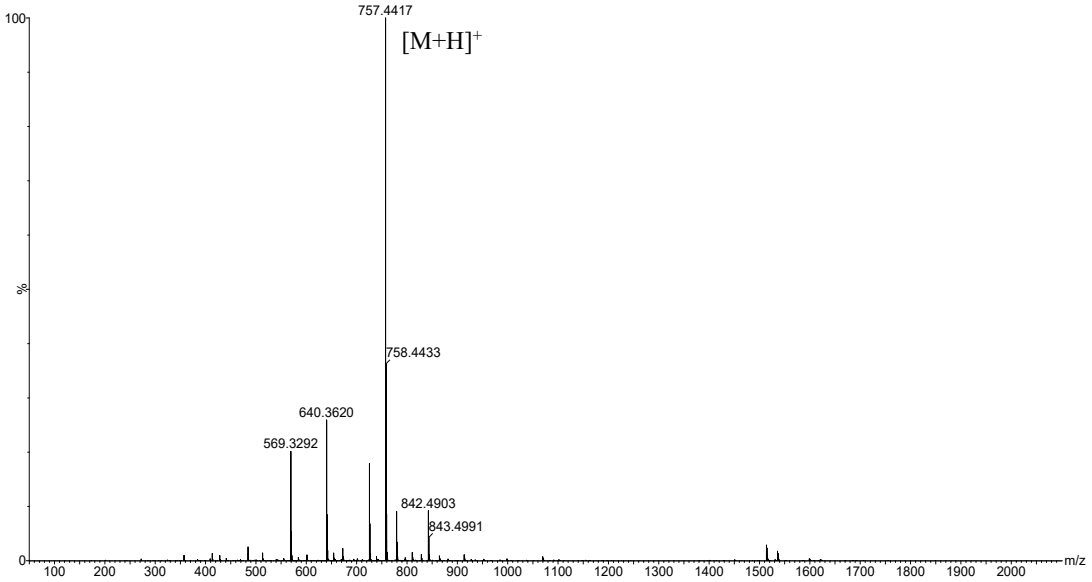

Figure 4.22 MS spectra Boc-(Ala-Aib)$_4$-COOMe

Boc-(Ala-Aib)$_4$-COOH

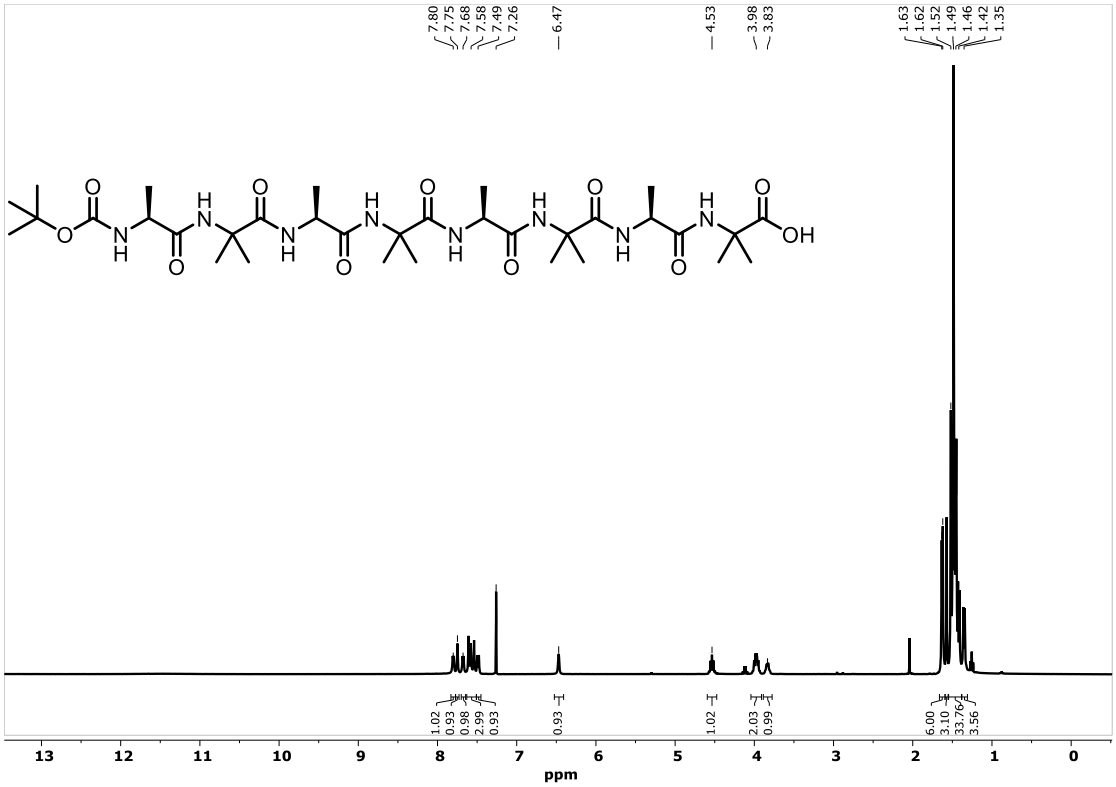

Figure 4.23 ^{1}H NMR (400 MHz, $CDCl_3$) of Boc-(Ala-Aib)$_4$-COOH

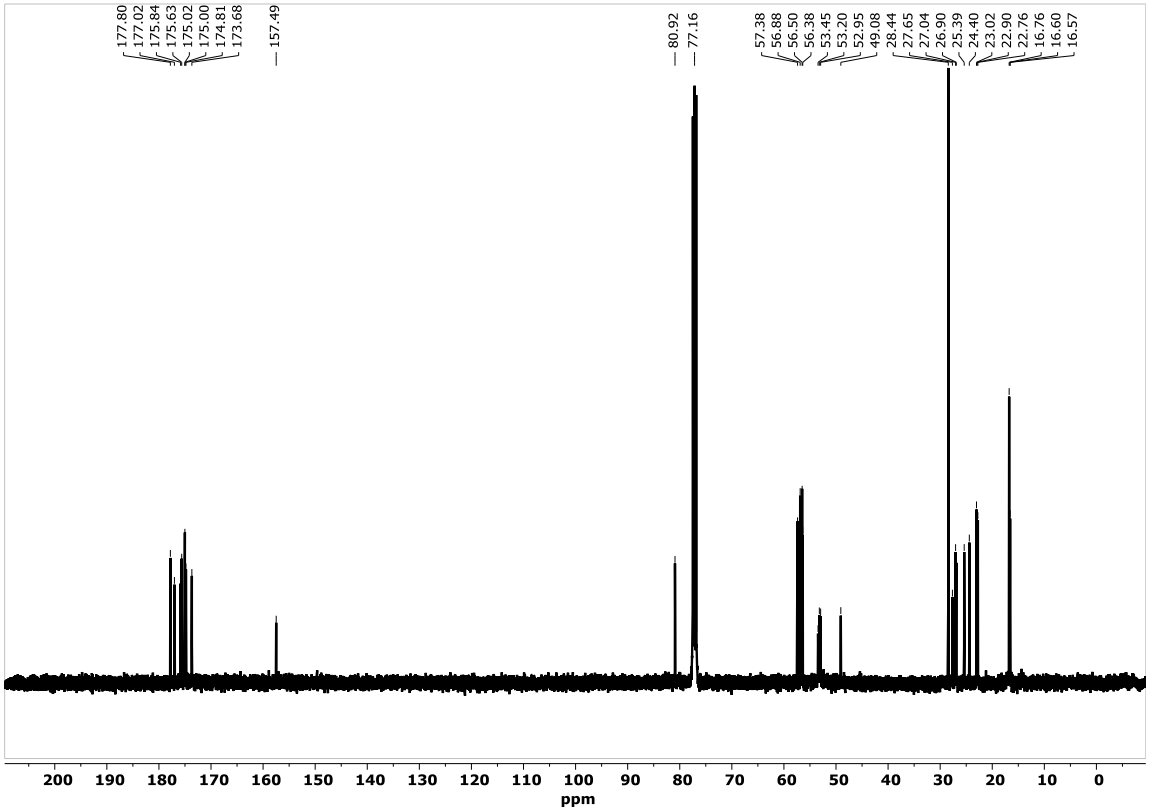

Figure 4.24 ^{13}C NMR (101 MHz, $CDCl_3$) of Boc-(Ala-Aib)$_4$-COOH

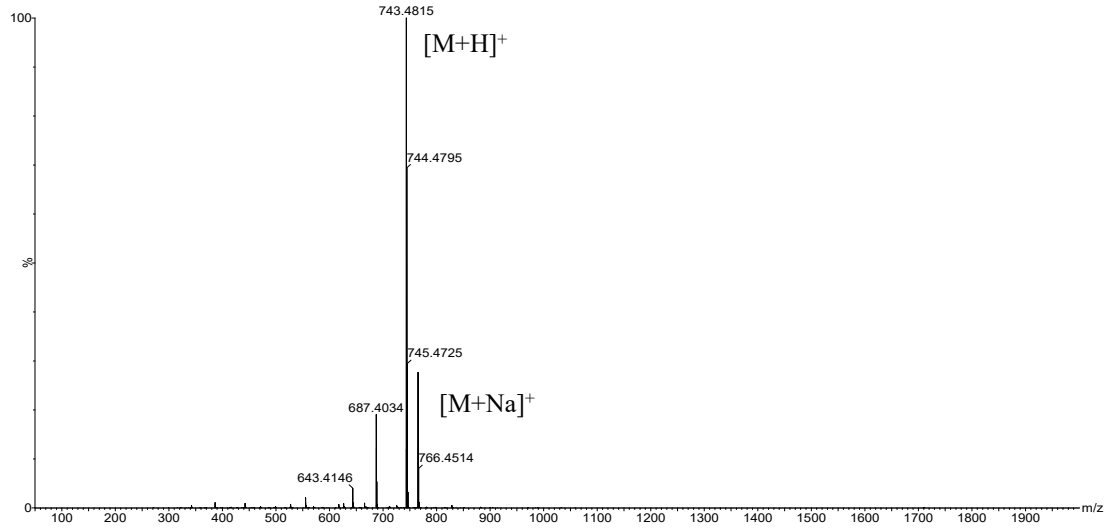

Figure 4.25 MS spectra Boc-(Ala-Aib)$_4$-COOH

Boc-(Ala-Aib)$_4$-CN(OCH$_3$)CH$_3$

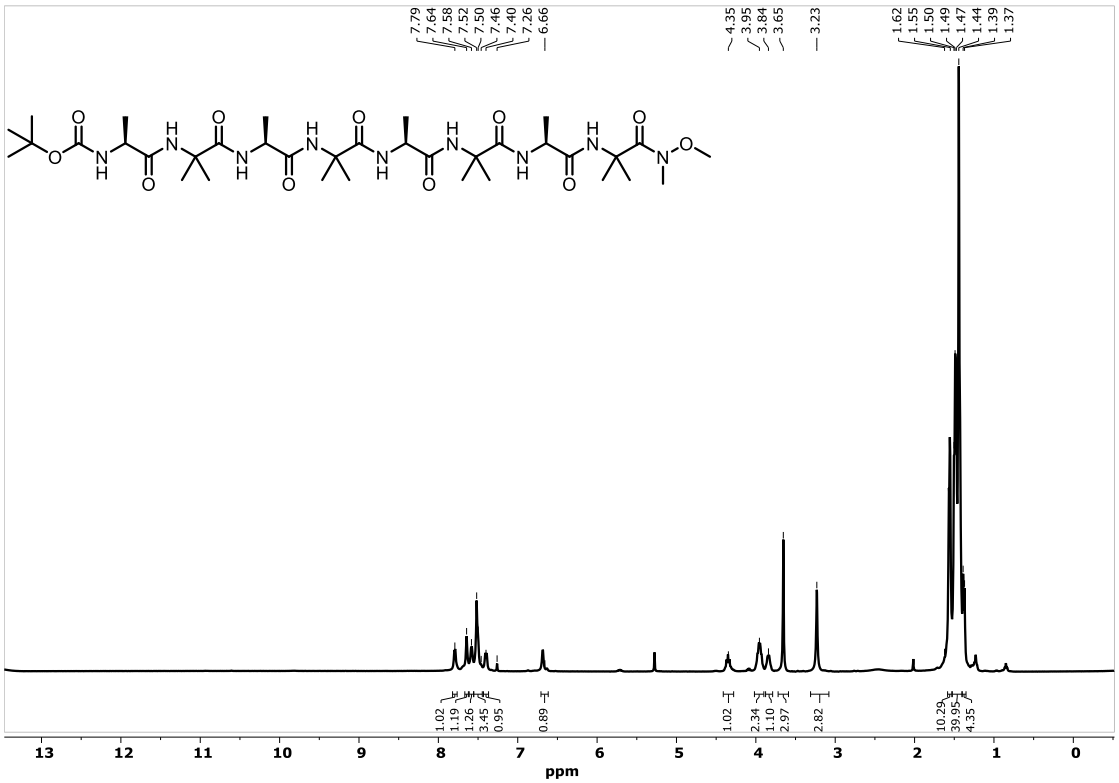

Figure 4.26 ^{1}H NMR (400 MHz, CDCl$_3$) of Boc-(Ala-Aib)$_4$-CN(OCH$_3$)CH$_3$

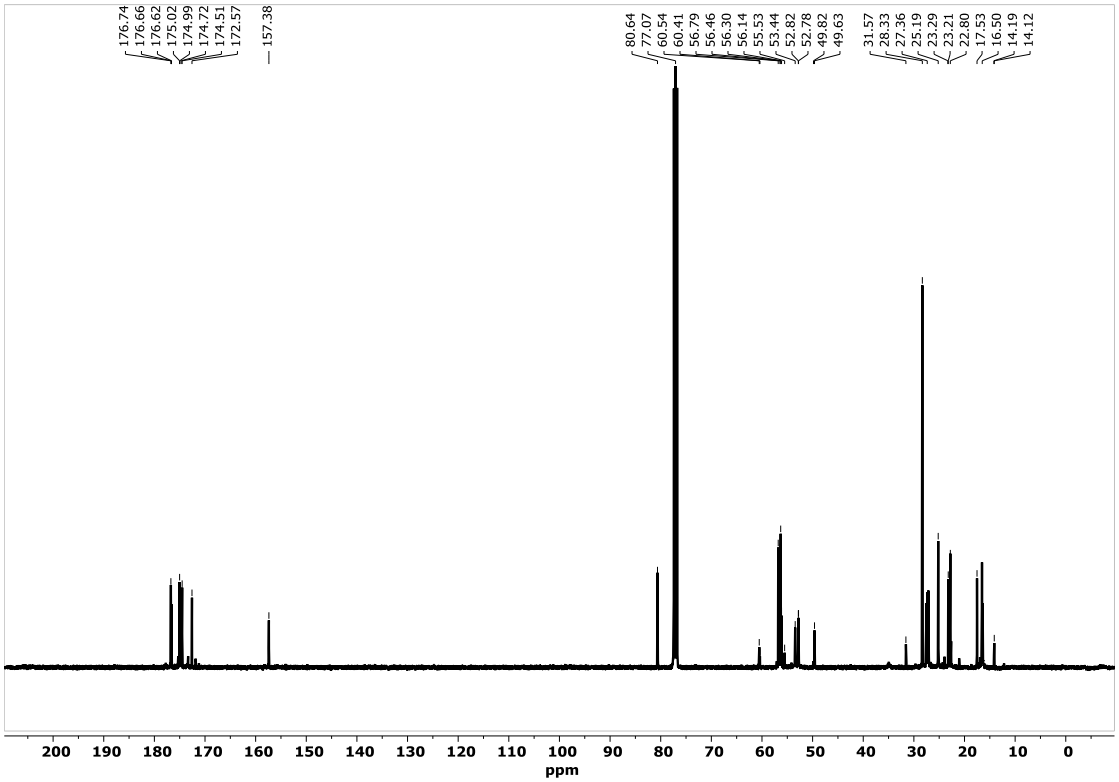

Figure 4.27 ^{13}C NMR (101 MHz, CDCl$_3$) of Boc-(Ala-Aib)$_4$-CN(OCH$_3$)CH$_3$

Boc-(Ala-Aib)$_4$-CHO

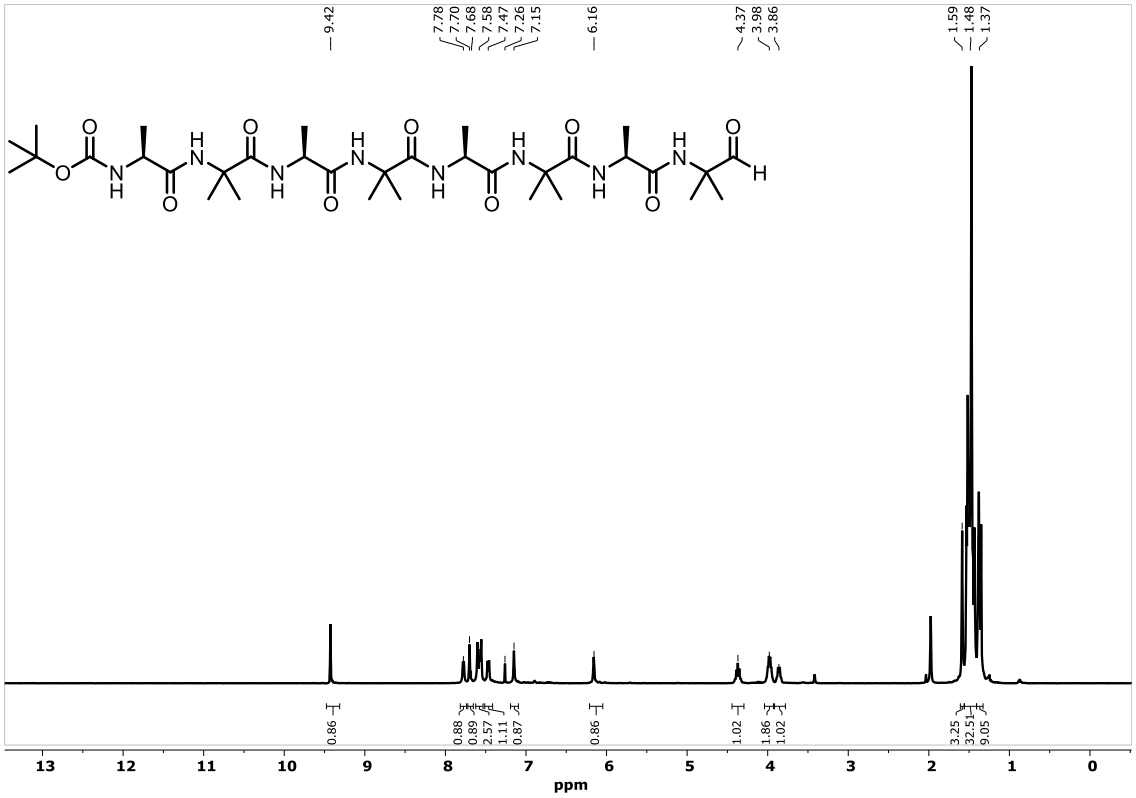

Figure 4.28 ^{1}H NMR (400 MHz, $CDCl_3$) of Boc-(Ala-Aib)$_4$-CHO

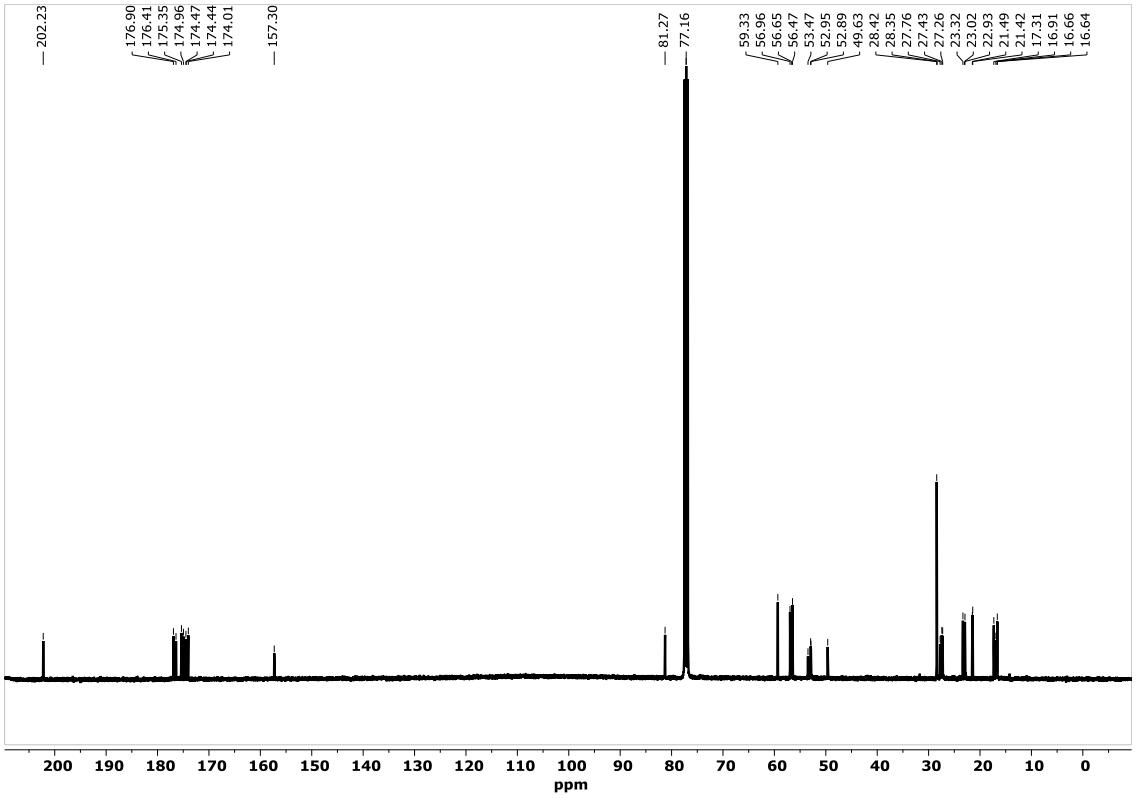

Figure 4.29 ^{13}C NMR (101 MHz, $CDCl_3$) of Boc-(Ala-Aib)$_4$-CHO

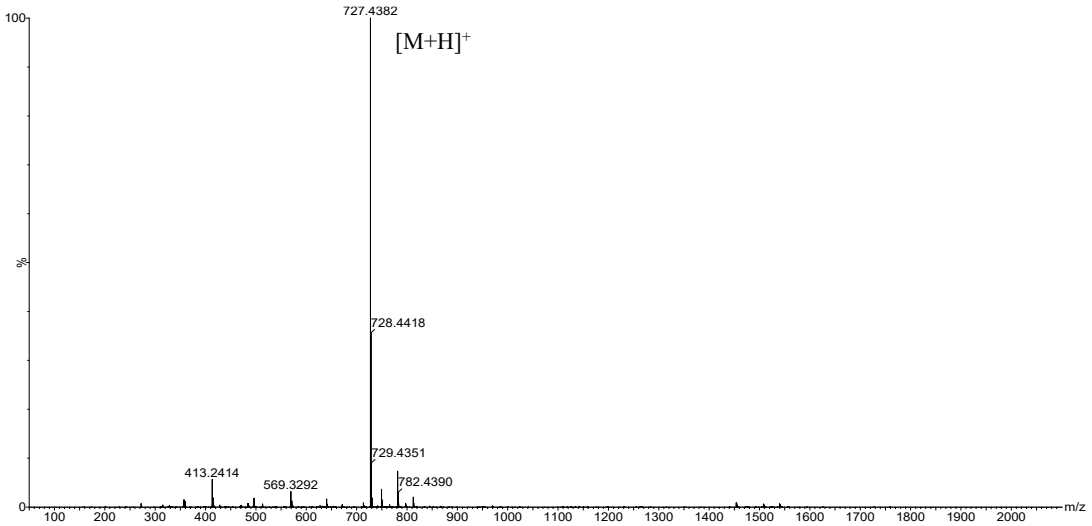

Figure 4.30 MS spectra Boc-(Ala-Aib)$_4$-CHO

NH$_2$-(Ala-Aib)$_4$-COOMe

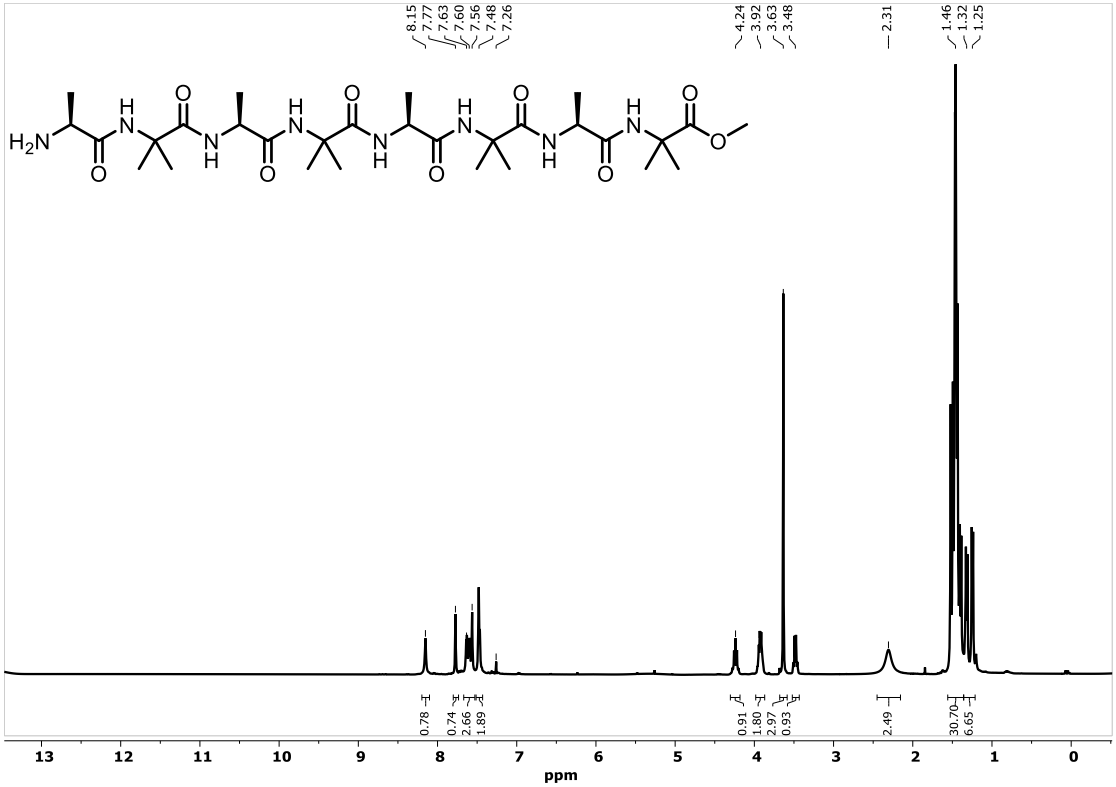

Figure 4.31 ^{1}H NMR (400 MHz, CDCl$_3$) of NH$_2$-(Ala-Aib)$_4$-COOMe

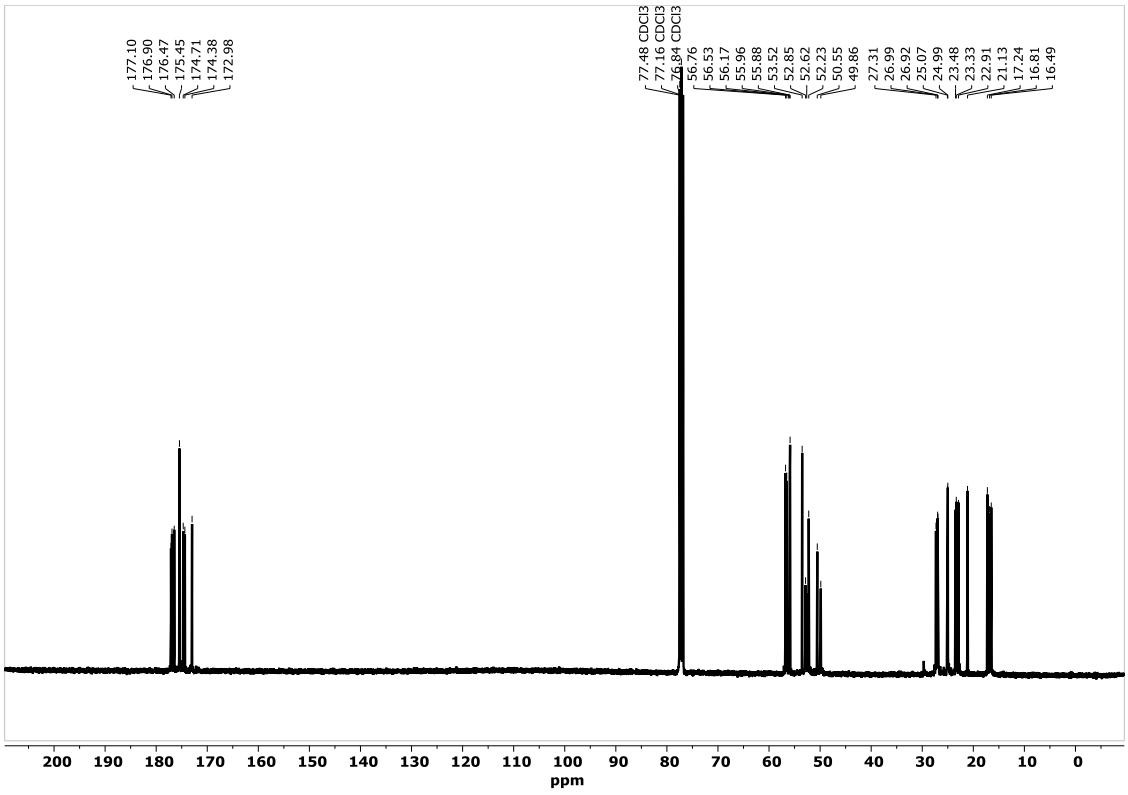

Figure 4.32 ^{13}C NMR (101 MHz, $CDCl_3$) of NH_2-(Ala-Aib)$_4$-COOMe

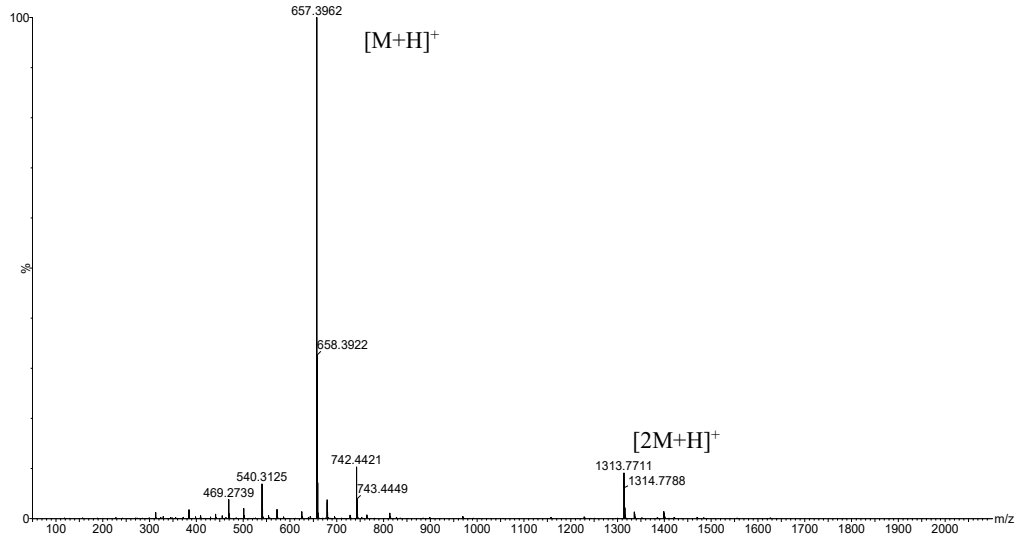

Figure 4.33 MS spectra NH_2-(Ala-Aib)$_4$-COOMe

Boc-(Ala-Aib)$_4$-CH$_2$-NH-(Ala-Aib)$_4$-COOMe

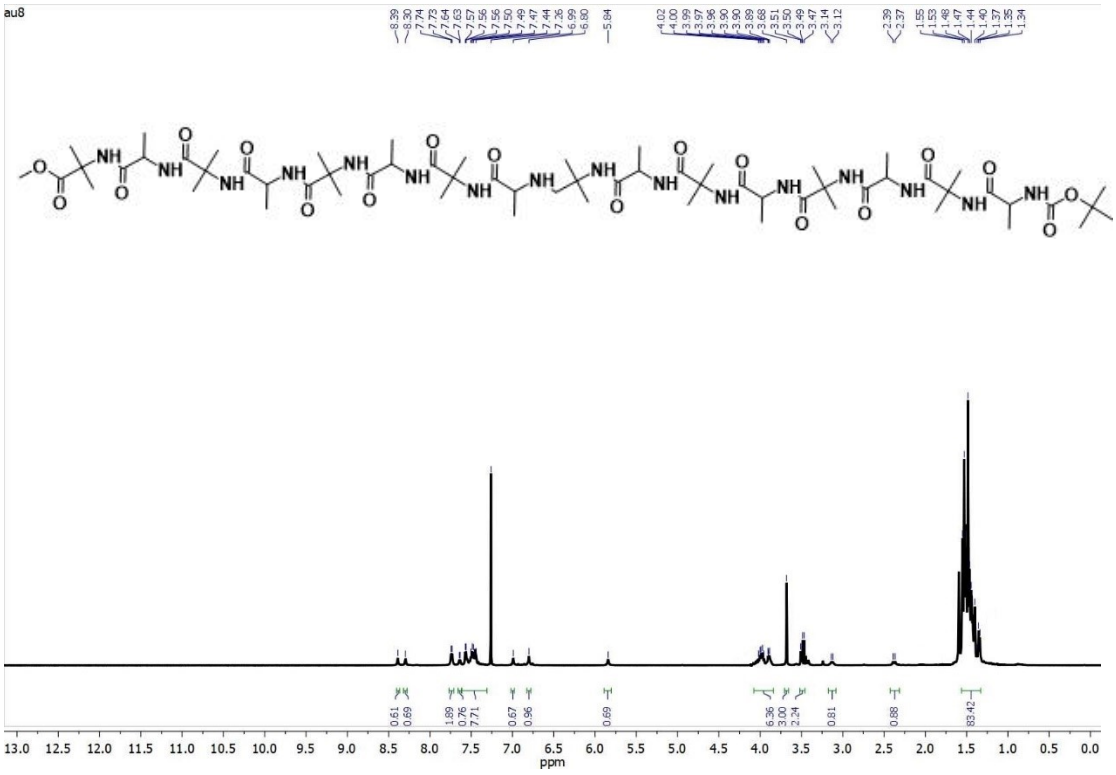

Figure 4.34 ^{1}H NMR (400 MHz, CDCl$_3$) of Boc-(Ala-Aib)$_4$-CH$_2$-NH-(Ala-Aib)$_4$-COOMe

Boc-(Ala-Aib)$_2$-CH$_2$-NH-(Ala-Aib)$_2$-COOMe

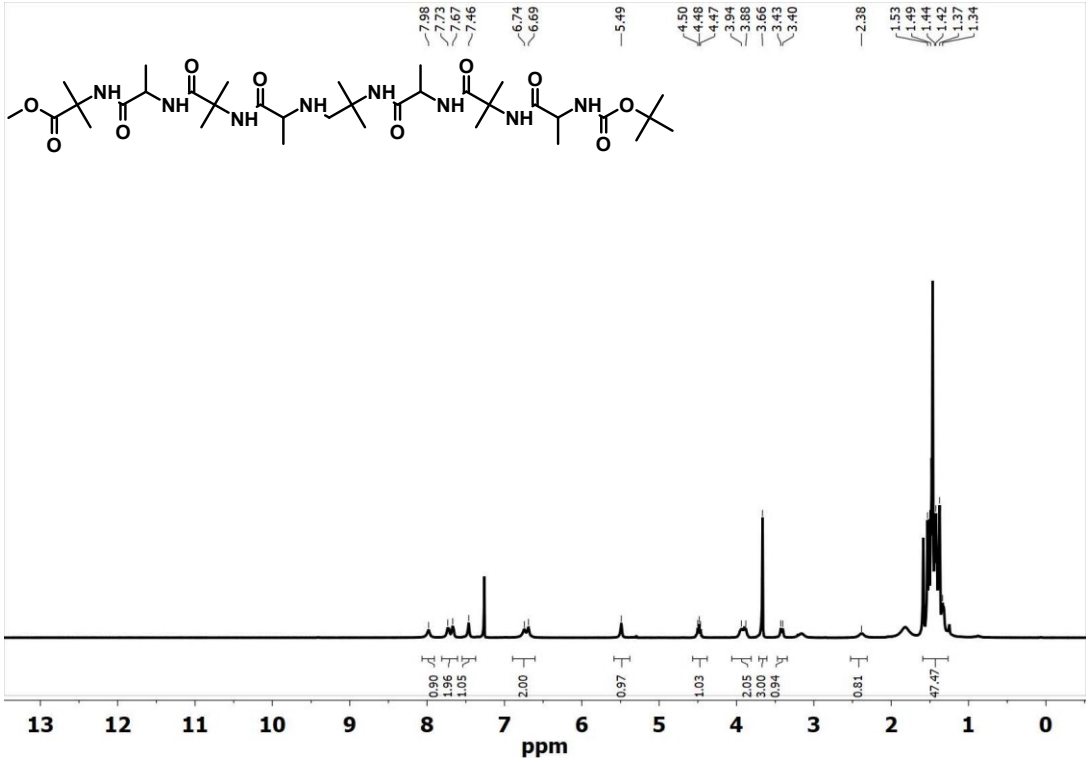

Figure 4.35 ^{1}H NMR (400 MHz, CDCl$_3$) of Boc-(Ala-Aib)$_2$-CH$_2$-NH-(Ala-Aib)$_2$-COOMe

Boc-(Ala-Aib)-CH$_2$-NH-(Ala-Aib)-COOMe

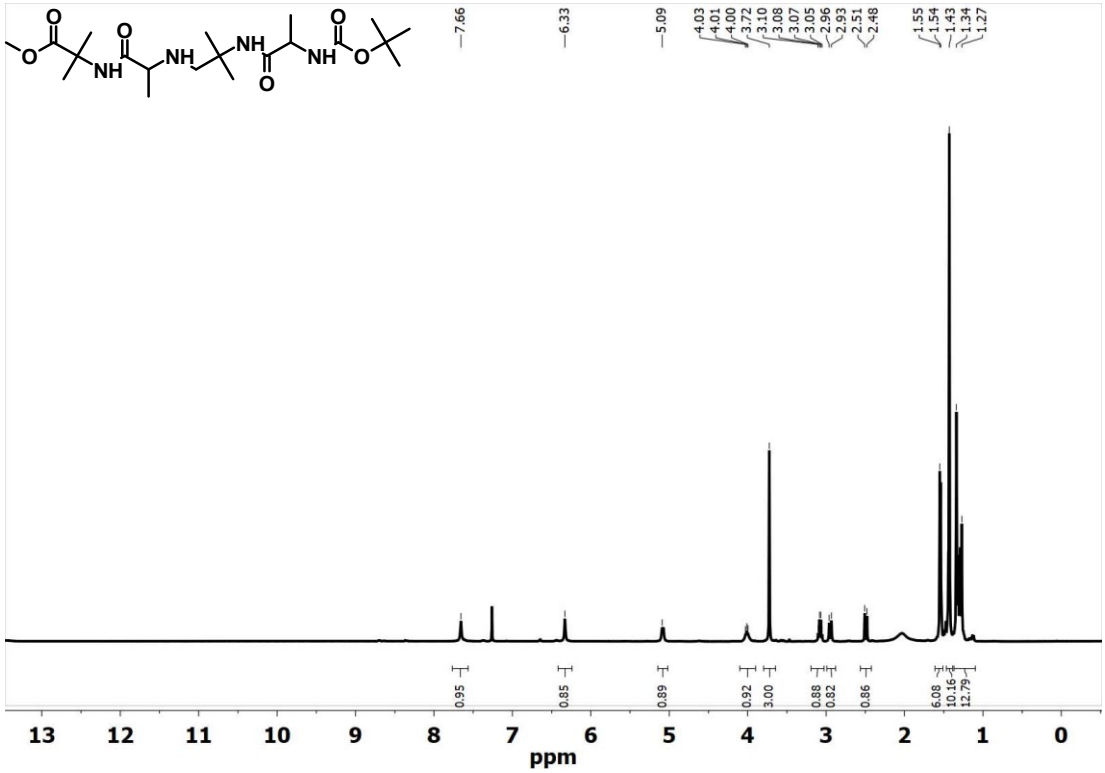

Figure 4.36 ^{1}H NMR (400 MHz, $CDCl_3$) of Boc-(Ala-Aib)-CH_2-NH-(Ala-Aib)-COOMe

Condensation product of nonaldehyde

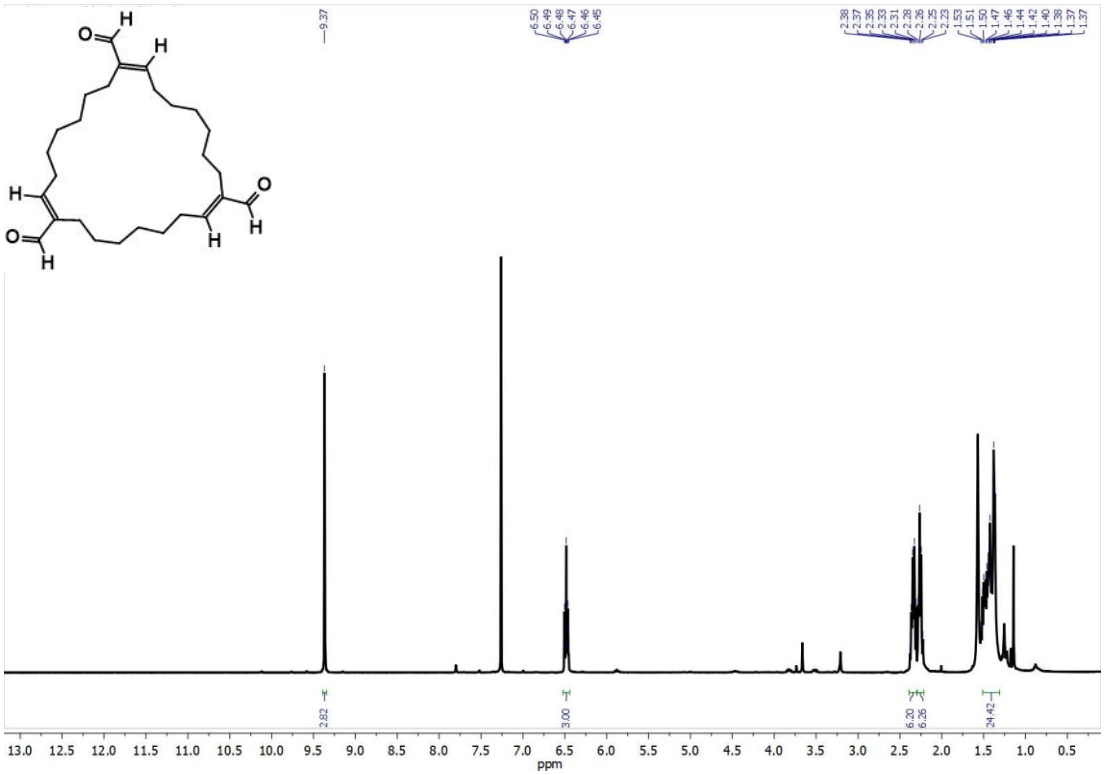

Figure 4.37 ^{1}H NMR (400 MHz, $CDCl_3$) of Condensation product of nonaldehyde

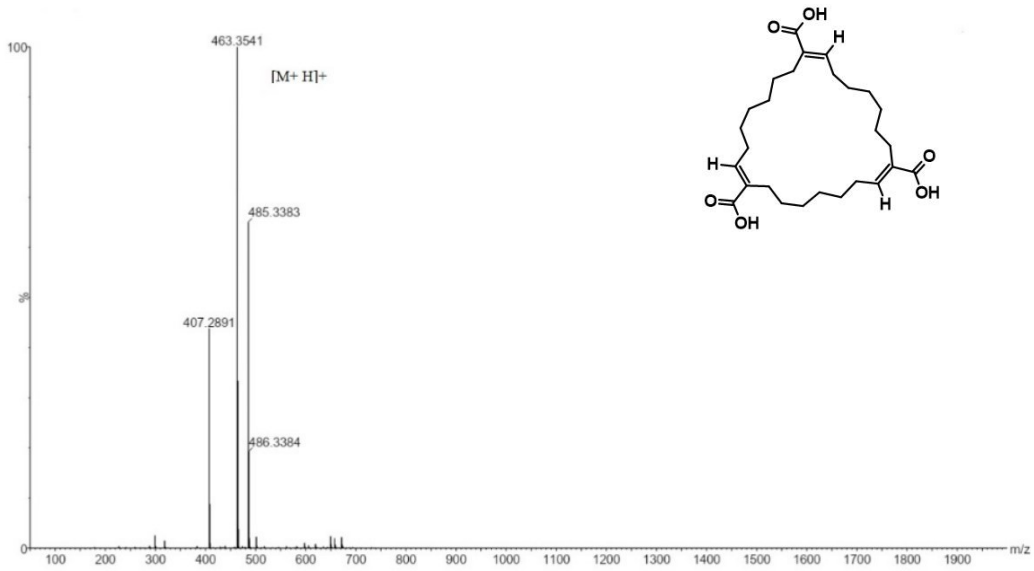

Figure 4.38 MS spectra NH_2-(Ala-Aib)$_4$- Condensation product of nonaldehyde oxidized

Condensation product of 9-((3-(((9-oxononyl)oxy)methyl)benzyl)oxy)nonanal

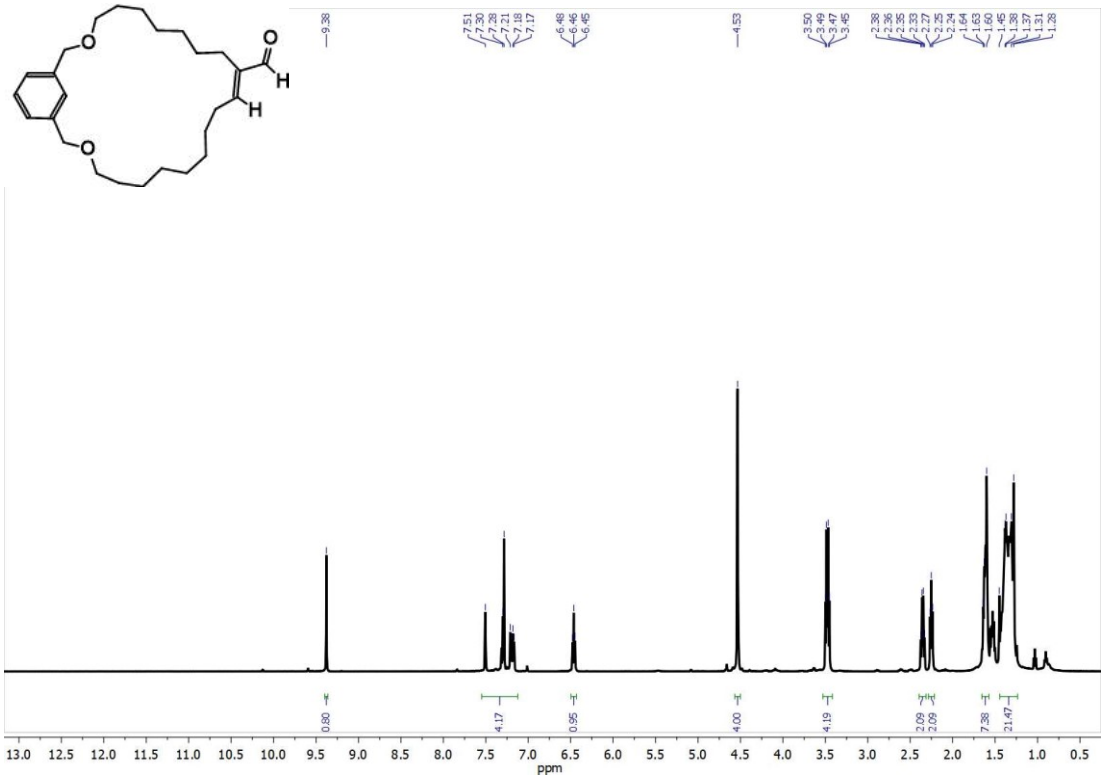

Figure 4.37 ^{1}H NMR (400 MHz, $CDCl_3$) of Condensation product of 9-((3-(((9-oxononyl)oxy)methyl)benzyl)oxy)nonanal

NH_2-Val-NH-CH_2-Ph-Cl

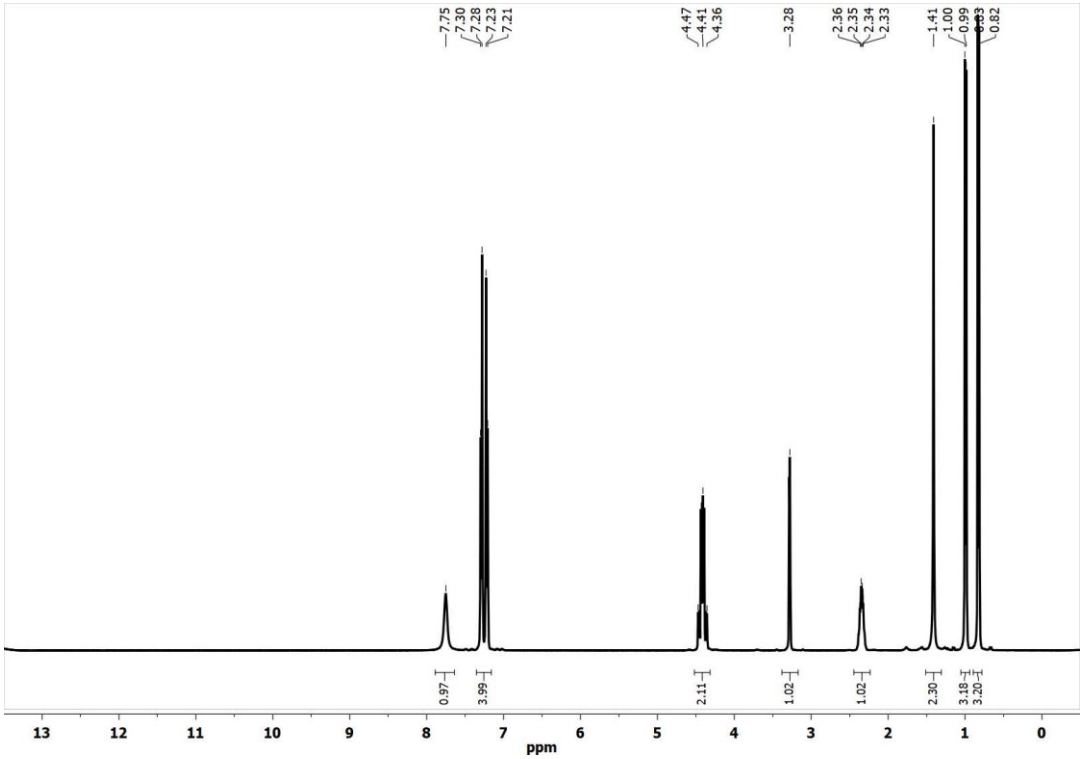

Figure 4.38 ^1H NMR (400 MHz, $CDCl_3$) of NH_2-Val-NH-CH_2-Ph-Cl

4.4.7 Crystal data

Table 4.1. Crystal data and structure refinement for Boc-AibΨ[CH=N]-L-Val-NH-*p*ClBn.

Identification code	mc306	
Empirical formula	$C_{21}H_{32}ClN_3O_3$	
Formula weight	409.94	
Temperature	293(2) K	
Wavelength	0.71073 Å	
Crystal system	Monoclinic	
Space group	C2	
Unit cell dimensions	a = 17.8122(8) Å	α= 90°
	b = 5.8142(2) Å	β= 104.385(4)°
	c = 23.0959(10) Å	γ = 90°
Volume	2316.91(17) $Å^3$	
Z	4	
Density (calculated)	1.175 Mg/m^3	
Absorption coefficient	0.189 mm^{-1}	
F(000)	880	
Crystal size	0.50 × 0.10 × 0.05 mm^3	
Theta range for data collection	2.599 to 25.027°.	
Index ranges	$-20 \le h \le 20, -6 \le k \le 6, -27 \le l \le 27$	
Reflections collected	14648	
Independent reflections	3887 [R(int) = 0.0249]	
Completeness to theta = 25.027°	98.1 %	
Absorption correction	Semi-empirical from equivalents	
Max. and min. transmission	1.00000 and 0.79121	
Refinement method	Full-matrix least-squares on F^2	
Data / restraints / parameters	3887 / 1 / 260	

Goodness-of-fit on F^2	1.031
Final R indices [I>2sigma(I)]	$R_1 = 0.0451$, $wR_2 = 0.1094$
R indices (all data)	$R_1 = 0.0523$, $wR_2 = 0.1148$
Absolute structure parameter	-0.03(3)
Extinction coefficient	n/a
Largest diff. peak and hole	0.330 and -0.261 e.Å^{-3}

Table 4.2. Selected torsion angles [°] for Boc-AibΨ[CH=N]-L-Val-NH-*p*ClBn.

C01-OU-C0-N1	164.4(4)
OU-C0-N1-C1A	166.9(3)
C0-N1-C1A-C1	51.7(4)
N1-C1A-C1-N2	-128.2(3)
C1A-C1-N2-C2A	-176.4(3)
C1-N2-C2A-C2	-101.8(3)
N2-C2A-C2B-C2G1	62.4(3)
N2-C2A-C2B-C2G2	-62.9(4)
N2-C2A-C2-NT	8.0(4)
C2A-C2-NT-CT1	-174.3(3)
C2-NT-CT1-CT2	-112.0(3)
NT-CT1-CT2-CT3	35.7(4)
NT-CT1-CT2-CT7	-149.0(3)

Table 4.3. Hydrogen bonds for Boc-AibΨ[CH=N]-L-Val-NH-*p*ClBn [Å and °].

D-H...A	d(D-H)	d(H...A)	d(D...A)	<(DHA)

NT-HT...O0	0.86	2.19	2.968(3)	149.7
N1-H1...O2#1	0.86	2.34	3.012(3)	134.8

Symmetry transformations used to generate equivalent atoms:

#1 x-1/2,y+1/2,z

5. CONCLUSIONS

During this thesis project we have performed the synthesis of several foldamers, excellent substrates for the study of reactions that are able to reproduce biological behaviors of proteins and enzymes.

First of all, their secondary structure has been studied with amino acids, such as Aib, which allowed a 3_{10}-helix structure, more tightly bound and longer than the classical α-helices. It was also identified the possibility to build a catalytic center within the backbone of these structures, thus reducing the difficulties of synthesis of larger complexes that contained the reaction centers as side chains. In fact, the ability to have the reaction centers within a rigid structure such as the foldamer helix allows the products of reactions to be controlled by forcing the substrates to be in a certain position. The synthesis strategy that enabled this design involves a reductive amination reaction between an aldehyde-terminated peptide and a primary amine-terminated peptide resulting in the formation of the Shiff-base followed by reduction to a secondary amine.

We obtained the crystallographic structure not only of foldamers that included the secondary amine within the backbone, but also the crystallographic characterization of an imino surrogate for a peptide bond between two amino acids, which as far as we know, is unprecedented.

In a second step based on the secondary structures of foldamers a catalytic center was built around the secondary amine formed in the backbone as a result of reductive amination. With the use of the amino acid Dap, which sees a primary amine in its side chain, it was therefore possible to construct a center that would see a primary amine and a secondary amine spaced by two carbons as reaction centers. Different residues (Val, Asp, Ser) have also been used to synthesize foldamers presenting isopropyl, carboxylic acids or hydroxyls adjacent to the secondary amine, thus going on to form different three-dimensional catalytic centers that have considerable diversity in aldol condensation reactions.

As an initial example of reactivity, the new foldamers were compared with foldamers recently developed by Gellman et al. for the cyclization of linear dialdehydes via imine/enamine intermediate resulting in C-C bond formation in the ring closure. The

results obtained presented a higher efficiency of the foldamers constructed by us, indicating that the pre-organization of the reaction center and imposition of substrates to be in a certain position leads to significant improvements in the efficiency of the reaction, even if following a very simple foldamer synthesis strategy (*click reaction*).

Future works could include the study of new reaction centers given the versatility of these foldamers. In fact, according to the choice of amino acid will be possible to design and to build new catalytic centers.

6. REFERENCES

1. Nestl, B. M., Hammer, S. C., Nebel, B. A. & Hauer, B. New Generation of Biocatalysts for Organic Synthesis. *Angewandte Chemie International Edition* **53**, 3070–3095 (2014).
2. Miller, S. J. In Search of Peptide-Based Catalysts for Asymmetric Organic Synthesis. *Accounts of Chemical Research* **37**, 601–610 (2004).
3. Wendlandt, A. E., Vangal, P. & Jacobsen, E. N. Quaternary stereocentres via an enantioconvergent catalytic SN1 reaction. *Nature 2018 556:7702* **556**, 447–451 (2018).
4. Park, Y. *et al.* Macrocyclic bis-thioureas catalyze stereospecific glycosylation reactions. *Science* **355**, 162–166 (2017).
5. Davie, E. A. C., Mennen, S. M., Xu, Y. & Miller, S. J. Asymmetric Catalysis Mediated by Synthetic Peptides. *Chemical Reviews* **107**, 5759–5812 (2007).
6. Roy, A., Prabhakaran, P., Baruah, P. K. & Sanjayan, G. J. Diversifying the structural architecture of synthetic oligomers: the hetero foldamer approach. *Chemical Communications* **47**, 11593–11611 (2011).
7. Gellman, S. H. Foldamers: A Manifesto. (1998).
8. Hill, D. J., Mio, M. J., Prince, R. B., Hughes, T. S. & Moore, J. S. A Field Guide to Foldamers. *Chemical Reviews* **101**, 3893–4011 (2001).
9. Horne, W. S., Price, J. L. & Gellman, S. H. Interplay among side chain sequence, backbone composition, and residue rigidification in polypeptide folding and assembly. *Proceedings of the National Academy of Sciences* **105**, 9151–9156 (2008).
10. Girvin, Z. C., Andrews, M. K., Liu, X. & Gellman, S. H. Foldamer-templated catalysis of macrocycle formation. *Science* **366**, 1528–1531 (2019).
11. Barlow, D. J. & Thornton, J. M. Helix geometry in proteins. *Journal of Molecular Biology* **201**, 601–619 (1988).
12. Richardson, J. S. & Richardson, D. C. Amino Acid Preferences for Specific Locations at the Ends of α Helices. *Science* **240**, 1648–1652 (1988).
13. Millhauser4, G. L. Biochemistry © New Concepts in Biochemistry Views of Helical Peptides: A Proposal for the Position of 3io-Helix along the Thermodynamic Folding Pathway* 1 **^. *M<XVCh* **28**, (1995).
14. Crisma, M., Formaggio, F., Moretto, A. & Toniolo, C. Peptide helices based on α-amino acids. *Biopolymers - Peptide Science Section* **84**, 3–12 (2006).
15. Goodman, C. M., Choi, S., Shandler, S. & DeGrado, W. F. Foldamers as versatile frameworks for the design and evolution of function. *Nature Chemical Biology 2007 3:5* **3**, 252–262 (2007).
16. Appella, D. H., Christianson, L. A., Karle, I. L., Powell, D. R. & Gellman, S. H. β-Peptide foldamers: Robust helix formation in a new family of β-amino acid oligomers. *Journal of the American Chemical Society* **118**, 13071–13072 (1996).

17. Tanaka, F., Fuller, R. & Barbas, C. F. Development of Small Designer Aldolase Enzymes: Catalytic Activity, Folding, and Substrate Specificity†. *Biochemistry* **44**, 7583–7592 (2005).

18. Müller, M. M. *et al.* A Rationally Designed Aldolase Foldamer. *Angewandte Chemie* **121**, 940–943 (2009).

19. Semetey, V. *et al.* Stable Helical Secondary Structure in Short-Chain N,N'-Linked Oligoureas Bearing Proteinogenic Side Chains**. **114**, 11 (2002).

20. Bécart, D. *et al.* Helical Oligourea Foldamers as Powerful Hydrogen Bonding Catalysts for Enantioselective C-C Bond-Forming Reactions. *Journal of the American Chemical Society* **139**, 12524–12532 (2017).

21. Aitken, L., Arezki, N., Dell'Isola, A. & Cobb, A. A. Asymmetric Organocatalysis and the Nitro Group Functionality. *Synthesis* **45**, 2627–2648 (2013).

22. Juliá, S. *et al.* Synthetic enzymes. Part 2. Catalytic asymmetric epoxidation by means of polyamino-acids in a triphase system. *Journal of the Chemical Society, Perkin Transactions 1* 1317–1324 (1982) doi:10.1039/P19820001317.

23. Kinghorn, M. J. *et al.* Proximity-Induced Reactivity and Product Selectivity with a Rationally Designed Bifunctional Peptide Catalyst. *ACS Catalysis* **7**, 7704–7708 (2017).

24. Ouellet, S. G., Walji, A. M. & Macmillan, D. W. C. Enantioselective Organocatalytic Transfer Hydrogenation Reactions using Hantzsch Esters. doi:10.1021/ar7001864.

25. Fessner, W. D. *et al.* The Mechanism of Class II, Metal-Dependent Aldolases. *Angewandte Chemie International Edition in English* **35**, 2219–2221 (1996).

26. Lai, C. Y., Nakai, N. & Chang, D. Amino Acid Sequence of Rabbit Muscle Aldolase and the Structure of the Active Center. *Science* **183**, 1204–1206 (1974).

27. Yamada, Y. M. A. *et al.* Direct Catalytic Asymmetric Aldol Reactions of Aldehydes with Unmodified Ketones. *Angewandte Chemie International Edition in English* **36**, 1871–1873 (1997).

28. Yamada, Y. M. A. & Shibasaki, M. Direct catalytic asymmetric aldol reactions promoted by a novel barium complex. *Tetrahedron Letters* **39**, 5561–5564 (1998).

29. List, B., Lerner, R. A. & Barbas, C. F. Proline-Catalyzed Direct Asymmetric Aldol Reactions. *Journal of the American Chemical Society* **122**, 2395–2396 (2000).

30. Newman, D. J. & Cragg, G. M. CHAPTER 1 Bioactive Macrocycles from Nature. 1–36 (2014) doi:10.1039/9781782623113-00001.

31. Rosenquist, Å. *et al.* Discovery and Development of Simeprevir (TMC435), a HCV NS3/4A Protease Inhibitor. *Journal of Medicinal Chemistry* **57**, 1673–1693 (2014).

32. Iyoda, M., Yamakawa, J. & Rahman, M. J. Conjugated Macrocycles: Concepts and Applications. *Angewandte Chemie International Edition* **50**, 10522–10553 (2011).

33. Martí-Centelles, V., Pandey, M. D., Burguete, M. I. & Luis, S. v. Macrocyclization Reactions: The Importance of Conformational, Configurational, and Template-Induced Preorganization. *Chemical Reviews* **115**, 8736–8834 (2015).

34. Galli, C. & Mandolini, L. The Role of Ring Strain on the Ease of Ring Closure of Bifunctional Chain Molecules. doi:10.1002/1099-0690.

35. Pedersen, C. J. *et al.*) A. Luttringhaus and I. Sichert-Modrow. *J. Am. Chem. Soc* **2**, 209.

36. Fürstner, A. Recent advancements in ring closing olefin metathesis. *Topics in Catalysis* **4**, 285–299 (1997).

37. Blackwell, H. E. *et al.* Ring-Closing Metathesis of Olefinic Peptides: Design, Synthesis, and Structural Characterization of Macrocyclic Helical Peptides. (2001) doi:10.1021/jo015533k.

38. Shen, X. *et al.* Kinetically E-selective macrocyclic ring-closing metathesis. *Nature Publishing Group* **541**, (2017).

39. Müller, M. M. *et al.* A Rationally Designed Aldolase Foldamer. *Angewandte Chemie* **121**, 940–943 (2009).

40. Wang, P. S. P., Nguyen, J. B. & Schepartz, A. Design and high-resolution structure of a β3-peptide bundle catalyst. *Journal of the American Chemical Society* **136**, 6810–6813 (2014).

41. Venkatachalam, C. M. Stereochemical criteria for polypeptides and proteins. V. Conformation of a system of three linked peptide units. *Biopolymers* **6**, 1425–1436 (1968).

42. Toniolo, C., Crisma, M., Formaggio, F. & Peggion, C. Control of Peptide Conformation by the Thorpe-Ingold Effect (C-Tetrasubstitution). (2002) doi:10.1002/1097-0282(2001)60:6.

43. Aravinda, S., Shamala, N. & Balaram, P. Aib Residues in Peptaibiotics and Synthetic Sequences: Analysis of Nonhelical Conformations. *Chemistry & Biodiversity* **5**, 1238–1262 (2008).

44. Erkkilä, A. & Pihko, P. M. Rapid Organocatalytic Aldehyde-Aldehyde Condensation Reactions. *European Journal of Organic Chemistry* **2007**, 4205–4216 (2007).

45. Roels, J. & Metz, P. Oxidation of α,ω-diols using the Dess - Martin periodinane. *Synlett* **2001**, 789–790 (2001).

Ringrazio in primo luogo il prof. Alessandro Moretto, per la sua disponilità, l'aiuto e i consigli, che non solo mi hanno portata ad aggiungere nuove conoscenze alla sintesi organica, ma mi hanno fatta anche appasionare a questo progetto di tesi.
A Matteo e Giulia, che hanno sempre trovato del tempo in laboratorio per aiutarmi e spiegarmi le cose che non capivo.
Alla mia controrelatrice, la Prof.ssa Barbara Fresch per avermi ascoltata e consigliata ad ogni incontro.
Un ringraziamento va anche fatto ai miei genitori e a mio fratello, che mi hanno permesso di intraprendere questo percorso di studi e mi hanno sostenuta ogni giorno. A Biagio per il supporto e la pazienza.